

Alma Mater Studiorum – Università di Bologna

DOTTORATO DI RICERCA IN

CELLULAR, MOLECULAR AND INDUSTRIAL BIOLOGY

Ciclo: XXIV

Settore Concorsuale di afferenza: BIOLOGICAL, BIOMEDICAL AND
BIOTECHNOLOGICAL SCIENCES

TITOLO TESI

ATOMIC FORCE MICROSCOPY STUDIES OF THE AMYLOIDOGENIC PROCESSES OF
INTRINSICALLY UNSTRUCTURED PROTEINS RELATED TO NEURODEGENERATIVE
DISEASES

Presentata da: DHRUV KUMAR

Coordinatore Dottorato

PROF. VINCENZO SCARLATO

Relatore

PROF. BRUNO SAMORI

Tutore

DR. MARCO BRUCALE

Esame finale anno 2012

Atomic Force Microscopy Studies of the Amyloidogenic Processes of Intrinsically Unstructured Proteins Related to Neurodegenerative Diseases



By

Dhruv Kumar

Ph.D. Cycle-XXIV

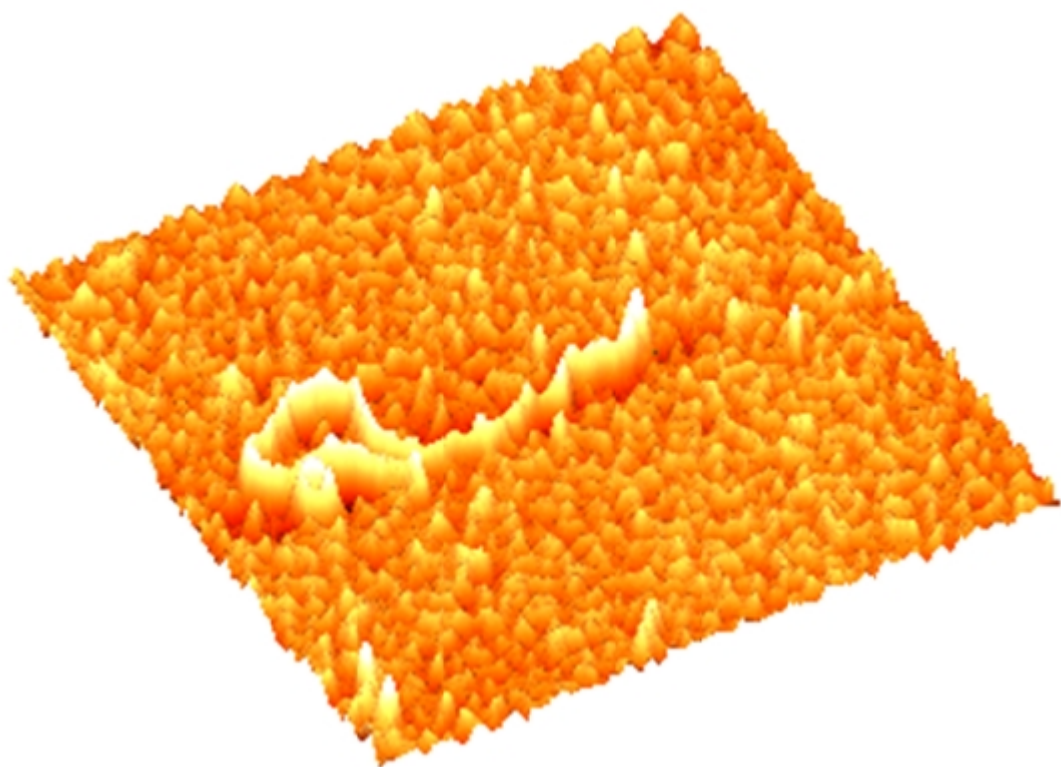
PhD School in Biological, Biomedical, and Biotechnological Sciences

PhD program in Cellular, Molecular, and Industrial Biology

**NanoBiotechnology and NanoBioscience lab
Department of Biochemistry,
University of Bologna, Italy**

PhD Supervisor: Prof. Bruno Samori (PhD)
PhD Co-supervisor: Dr. Marco Brucale (PhD)
PhD Coordinator: Prof. Vincenzo Scarlato (PhD)

March 2012



“You have to dream before your dream can come true”

Abdul kalam

To my parents and my family

Abstract

Protein aggregation and formation of insoluble aggregates in central nervous system is the main cause of neurodegenerative disease. Parkinson's disease is associated with the appearance of spherical masses of aggregated proteins inside nerve cells called Lewy bodies. α -Synuclein is the main component of Lewy bodies. In addition to α -synuclein, there are more than a hundred of other proteins co-localized in Lewy bodies: 14-3-3 η protein is one of them. In order to increase our understanding on the aggregation mechanism of α -synuclein and to study the effect of 14-3-3 η on it, I addressed the following questions. (i) How α -synuclein monomers pack each other during aggregation? (ii) Which is the role of 14-3-3 η on α -synuclein packing during its aggregation? (iii) Which is the role of 14-3-3 η on an aggregation of α -synuclein "seeded" by fragments of its fibrils?

In order to answer these questions, I used different biophysical techniques (e.g., Atomic force microscope (AFM), Nuclear magnetic resonance (NMR), Surface plasmon resonance (SPR) and Fluorescence spectroscopy (FS)).

To answer the first question, I compared by AFM imaging the *in vitro* aggregation of α -synuclein with that of α -synuclein dimers (**NC**-, **NN**-, and **CC**-terminal dimers) and with that of a so-called Synucle-Nuclein construct. The Synucle-Nuclein construct is a dimer where an α -synuclein moiety lacking N-terminal region (Synucle) is connected to another moiety of α -synuclein lacking C-terminal region (Nuclein). In this construct the two NAC (Non Amyloid-beta Component) regions that drive the formation of β -sheet like structure in the fibrils are tethered together, contrary to the cases of the other three dimers. I found that only the **NC**-terminal dimer aggregates into mature fibrils like α -synuclein does, whereas both **NN**- and **CC**-terminal dimers form amorphous aggregates. Also the Synucle-Nuclein construct aggregates into mature fibrils, but they are shorter in length than those of α -synuclein. This is a strong indication that in α -synuclein fibrils the monomer moieties are packed in a head to tail fashion, and that the NAC β -sheet packing is the core of the fibrils.

To answer the second question, I studied the *in vitro* aggregation of α -synuclein and α -synuclein dimers in the presence of different molar concentration of 14-3-3 η . Imaging with AFM, I found that 14-3-3 η affects the aggregation pathway of α -synuclein by modifying the shape of the growing oligomers and protofibrils. NMR and SPR revealed that 14-3-3 η does not interact with α -synuclein monomer. AFM showed that 14-3-3 η does not interact also with α -synuclein mature fibrils. In order to prove that 14-3-3 η targets the oligomeric species, I labeled both α -synuclein and 14-3-3 η with a fluorophore, and by FS I could demonstrate that 14-3-3 η intercalates into the growing oligomers both in the case of α -synuclein and in the case of **NC**-terminal dimers. This result

was confirmed by the data obtained on trying to answer the third question, when I studied α -synuclein aggregation in the presence of both 14-3-3 η and fragments of α -synuclein mature fibrils. These fragments were prepared by ultrasonication of α -synuclein mature fibrils. By exposing their “living ends”, they can favor and “seed” the aggregation of monomeric α -synuclein. Imaging with AFM, I found that 14-3-3 η slows down the addition of monomeric α -synuclein to the exposed living ends of those seeds. These AFM data on the growth of α -synuclein seeds in the presence of 14-3-3 η and those obtained by FS on the inclusion of 14-3-3 η into the growing oligomers and fibrils of α -synuclein demonstrate that the 14-3-3 η can inhibit the α -synuclein aggregation by an intercalation mechanism. This capability might explain the co-localization of 14-3-3 η and α -synuclein in Lewy bodies.

Key words: α -Synuclein, A β -protein, 14-3-3 η , Neurodegenerative disease, Protein aggregation, AFM etc.

Acknowledgements

Firstly, I would like express my deepest gratefulness to my principle supervisor, **Prof. Bruno Samori** for providing me an exciting research project and research environment. He has been a great mentor and I am deeply grateful for all the encouragement, guidance, support and love he has provided over the last three years. I would like to express my great gratitude to my co-supervisor **Dr. Marco Brucale** for providing me a stimulating and enjoyable environment to work in and great support throughout my Ph.D. I would like to give thank to my PhD coordinator **Prof. Vicenza Scarlato** for coordinating PhD program, and available always for the project discussion and for help. Thanks are also given to all other colleagues and friends (**Prof. Giampaolo, Daniele, Alixendera, Rosita, Massimo, Aldo, Danial, Manuele, Simone, Silvia, Francesca, Federica, Andrea and others**) at Samori lab (Nanobioscience lab) for their support, discussion and encouragements.

I am also thankful to the **Ministry of external affairs (MHRD) India and Italy** for providing me partially financial support during my PhD and **Institute of advanced studies** (Brain's in competition program), Bologna, Italy for providing me free accommodation throughout my Ph.D.

I would like to thank our project collaborators (**Prof. Luigi Bubacco, laura, Isabella, Nicoletta and Marco**) at the Molecular Biology lab, University of Padova for providing me protein samples (α -Synuclein and 14-3-3 protein) for the single molecule and aggregation experiments and **Prof. Hilal lashuel** at laboratory of molecular and chemical biology of neurodegeneration, EPFL, Lausanne for providing me amyloid beta protein.

I would like to thank my friends (**Saurabh, Deepak, Prashant, S.M. Velu, Rashmi, Priyank Shukla, and Shalini Tiwari**) who always encouraged me and boost me to work hard.

I would like to thank **Prof. Dwijendra K. Gupta** for his great support and encouragement throughout my Ph.D.

I would like to thank **Prof. Paolo Neyroz** at department of Pharmacy, University of Bologna for providing me Fluorescence polarization spectroscope and **Dr. Marzia Govoni** at department of virology, University of Bologna for providing me Ultrasonic Sonicator.

Finally, I express my warmest gratefulness and love to my parents, my younger brother (Dhanesh), my sweet heart wife and my lovely little master (Karamveer) to whom I am deeply indebted for their constant words of encouragement, love, moral support and happiness.

Declaration

I, **Dhruv Kumar** confirm that the research work presented in this thesis is my own. Where information has been derived from other sources, I confirm that this has been indicated in the thesis.

(Dhruv Kumar)

List of abbreviation

AD:	Alzheimer's disease
AFM:	Atomic force microscope
ALS:	Amyotrophic lateral sclerosis
APP:	Amyloid precursor protein
Aβ:	Amyloid-beta
CD:	Circular dichroism
CM-AFM:	Contact mode atomic force microscopy
CNS:	Central nervous system
DLB:	Dementia with lewy bodies
DTT:	Dithiothreitol
FP:	Fluorescence polarization
GAGs:	Glycosaminoglycans
HD:	Huntington disease
HPLC:	High performance liquid chromatography
HTT:	Huntingtin
LBD:	Lewy body disease
LBS:	Lewy-bodies
LN:	Lewy neurites
MSA:	Multiple system atrophy
NAC:	Non amyloid component
NCM-AFM:	Non-contact mode atomic force microscopy
NMR:	Nuclear magnetic resonance
PBS:	Phosphate buffered saline
PD:	Parkinson's disease
PMDs:	Protein misfolded diseases
PrPSc:	Prion protein
PS1:	Presenilin 1
PSP:	Progressive supranuclear palsy
SDS-PAGE:	Sodium dodecyl sulfate polyacrylamide gel electrophoresis
SEM:	Scanning electron microscope
SN:	Substantia nigra
SOD:	Superoxide dismutase

SOD1: Superoxide dismutase-1
STM: Scanning tunneling microscope
SUVs: Small unilamellar vesicles
TEM: Transmission electron microscope
TM-AFM: Tapping mode atomic force microscopy
WT: Wild type

List of figures

Figure 1.1: Model for protein misfolding and fibrillization.....	6
Figure 1.2: Working principle of tapping mode atomic force microscopy.....	9
Figure 1.3: Non-contact mode atomic force microscope.....	12
Figure 1.4: A typical AFM force curve.....	17
Figure 1.5: Scheme showing polarization of plane polarized light by fluorescent molecule in fluorescent polarization experiment.....	20
Figure 1.6: The human synuclein family.....	23
Figure 1.7: Schematic representation of primary structure of α -synuclein.....	25
Figure 1.8: Putative pathological mechanisms of α -synuclein.....	29
Figure 1.9: Comparison of NAC with A β , PrP, and IAPP sequences.....	31
Figure 1.10: Model of disease pathway in Parkinson's disease.....	35
Figure 1.11: The α -synuclein pathology of Parkinson's disease.....	36
Figure 1.12: Summary schematic of α -synuclein toxicity in a dopaminergic neuron.....	37
Figure 1.13: Alignment of α -synuclein and the 14-3-3 family of proteins.....	39
Figure 1.14: A β production.....	42
Figure 1.15: Crystal structure of 14-3-3 η dimer.....	44
Figure 1.16: Crystal structural model of 14-3-3 ζ	46
Figure 1.17: Multiple sequence alignment of α -synuclein and 14-3-3 η showing alignment score 47...52	52
Figure 1.18: Multiple sequence alignment of 14-3-3 γ and 14-3-3 η	53
Figure 2.1: AFM image analysis of early-formed α -synuclein oligomers.....	55
Figure 2.2: AFM image analysis of belatedly-formed α -synuclein oligomers.....	56
Figure 2.3: AFM image analysis of non-spherical α -synuclein oligomers.....	57
Figure 2.4: AFM image analysis of α -synuclein protofilaments.....	58
Figure 2.5: AFM image analysis of α -synuclein protofibrils.....	59
Figure 2.6: AFM image analysis of α -synuclein mature fibrils.....	60
Figure 2.7: Model of the hierarchical structure and the roles of the terminal regions in the assembly of α -synuclein fibril.....	61
Figure 2.8: AFM image analysis of α -synuclein mature fibrils induced by seeds.....	63
Figure 2.9: AFM image analysis of NN-terminal dimer.....	64
Figure 2.10: AFM image analysis of CC-terminal dimer.....	66
Figure 2.11: AFM image analysis of NC-terminal dimer.....	67
Figure 2.12: AFM image analysis of Synucle-Nuclein construct.....	69

Figure 2.13: AFM image analysis of A β mature fibrils.....	71
Figure 2.14: NMR analysis of interaction between α -synuclein and 14-3-3 η	72
Figure 2.15: SPR analysis of interaction between α -synuclein and 14-3-3 η	73
Figure 2.16: AFM image analysis of α -synuclein mature fibrils obtained in the presence and absence of 14-3-3 η	74
Figure 2.17: AFM image of curved object obtained during α -synuclein aggregation in the presence 14-3-3 η by following different stoichiometric ratio.....	75
Figure 2.18: Height and curvature distribution of curved object following different stoichiometric ratio of 14-3-3 η and α -synuclein (1:1, 1:4, 1:7, 1:12, 1:20, 1:24, 1:30 1: ∞).....	76
Figure 2.19: AFM image of immunogold labeled curved object α -synuclein with 14-3-3 η in the presence of 14-3-3 η specific antibody.....	78
Figure 2.20: TEM image analysis of immunogold labeled curved objects in the presence of 14-3-3 η specific antibody.....	79
Figure 2.21: Fluorescence emission spectra of α -synuclein aggregates.....	79
Figure 2.22: Fluorescence spectra of curved object binding with ThT.....	80
Figure 2.23: AFM image of seeded growth of α -synuclein aggregation suppressed by 14-3-3 η	81
Figure 2.24: AFM image of curved object obtained during the NC-terminal dimer aggregation in the presence 14-3-3 η	82
Figure 2.25: AFM image of curved object obtained during the amyloid-beta aggregation in the presence 14-3-3 η	83
Figure 2.26: AFM image of α -synuclein aggregation unaffected by 14-3-3 γ dimer.....	83
Figure 2.27: AFM image of seeded growth of α -synuclein aggregation unaffected by 14-3-3 γ	84
Figure 3.1: General scheme of WSXM showing the most representative process.....	88

List of tables

<i>Table 1.1: Common neurodegenerative diseases characterized by deposition of aggregated proteins.....</i>	5-6
<i>Table 1.2: Physical methods used in the literature to analyze protein aggregation.....</i>	8
<i>Table 1.3: Milestones in 14-3-3 research.....</i>	48-49

Publication arising from the thesis

1. **Chaperone like protein 14-3-3 η interacts with human α -synuclein aggregation intermediates rerouting the intracellular amyloidogenic pathway** – Manuscript Under preparation.
2. **Structure and aggregation of α -Synuclein covalent tandem dimers** – Manuscript Under preparation.

Contents table

<i>Abstract</i>	(I-II)
<i>Acknowledgements</i>	(III)
<i>Declaration</i>	(IV)
<i>List of abbreviation</i>	(V-VI)
<i>List of figures</i>	(VII-VIII)
<i>List of tables</i>	(IX)
<i>Publication arising from the thesis</i>	(X)

Chapter-1 (Introduction)

[1.1] Protein misfolding in neurodegenerative disease.....	2-7
[1.1.1] Role of misfolded proteins in neurodegenerative disease.....	2-3
[1.1.2] Mechanisms of protein misfolding.....	3-4
[1.1.3] Protein misfolding in the presence of seeds.....	4-4
[1.1.4] Protein aggregation in neurodegenerative disease.....	5-5
[1.1.5] General mechanisms of brain amyloid formation.....	6-7
[1.2] Biophysical techniques.....	7-22
[1.2.1] Atomic force microscope.....	9-19
[1.2.1.1] Atomic force microscopy	10-10
[1.2.1.2] Mode of operation.....	10-13
[1.2.1.3] AFM as an imaging device.....	13-14
[1.2.1.4] Imaging conditions.....	14-15
[1.2.1.5] Choice of probe and substrate.....	15-15
[1.2.1.6] Force spectroscopy.....	16-16
[1.2.1.7] Anatomy of a force curve.....	16-17
[1.2.1.8] AFM calibration.....	17-18
[1.2.1.9] AFM vs other imaging technique.....	18-18
[1.2.2] Fluorescence polarization.....	18-22
[1.3] α -Synuclein.....	22-40
[1.3.1] Historical overview.....	22-22
[1.3.2] Synuclein family.....	22-24
[1.3.3] Structural and conformational aspects of α -Synuclein.....	24-28

[1.3.3.1] α -Synuclein as an intrinsically disordered protein.....	25-25
[1.3.3.2] Conformational equilibria in α -synuclein.....	25-28
[1.3.4] α -Synuclein aggregation.....	28-33
[1.3.4.1] Role of partial folded structure in aggregation or fibril formation.....	28-28
[1.3.4.2] Mechanism of α -synuclein aggregation.....	28-30
[1.3.4.3] Aggregation of α -synuclein fragments.....	30-31
[1.3.4.4] α -Synuclein mutants.....	31-31
[1.3.4.5] Seeded growth of α -synuclein.....	32-32
[1.3.4.6] Factors affecting α -synuclein aggregation.....	32-32
[1.3.4.7] Proteins inhibiting α -synuclein aggregation.....	33-33
[1.3.5] α -Synuclein and neurodegenerative disease.....	33-38
[1.3.5.1] α -Synuclein and parkinson's disease.....	35-36
[1.3.5.2] α -Synuclein toxicity.....	36-38
[1.3.6] α -Synuclein interacting molecules.....	38-40
[1.3.6.1] α -Synuclein shares physical and functional homology with 14-3-3 proteins.....	39-40
[1.4] Amyloid-beta ($A\beta$).....	40-42
[1.4.1] Amyloid-beta in neurodegenerative disease.....	41-42
[1.5] 14-3-3 Proteins.....	42-53
[1.5.1] General properties.....	43-43
[1.5.2] Structural basis.....	43-47
[1.5.2.1] 14-3-3 monomer contains a conserved amphipathic groove.....	43-45
[1.5.2.2] 14-3-3 dimer can simultaneously bind two ligands.....	46-47
[1.5.3] Disease associated with 14-3-3 proteins.....	47-49
[1.5.4] Co-localization of 14-3-3 protein in Lewy- bodies.....	50-51
[1.5.5] Sequence similarity between 14-3-3 η and α -synuclein.....	52-52
[1.5.6] Sequence similarity between 14-3-3 η and 14-3-3 γ	53-53

Chapter-2 (Results and Discussion)

Morphological Analysis of Proteins

[2.1] α -Synuclein.....	55-62
[2.1.1] Monomer.....	55-55

[2.1.2] Oligomers.....	55-57
[2.1.3] Morphologically distinct oligomers.....	57-58
[2.1.4] Protofilaments.....	58-58
[2.1.5] Protofibrils.....	58-59
[2.1.6] Mature fibrils.....	59-62
[2.2] Seeded growth of α -synuclein.....	62-64
[2.3] α -Synuclein dimers and constructs.....	64-70
[2.3.1] NN-terminal dimer.....	64-65
[2.3.2] CC-terminal dimer.....	65-67
[2.3.3] NC-terminal dimer.....	67-68
[2.3.4] Synucle-Nuclein constructs.....	68-70
[2.4] Amyloid-beta ($A\beta$) aggregation.....	70-71
[2.5] Effect of 14-3-3 η on α -synuclein aggregation.....	71-83
[2.5.1] Interaction between 14-3-3 η and α -synuclein monomer.....	71-73
[2.5.2] Effect of 14-3-3 η on α -synuclein mature fibrils.....	73-74
[2.5.3] Effect of 14-3-3 η on α -synuclein oligomers.....	74-81
[2.5.4] Effect of 14-3-3 η on seeded growth of α -synuclein aggregation.....	81-81
[2.5.5] Effect of 14-3-3 η on NC-terminal dimer.....	82-82
[2.5.6] Effect of 14-3-3 η on $A\beta$ aggregation.....	82-83
[2.6] Effect of 14-3-3 γ on α -synuclein aggregation.....	83-84
[2.6.1] Effect of 14-3-3 γ on α -synuclein aggregation.....	83-84
[2.6.2] Effect of 14-3-3 γ on seeded growth of α -synuclein aggregation.....	84-84

Chapter-3 (Materials and Methods)

[3.1] Cloning, expression and purification.....	86-86
[3.2] Atomic force microscopy	86-89
[3.2.1] Protein aggregation.....	86-86
[3.2.2] Sample preparation.....	86-86
[3.2.3] AFM imaging.....	86-87
[3.2.4] AFM image analysis.....	87-89
[3.2.5] Fibril formation and preparation for ultrasonication experiment.....	89-89

Chapter-4 (Conclusions)

[4.1] Conclusions91-92

Bibliography.....93-107

Curriculum Vitae.....108-111

Chapter-1

(Introduction)

Neurodegenerative disease is a group of brain related disorder. They involve in the damage and death of neuronal cells in nervous system associated with the protein misfolding and aggregation, which affect the normal function of human brain. In general, neuronal cell death and damage originates by the aggregation of misfolded proteins into the beta sheet like structure in the nervous system. There are several factors that influence the aggregation and accumulation of misfolded proteins into the beta sheet like structure, whereas the exact relation between protein aggregation and cell death is still not very well understood.

[1.1] Protein misfolding in neurodegenerative disease

Most of the neurodegenerative diseases are associated with the misfolding of intrinsically unstructured proteins into β -sheet like structures. The intrinsically unstructured proteins acquire different conformations when they aggregate to form β -sheet like structure [Sandal et al., 2008]. These conformations are stabilized by the intermolecular interactions, leading to the formation of oligomers, proto-fibrils and fibrils, and finally mature fibrils accumulate as amyloid deposits in affected tissues [Soto et al., 2003; Soto et al., 2008]. Aggregates of amyloid-beta ($A\beta$) in alzheimer's disease (AD) and prion protein (PrPSc) in prion diseases accumulate extracellularly, and other misfolded aggregates accumulate intracellularly, such as α -synuclein in parkinson's disease (PD), superoxide dismutase (SOD) in amyotrophic lateral sclerosis (ALS), tau in tauopathies or AD, and huntingtin (HTT) in huntington disease (HD) [Soto, 2003].

[1.1.1] Role of misfolded proteins in neurodegenerative disease

Over the past two decades misfolded proteins have been widely considered to be the triggering factors in the neurodegenerative disease (e.g. PD, AD, HD, Prion Disease etc.). Perhaps the most convincing pieces of evidence in favor of this observation came from genetic studies. Most of the neurodegenerative diseases mainly arise sporadically, without detectable genetic origins; however, a portion (usually small) of the cases can be inherited (e.g. A30P, E46K, A53T mutations in α -synuclein). Interestingly, mutations in the genes encoding the protein component of the misfolded aggregates have been shown to be genetically associated with inherited forms of the disease [Selkoe et al., 1996; Buxbaum et al., 2000; Hardy, 2001; Soto, 2001]. The familial forms usually have an earlier onset and higher severity than sporadic cases. Mutations in the respective misfolded proteins have been associated with familial forms of many diseases, including PD, AD, HD, ALS and various rarer amyloid-related diseases such as cerebral haemorrhage with amyloidosis of the dutch and icelandic type, and cerebral amyloidosis of the British and Danish type [Selkoe et al., 1996;

Buxbaum et al., 2000; Hardy,2001; Soto, 2001]. The fact that mutations in the genes encoding the misfolded proteins produce inheritable disease is by itself a very strong argument for a crucial role of protein misfolding in the disease.

Other evidence for the important role of protein misfolding came from the studies aiming to generate transgenic animal models for protein misfolded diseases (PMDs). Insertion of human genes encoding mutant proteins with a high propensity to misfold and aggregate leads to the emergence of several pathological hallmarks of the different diseases. Human α -synuclein gene expression in transgenic mice induces some of the hallmarks of PD, as dopaminergic cell loss, Lewy-body accumulation and motor dysfunction [Meredith et al., 2008]. In case of prion protein, mice generate spontaneous neurodegeneration accompanied by brain vacuolization as happens in natural transmissible spongiform encephalopathy (TSEs) [DeArmond et al., 1995]. In the case of AD, the most common transgenic models over-express the amyloid precursor protein (APP) and/or the presenilin 1 (PS1), both genes associated to familial forms of AD [Selkoe 1996]. Transgenic mice expressing human mutated APP show amyloid plaques, cognitive impairment, cell death and related inflammatory processes [Duyckaerts et al., 2008]. All these findings suggest that misfolding and aggregation of amyloid proteins play an essential role in the pathology and could be the main cause of Neurodegenerative disease.

[1.1.2] Mechanisms of protein misfolding

Protein misfolding arises from the imperfect folding process that results in the formation of the proteins with different conformations from its native state [Sandal et al., 2008]. Protein misfolding can go on by several reasons [Soto, 2001; Kelly, 1996]. (i) Somatic mutations in the gene sequence leading to the production of a protein unable to adopt the native folding. (ii) Errors on the processes of transcription or translation leading to the production of modified proteins unable to properly fold. (iii) Failure of the folding and chaperone machinery. (iv) Mistakes on the post-translational modifications or trafficking of proteins. (v) Structural modification produced by environmental changes. (vi) Induction of protein misfolding by seeding and cross-seeding mechanisms.

The most common destiny for misfolded proteins is self-aggregation, because the mistaken exposure of fragments to the solvent that are normally buried inside the protein, lead to a high degree of stickiness. The β -sheet structural motif offers the most favorable organization for these intermolecular aggregates and can accommodate an almost unlimited number of polypeptide chains [Kelly, 1996; Nelson et al., 2005]. As a result, misfolded proteins exist as a large and

heterogeneous range of polymeric sizes, which are usually classified in very well defined categories, such as oligomers, protofibrils and fibrils [Caughey et al., 2003; Glabe, 2006; Walsh et al., 2007]. Soluble oligomers are small assemblies of misfolded proteins that are present in the buffer soluble fraction of tissue extracts and usually include structures ranging in size from dimers to 24-mers [Glabe, 2006; Walsh et al., 2007]. Recent undeniable facts coming from several autonomous studies of different proteins indicates that oligomers might be the most toxic species in the misfolding and aggregation pathway [Caughey et al., 2003; Glabe, 2006; Walsh et al., 2007]. Protofibrils are larger aggregates that can be seen by using electron microscopy and atomic force microscopy as curvilinear structures of 4–11 nm diameter and <200 nm long [Caughey et al., 2003; Walsh et al., 1999]. Protofibrils increase in size with increased time and protein concentration, and are lengthened by growth on their ends [Harper et al., 1999]. Annular protofibrils are pore-like assemblies that accumulate in the cell membrane and may contribute to cell death [Srinivasan et al., 2004; Lashuel et al., 2002]. Protofibrils and annular protofibrils have also been shown to be highly toxic in various *in vitro* studies [Lashuel et al., 2002; Hartley et al., 1999]. Amyloid fibrils are long, straight and unbranched structures of around 10 nm diameter and usually several micrometers lengths [Nelson et al., 2005]. They bind the dyes Congo red and thioflavin and show a typical “cross- β ” X-ray diffraction pattern consisting of two major reflections at 4.7 Å and 10 Å found on orthogonal axes [Nelson et al., 2005]. Fibrils can also elicit toxicity in cultured cells, but usually at much higher concentrations than oligomers and protofibrils [Caughey et al., 2003].

[1.1.3] Protein misfolding in the presence of seeds

The mechanism of protein misfolding and aggregation in the presence of seeds (fragmented mature fibrils) is called as “seeding-nucleation” model [Soto et al., 2006; Jarrett et al., 1993]. In this process, the early steps of misfolding are thermodynamically unfavorable and progress gradually, until the minimum stable oligomeric unit is formed, then grows exponentially at a fast speed. There are two kinetic phases in the seeding-nucleation model of polymerization. Firstly, during the lag phase, a low amount of misfolded and oligomeric structures are produced in a slow process, generating seeds for the next step. Once nuclei are formed, the elongation phase takes place and results in fast growing of the polymers. The addition of pre-formed seeds can reduce the length of the lag phase, accelerating the exponential phase. Fragmented fibrils are considered as the best seeds to propagate the misfolding process in an exponential manner.

[1.1.4] Protein aggregation in neurodegenerative disease

Protein aggregation is the principle phenomena of amyloid like proteins in neurodegenerative diseases such as PD, AD and Prion disease. The rate of morbidity and mortality is higher in the developed world [Hebert et al., 2001; Hebert et al., 2003]. Largely as a result of increased life expectancy and changing population demographics, neurodegenerative dementias and neurodegenerative movement disorders are becoming more common [Brookmeyer et al., 1998; Samii et al., 2004]. Converging lines of investigation have revealed a potential single common pathogenic mechanism underlying many diverse neurodegenerative disorders (i.e., the aggregation and deposition of misfolded proteins). As summarized in **Table 1.1**, nearly every major neurodegenerative disease is characterized pathologically by the insidious accumulation of insoluble filamentous aggregates of normally soluble proteins in the central nervous system (CNS). Because these filamentous aggregates display the ultrastructural and tinctorial properties of amyloid (i.e., 10 nm wide fibrils with crossed β -sheet structures), these diseases can be grouped together as brain amyloidoses.

From a pathological point of view, neurodegenerative entities are defined by the type and pattern of amyloid deposition in the brain. Unfortunately, the type and pattern of brain amyloidosis does not always correlate well with the observed clinical phenotype. This disconnect has led to a confusing nosology that sometimes requires clinicians to describe phenotypes on the basis of the presumed presence of pathological lesions (e.g., dementia with Lewy bodies) and sometimes requires pathologists to describe lesions using clinical language regardless of the patient's actual clinical presentation (e.g., progressive supranuclear palsy, PSP). The best way to circumvent this chaos may be the use of chemical analytes of biological fluids and neuroimaging biomarkers that allow clinicians to distinguish between these related brain amyloidoses on the basis of the nature and extent of the brain pathology as well as the specific amyloidogenic protein(s) involved in disease pathogenesis.

Recognizing that all these related neurodegenerative diseases share common mechanisms involving CNS accumulation of misfolded proteins suggests that these disorders may have similar targets for the development of diagnostic and therapeutic agents.

Table 1.1: Common neurodegenerative diseases characterized by deposition of aggregated proteins

Neurodegenerative Disease	Related Proteins
Alzheimer's disease	Amyloid- β ($A\beta$), α -Synuclein, Tau
Amyotrophic lateral sclerosis	Superoxide dismutase-1 (SOD1)

Cortical basal degeneration/Progressive supranuclear palsy	Tau
Dementia with Lewy Bodies	α -Synuclein
Huntington disease	Huntingtin (containing polyglutamine repeat expansion)
Multiple system Atrophy	α -Synuclein
Parkinson's disease	α -Synuclein
Pick's disease	Tau
Prion diseases	Protease-resistant prion protein (PrP)
Spinocerebellar ataxia	Ataxin (containing polyglutamine repeat expansion)

[1.1.5] General mechanisms of brain amyloid formation

Brain amyloidosis begins with the production of a soluble native protein that is misfolded to yield the precursor for fibril formation (**Figure 1.1**). The misfolded protein can self-aggregate to form oligomers, protofibrils, or other intermediates that promotes fibril formation [Caughey et al., 2003]. Oligomers of A β can be detected *in vitro* [Huang et al., 2000], in cell culture and transgenic mouse models of Alzheimer's disease [Walsh et al., 2000; Podlisny et al., 1998; Takahashi et al., 2004], and in postmortem Alzheimer's disease brain specimens [Kay et al., 2003].

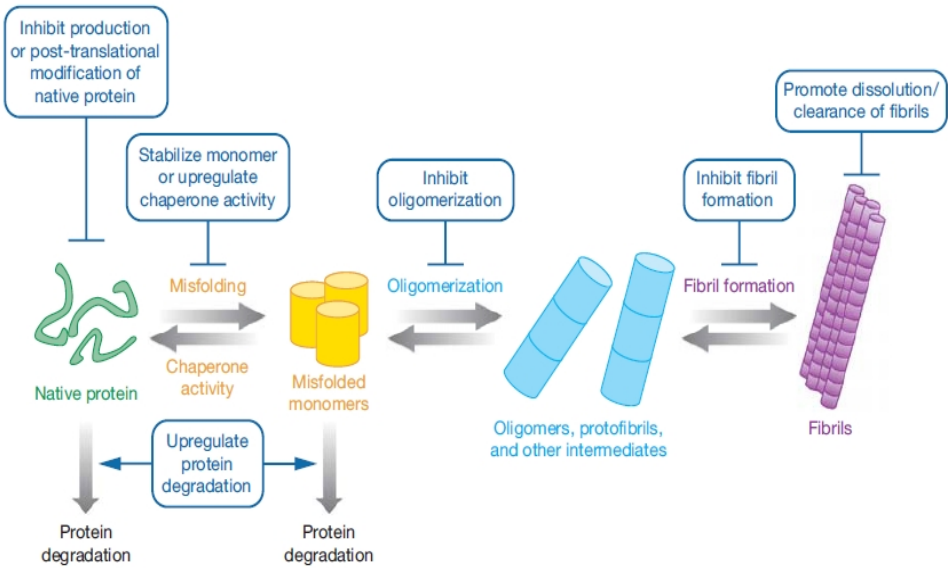


Figure 1.1: Model for protein misfolding and fibrillization. Soluble native protein is misfolded and associates in the form of oligomers and other intermediates that eventually give rise to fibrils. Potential opportunities for therapeutic intervention are shown in blue boxes. [Reproduced from Skovronsky et al. 2006]

Although, oligomers of α -synuclein have been studied very well, it is obvious that other amyloidogenic proteins such as A β or polyglutamine-containing proteins can also form oligomers. Remarkably, oligomers composed of each of these amyloidogenic proteins (which share no primary sequence homology) show a similar conformation-dependent structure [Kayed et al., 2003]. These studies may suggest a common mechanism of amyloid formation that depends upon structural determinants within the oligomers. Further support of this hypothesis, the observation comes from the different forms of amyloid that interact with each other *in vitro*. For example, α -synuclein can initiate fibrillization of tau, and co-incubation of tau and α -synuclein synergistically promotes fibrillization of both proteins [Giasson et al., 2003].

There are various factors that influence the balance between native protein, misfolded protein, oligomers, and fibrils both *in vivo* and *in vitro*. For example, in the disease state, overproduction of the amyloidogenic protein constituent, wrong covalent bond modification, failed degradation, or insufficient molecular chaperone activity may all contribute in shifting the balance towards misfolded protein and oligomer formation. Each of these steps represents a potential target for therapeutic intervention, with therapies being developed currently for different forms of amyloid.

[1.2] Biophysical techniques

There are several techniques that can be used for the study of protein aggregation and its characterization. Each techniques have their own advantages and disadvantages. These techniques are summarized in **Table 1.2** and in detail [see review in Morris et al., 2009]. Methods indicated in **Table 1.2** is if the physical methods listed there are used as direct or indirect¹ methods for the systems at hand, and if they can be used in-situ or involve ex-situ use and sample preparation. In protein aggregation, as with all science, the use of multiple, complimentary, ideally direct, in-situ physical methods are of course preferred.

In this thesis we have used the Atomic Force Microscope (AFM) and Fluorescence polarization (FP) to study the aggregation of α -synuclein. Apart from the AFM and FP we have also used ultrasonic sonicator to prepare seeds from the mature fibrils of α -synuclein.

Table 1.2: Physical methods used in the literature to analyze protein aggregation (In detail See review in Morris et al., 2009)

S.No	Method	Direct/ Indirect ¹	In-situ/Ex- situ	Measure Kinetics?	Selected References
1.	Atomic force microscopy	Direct	In-situ	Yes	Harper et al., 1997
2.	Calorimetry	Direct	In-situ	Yes	Bondos et al., 2006
3.	Circular dichroism	Direct	Concentration Dependent ^a	Yes	Woody et al., 1996
4.	Dyes	Indirect	Concentration Dependent ^a	Yes	Munishkina et al., 2007
5.	Electron microscopy	Direct	Ex-situ	No	Bondos et al., 2006
6.	Electron paramagnetic resonance spectroscopy	Indirect	Concentration Dependent ^a	Yes	Lundberg et al., 1997
7.	Flow birefringence	Direct	In-situ	Yes	Kasai et al., 1972
8.	Fluorescence spectroscopy with an intrinsic fluorophore	Direct	Concentration Dependent ^a	Yes	Munishkina et al., 2007
9.	Fluorescence spectroscopy with an extrinsic fluorophore	Indirect	Concentration Dependent ^a	Yes	Munishkina et al., 2007
10.	Fourier transform infrared Spectroscopy	Direct	Concentration Dependent ^a	Yes	Bondos et al., 2006
11.	Light scattering	Direct	In-situ	Yes	Lomakin et al., 1997
12.	Mass spectrometry	Direct	Ex-situ	No	Lashuel et al., 2002
13.	Nuclear magnetic resonance Spectroscopy	Direct	Concentration Dependent ^a	Yes	Fernandez et al., 2004
14.	Quartz crystal oscillator Measurements	Direct	Concentration Dependent ^a	Yes	Knowles et al., 2007
15.	Turbidity	Direct	In-situ	Yes	Beme et al., 1974
16.	Viscosity	Direct	In-situ	Yes	Harding et al., 1997
17.	X-ray diffraction	Direct	Concentration Dependent ^a	No ^b	Sunde et al., 1997

¹We were unable to find a definition for direct vs. indirect physical methods in the literature. Therefore, we will use the term direct physical method to mean a method that measures a property that is directly affected by the aggregation process, while an indirect method measures a property that is only indirectly affected by the aggregation process

^aBy “concentration dependent” we mean this method can be in-situ if the aggregation conditions are within the detection limits of the physical method.

^bOr “yes” in principle if Synchrotron radiation is used.

[1.2.1] Atomic force microscope

Atomic force microscope (AFM) is a technique to explore the molecular behavior, molecular motions, fluctuations and growth of the molecule (both biological and non-biological) at nano-scale level. AFM is a member of the scanning probe microscopes family; it was developed by Gerd Binnig and Carl Quate in 1986 at IBM research laboratory Zurich and at Stanford, Ca respectively. AFM is derived from the scanning tunneling microscope (STM), where a sharp metal tip is scanned over a conducting surface detecting minute changes in sample topography through the strong distance dependence of the tunneling current. Atomic force microscopy relies on the tip-sample interaction forces for topography contrast. These forces are nonspecific and do not require conductive samples, a major limitation of STM in the study of biomaterials.

The working principle of AFM is that a small cantilever (typical length $\sim 100 \mu\text{m}$) with a sharp tip (1-10 nm end-of-curvature) scans a sample surface. As the tip encounters height differences or experiences changing tip-sample interaction forces, the cantilever bends (**Figure 1.2**). This deflection is detected and a feedback system moves the probe to keep the deflection at a set value. In tapping mode AFM, the cantilever is oscillated, and feedback is usually done on either the tapping amplitude or frequency signal. In this way, an AFM maps the nanometer to micrometer scale topography and surface properties of the sample in a less invasive way.

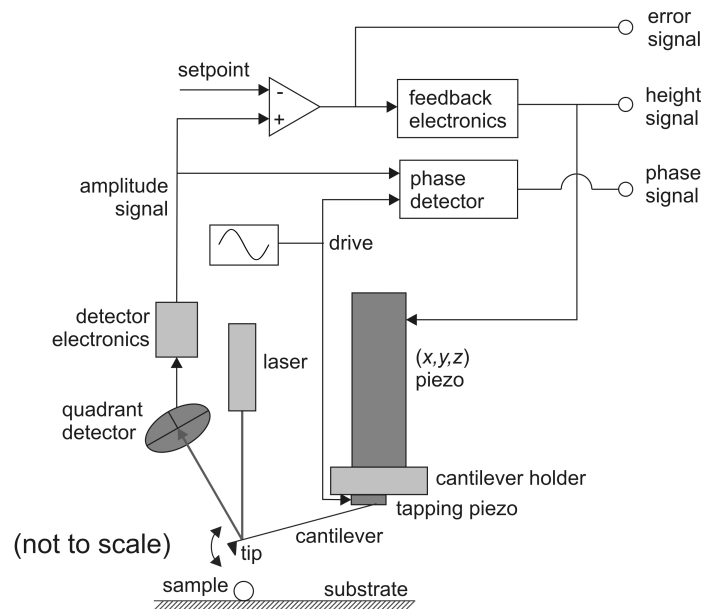


Figure 1.2: Working principle of tapping mode atomic force microscopy. This simplified schematic gives an overview of the main components of a beam deflection type AFM in amplitude-modulation tapping mode and explains the origins of the signals that will be referred to in the text. Comparing the amplitude signal with a pre-set setpoint value yields the error signal. The feedback electronics uses this signal to adjust the voltage to the z-piezo, changing the height of the cantilever relative to the surface. Meanwhile, the phase detector compares the

phase of the amplitude signal with that of the tapping drive signal to yield the phase signal. [Reproduced from Ph.D. thesis Rajji 2008]

There are several ways to setup an AFM, but the scheme shown in **Figure 1.2** is a commonly used one. There are several methods of cantilever deflection detection (optically: with quadrant detectors or interferometry, or mechanically using bimetals, to name a few), and there are several ways of controlling the motion of tip relative to sample (the piezo elements or other actuators can be in the piezo tube attached to the cantilever, or they can be in the sample stage), but the general working principle remains the same.

[1.2.1.1] Atomic force microscopy

The working principles of AFM are very simple. An atomically sharp tip is scanned over a surface with feedback mechanisms that enable the piezo-electric scanners to maintain the tip at a constant force (to obtain height information), or height (to obtain force information) above the sample surface. Tips are typically made up of Si₃N₄ or Si, and extended down from the end of a cantilever. The nanoscope AFM head employs an optical detection system in which the tip is attached to the underside of a reflective cantilever. A diode laser is focused onto the back of a reflective cantilever. As the tip scans the surface of the sample, moving up and down with the contour of the surface, the laser beam is deflected off the attached cantilever into a dual element photodiode. The photodetector measures the difference in light intensities between the upper and lower photodetectors, and then converts into voltage. Feedback from the photodiode difference signal, through software control from the computer, enables the tip to maintain either a constant force or constant height above the sample. In the constant force mode the piezo-electric transducer monitors real time height deviation. In the constant height mode the deflection force on the sample is recorded. The latter mode of operation requires calibration parameters of the scanning tip to be inserted in the sensitivity of the AFM head during force calibration of the microscope.

[1.2.1.2] Mode of operation

Contact mode

In contact mode atomic force microscopy (CM-AFM), the tip scans the sample in close contact with the surface, and the force between the tip and the surface kept constant during scanning by maintaining a constant deflection. This is the simplest mode used in the force microscope. The repulsive force on the tip is a mean value of 10^{-9} N. This force is set by pushing the cantilever against the sample surface with a piezoelectric positioning element. In contact mode AFM the

deflection of the cantilever is sensed and compared in a DC feedback amplifier to some desired value of deflection. The tip is effectively 'dragged along' the sample while the feedback loop keeps the interaction force constant by maintaining the deflection at a setpoint value. If the measured deflection is different from the desired value the feedback amplifier applies a voltage to the piezo to raise or lower the sample relative to the cantilever to restore the desired value of deflection. The voltage that the feedback amplifier applies to the piezo is a measure of the height of features on the sample surface. It is displayed as a function of the lateral position of the sample. This mode allows for very high lateral resolution on periodic samples with low corrugation, but is typically too damaging for protein aggregates.

Non-contact mode

In non-contact mode atomic force microscopy (NCM-AFM), the tip of the cantilever does not come in contact with the sample surface. This is an important development in imaging that introduced a system for implementing the non-contact mode which is used in situations where tip contact might alter the sample in delicate ways. In this mode the tip floats 5-15 nm above the sample surface (**Figure 1.3**). Attractive Van der Waals forces acting between the tip and the sample are detected, and topographic images are constructed by scanning the tip above the surface. The attractive forces from the sample are substantially weaker than the forces used by contact mode. Therefore the tip must be given a small oscillation so that AC detection methods can be used to detect the small forces between the tip and the sample by measuring the change in amplitude, phase, or frequency of the oscillating cantilever in response to force gradients from the sample. For highest resolution, it is necessary to measure force gradients from Van der Waals forces which may extend only a nanometer from the sample surface. Measuring the tip to sample distance at each (x, y) data point allows the scanning software to construct a topographic image of the sample surface.

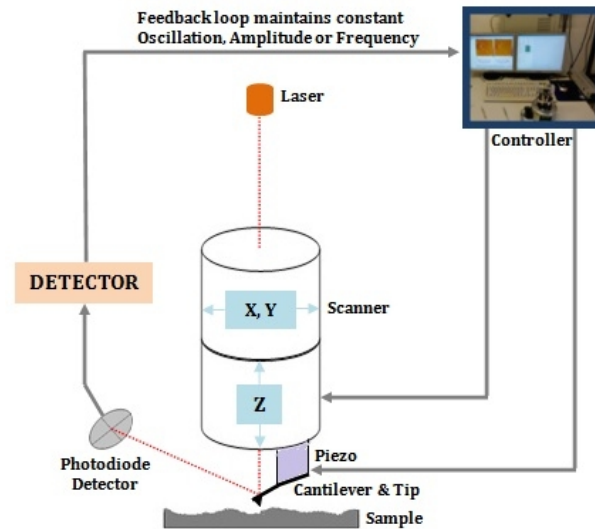


Figure 1.3: Non-contact mode atomic force microscope.

Figure 1.3 showing the scheme for dynamic mode of operation (both frequency and amplitude) in non contact mode. In frequency modulation, information about the tip sample interaction can be observed by monitoring the change in oscillation frequency. In amplitude modulation, feedback signal for the image can be observed by the monitoring change in the oscillation amplitude or phase.

Non contact mode is good for the scanning of soft material in both liquid and air surface, whereas contact mode results into the degradation and damage of material by penetrating the surface in liquid medium.

Tapping mode

In tapping mode atomic force microscopy (TM-AFM), the cantilever oscillates at or near its resonance frequency. Feedback can be performed on the measured tapping amplitude or frequency [Garcia and Perez, 2002; Higgins et al., 2005], giving rise to the terms amplitude modulated AFM and frequency modulated AFM respectively. The intermittent tip-sample contact reduces lateral forces being exerted on the sample. The resonance frequency f_{res} is typically in the 100 kHz range in air, and in the 30 kHz range in liquid, and tapping amplitudes range from several nm in liquid to 100's of nm in air. The minimum tapping amplitude that is necessary in air depends on the force needed to escape the thin water layer due to air humidity that is present on any surface exposed to air.

TM-AFM enables imaging of soft biological samples with minimal damage. This allows one to measure protein aggregate dimensions and material properties in a state as close as possible to the native state. In liquid, high frequency tapping may lead to apparent stiffening of soft biological samples, reducing tip induced damage even further on cells [Putman et al., 1994b].

TM-AFM mode is the most commonly used for imaging amyloid fibrils, and the amplitude of the tapping is one important factor that determines the extent of tip and sample wear. A second critical parameter is the setpoint ratio ($s = A_{set}/A_{free}$): the ratio of the tapping amplitude setpoint (to which the feedback loop regulates the measured amplitude, see **Figure 1.2**), to the tapping amplitude when the cantilever is suspended free in air or water.

Because both attractive and repulsive forces act on the cantilever, and because they depend on the tip-sample separation in a nonlinear way, two stable oscillation states coexist in amplitude modulated AFM [reviewed in Garcia and Perez, 2002]. The equation of motion for the cantilever has two solutions: a high and a low amplitude branch. This means that a given setpoint tapping amplitude can be achieved at two distinct tip-sample separations. If the driving amplitude is large enough, both branches will merge into one, and only one stable solution to the equation of motion will exist [Garcia and Perez, 2002]. For low driving amplitudes however, the AFM operator should be aware that branch hopping (and related height artifacts) may occur. It is useful to qualitatively define tapping regimes. If s is lower than 30 %, we consider the tapping 'hard', if $s > 70\%$, tapping is 'soft'. In tapping mode experiments on TTR105–115 fibrils in air, [Mesquida et al., 2007] found that fibrils were not damaged by setpoint ratios between 10-80 %. This indicates the range of setpoint ratios used in amyloid research: the appropriateness of 'hard' or 'soft' tapping depends on the sample and the probe utilized.

[1.2.1.3] AFM as an imaging device

The atomic force microscope (AFM) is a representative example of instruments known as scanning probe microscope. Scanning probe microscope works by monitoring the value of a physical variable that depends on the distance between the surface to image and a specific probe. The topography of the surface is then reconstructed in three-dimensional detail. The prototype scanning probe microscope was the scanning tunneling microscope (STM), in which the probe is a microscopic electrode and the physical variable is the current between the electrode and a conductive surface on which the sample is placed. The tunneling current, varying exponentially and very steeply with distance, is a sensible probe of surface topography. AFM instead works using

probe displacement as the variable, being similar conceptually to a miniature phonograph. The probe itself is a solid, sharp microscopic tip located at the end of a flexible cantilever.

The tip and the surface are put in contact or close proximity, and the cantilever deflection due to the tip sample interactions is the variable being monitored. The cantilever, normally, can be modeled as a simple Hookean spring and therefore its response is linear with applied force. In most cases, cantilever deflection is in turn probed and amplified by a laser beam that reflects on the cantilever very end, forming a so-called optical lever system. The laser beam reflected by the tip hits a photodiode, which records the displacement of the laser beam from a reference point. The system in this way achieves a resolution of the order of the nanometer.

A piezoelectric scanner is usually used to move the sample (or the tip) in three dimensions, allowing the tip to scan various portions of the sample. Piezoelectric scanners allow AFMs to reach 1 nm of lateral resolution. Atomic resolution has been reached vertically for hard materials in vacuum conditions. On the other hand, AFM can easily be applied to biological samples because it requires little or no sample preparation and works readily in physiological conditions (liquid buffer, room temperature etc.). Live eukaryotic cells can be extensively analyzed with the AFM [Mathur et al., 2001].

[1.2.1.4] Imaging conditions

AFM on biomaterials can be performed in air or in a liquid, such as an aqueous pH-buffering solution.

Imaging in air

The main advantages of imaging in air are, (i) that sample preparation is easier, sample no need to put in liquid, and (ii) the sample can be used for long time after preparation without degradation. A disadvantage of AFM in air compared to in liquid is that a tapping amplitude in the order of 100 nm is required (with associated high tapping force) to overcome the strong capillary force that is due to a thin water layer that tends to form on the substrate surface.

Imaging in liquid

One undeniable reason for imaging in liquid is that in liquid environment physiological conditions resembles much more close to the proteins and other biological systems. Also, in an aqueous environment it is possible to study biomolecular interactions.

In the case of amyloid fibrils, a disadvantage of imaging in liquid is their higher fragility in liquid than in air. Also, it is sometimes hard to bind the sample to the substrate (although that seems to be more of a problem for DNA than for protein aggregates). Another disadvantage is that the samples cannot be kept for the next use, since the evaporation of the water droplet leads to buffer salt deposition, while continued immersion in a large quantity of buffer would presumably lead to desorption of the aggregates. A major application for AFM imaging in buffer is that aggregations can be monitored in real-time through in situ imaging: when the buffer contains monomers of the protein of interest and the buffer conditions are right, surface templated aggregation may occur [Hoyer et al., 2004]. Also, the directionality of fibril growth becomes accessible [Blackley et al., 2000; Goldsbury et al., 1999; Zhu et al., 2002].

[1.2.1.5] Choice of probe and substrate

An AFM probe consists of a cantilever with a tip, and its properties are critical to the results of the imaging of biomolecular samples. The lateral resolution of AFM images depends on the sharpness of the tip that is used, and the cantilever stiffness and resonance frequency determine the force exerted on the sample, and any resulting damage.

The substrate used for imaging of amyloid fibrils is a relevant factor in in-situ aggregation studies: the fibrils may form a pattern based on the atomic structure of the substrate [Yang et al., 2002]. The properties of the surface on which the sample is deposited also influence the kinetics and morphology of amyloid fibril formation. In an in-situ TM-AFM study in liquid, the morphology of A β aggregates was different on hydrophilic mica than on hydrophobic graphite: on mica, particulate aggregates formed, whereas on graphite, linear assemblies similar to protofilaments formed [Kowalewski and Holtzman, 1999]. This dependence of fibril morphology on substrate hydrophobicity implies that fibril formation may be expedited on interfaces between aqueous solutions and lipid surfaces, as would occur at cellular membranes and lipoprotein particles in a living cell. A β 1–42 early aggregates deposit with a higher yield on hydrophilic mica than on hydrophobic graphite, and the opposite is true for mature fibrils [Arimon et al., 2005]. Finally, hydrophobic surface favor the formation of surface nanobubbles [Yang et al., 2007], which is undesirable when imaging proteins. For AFM imaging of protein fibrils, freshly cleaved mica appears to be the most convenient substrate.

[1.2.1.6] Force spectroscopy

In addition to these topographic measurements, the AFM can also provide much more information about the molecular motion behavior and fluctuation of the single molecule (both biological and non-biological) at nano-scale. The AFM can also record the amount of force felt by the cantilever as the probe tip is brought close to and even indented into a sample surface and then pulled away. This technique can be used to measure the long range attractive or repulsive forces between the probe tip and the sample surface, elucidating local chemical and mechanical properties like adhesion and elasticity, and even thickness of adsorbed molecular layers or bond rupture lengths.

Force curves (force-vs-distance curve) typically show the deflection of the free end of the AFM cantilever as the fixed end of the cantilever is brought vertically towards and then away from the sample surface. Experimentally, this is done by applying a triangle-wave voltage pattern to the electrodes for the z-axis scanner. This causes the scanner to expand and then contract in the vertical direction, generating relative motion between the cantilever and sample. The deflection of the free end of the cantilever is measured and plotted at many points as the z-axis scanner extends the cantilever towards the surface and then retracts it again. By controlling the amplitude and frequency of the triangle-wave voltage pattern, the researcher can vary the distance and speed that the AFM cantilever tip travels during the force measurement.

Similar measurements can be made with oscillating probe systems like Tapping Mode and non-contact AFM. This sort of work is just beginning for oscillating probe systems, but measurements of cantilever amplitude and/or phase versus separation can provide more information about the details of magnetic and electric fields over surfaces and also provide information about viscoelastic properties of sample surfaces.

[1.2.1.7] Anatomy of a force curve

A: In this region cantilever does not touch the surface, if the cantilever feels a long-range attractive (or repulsive) force it will deflect downwards (or upwards) before making contact with the surface.

B: As the probe tip is brought very close to the surface, it may jump into contact if it feels sufficient attractive force from the sample.

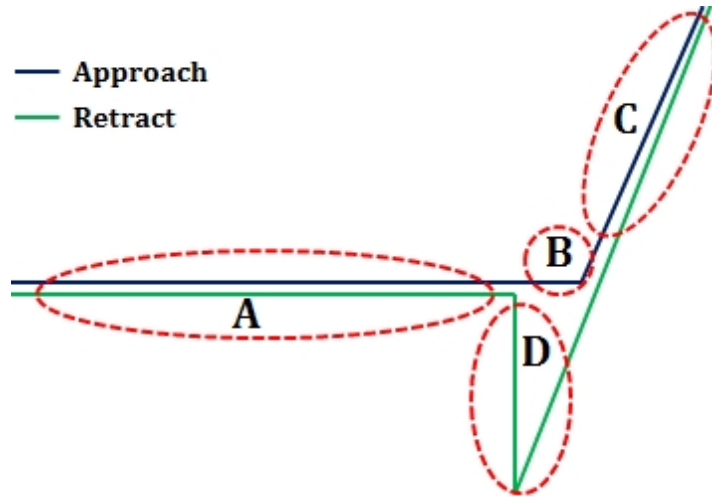


Figure 1.4: A typical AFM force curve.

C: Once the tip is in contact with the surface, cantilever deflection will increase as the fixed end of the cantilever is brought closer to the sample. If the cantilever is sufficiently stiff, the probe tip may indent into the surface at this point. In this case, the slope or shape of the contact part of the force curve can provide information about the elasticity of the sample surface.

D: After loading the cantilever to a desired force value, the process is reversed. As the cantilever is withdrawn, adhesion or bonds formed during contact with the surface may cause the cantilever to adhere to the sample some distance past the initial contact point on the approach curve (B).

A key measurement of the AFM force curve is the point at which the adhesion is broken and the cantilever comes free from the surface. This can be used to measure the rupture force required to break the bond or adhesion.

[1.2.1.8] AFM calibration

The cantilever elastic constant needs to be measured for each experiment: this is due to unavoidable inhomogeneities in the batches of commercial cantilevers. This is usually done day to day by the “thermal tune” method that is by measuring the thermal oscillation spectrum of the free cantilever (not in touch with any surface) and using the equipartition theorem to obtain the actual elastic constant. The cantilever is here treated as a simple oscillator and the Brownian motion of the main fundamental oscillation mode of the cantilever gives the elastic constant by the simple formula:

$$k = \frac{k_b T}{\langle x_c^2 \rangle} \quad (2.1)$$

where k_B the Boltzmann constant, T is is temperature and $\langle z_0^2 \rangle$ is the square mean cantilever deflection.

This latter variable is found by fitting the power spectrum of the cantilever thermal noise, with the advantage of avoiding interference from both non-thermal oscillation at other discrete frequencies and white noise.

In practice, it must be noticed that today more complex, empirical equations are used, to correct significant deviations from the ideal oscillator behaviour of the cantilever. The typical error is $\pm 20\%$ [Hutter et al., 1993; Florin et al., 1995]. The other essential parameter to be known is the optical lever sensitivity, i.e. the ratio between cantilever deflection and the photodiode output voltage difference. This depends from the optical properties of the cantilever, the medium (air or water), the eventually present fluid cell etc. and also needs to be measured for each cantilever. This is usually done by pressing the cantilever on a hard surface (i.e. glass or mica) at high forces: assuming that no substrate deformations happen, the cantilever deflection must be theoretically equal to the piezo movement and the ratio can be calculated. When this is done, the sample can be put in place under the tip. There are a number of free parameters that the experimenter must decide before starting the experiment (most of them can also be changed during operation): the speed, the length range, the maximum force acting on contact on the surface, the scan rate (number of points recorded per second) are usually the most important.

[1.2.1.9] AFM vs other imaging technique

AFM vs STM

It is an interesting to compare AFM and its precursor Scanning Tunneling Microscope. In some cases, the resolution of STM is better than AFM because of the exponential dependence of the tunneling current on distance. The force-distance dependence in AFM is much more complex when characteristics such as tip shape and contact force are considered. STM is generally applicable only to conducting samples while AFM is applied to both conductors and insulators. In terms of versatility, needless to say, the AFM wins. Furthermore, the AFM offers the advantage that the writing voltage and tip-to-substrate spacing can be controlled independently, whereas with STM the two parameters are integrally linked.

AFM vs SEM

Compared with Scanning Electron Microscope, AFM provides extraordinary topographic contrast direct height measurements and unobscured views of surface features (no coating is necessary).

AFM vs TEM

Compared with Transmission Electron Microscopes, three dimensional AFM images are obtained without expensive sample preparation and yield far more complete information than the two dimensional profiles available from cross-sectioned samples.

AFM vs Optical microscope

Compared with Optical Interferometric Microscope (optical profiles), the AFM provides unambiguous measurement of step heights, independent of reflectivity differences between materials.

[1.2.2] Fluorescence polarization

Fluorescence Polarization (FP) was first described by Perrin in 1926. When a small fluorescent molecule is excited with plane-polarized light, the emitted light is largely depolarized because molecules tumble rapidly in solution during their fluorescence lifetime (the time between excitation and emission). It is a powerful tool to study molecular interactions (protein-protein, protein-DNA and protein-ligands) by monitoring changes in the apparent size of fluorescently-labeled or inherently fluorescent molecules.

Principle behind fluorescence polarization

When a fluorescent molecule is excited with plane polarized light, light is emitted in the same polarized plane, provided that the molecule remains stationary throughout the excited state (which has duration of 4 nanoseconds for fluorescein). If the molecule rotates and tumbles out of this plane during the excited state, light is emitted in a different plane from the excitation light. If vertically polarized light is exciting the fluorophore, the intensity of the emitted light can be monitored in vertical and horizontal planes (degree of movement of emission intensity from vertical to horizontal plane is related to the mobility of the fluorescently labeled molecule (see **Figure 1.4**)). If a molecule is very large, little movement occurs during excitation and the emitted light remains highly polarized. If a molecule is small, rotation and tumbling is faster and the emitted light is depolarized relative to the excitation plane.

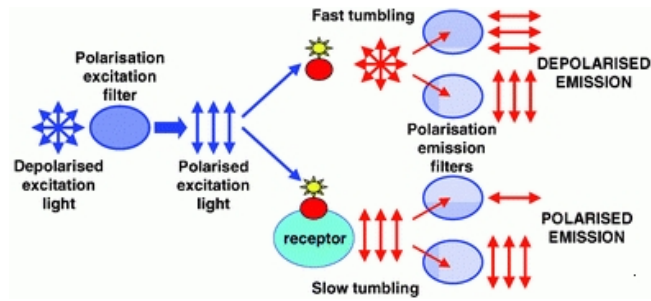


Figure 1.5: Scheme showing polarization of plane polarized light by fluorescent molecule in fluorescent polarization experiment.

Polarization is defined as a function of the observed parallel (I_{\parallel}) and perpendicular intensities (I_{\perp}):

$$P = \frac{I_{\parallel} - I_{\perp}}{I_{\parallel} + I_{\perp}} \quad (2.2)$$

If the emission is completely polarized in the parallel direction, i.e., the electric vector of the exciting light is totally maintained, then:

$$P = \frac{1-0}{1+0} = 1 \quad (2.3)$$

If the emitted light is totally polarized in the perpendicular direction then:

$$P = \frac{0-1}{0+1} = -1 \quad (2.4)$$

The limits of polarization are thus +1 to -1

Another term frequently used in the context of polarization is anisotropy (usually designated as either A or r) which is defined as:

$$r = \frac{I_{\parallel} - I_{\perp}}{I_{\parallel} + 2I_{\perp}} \quad (2.5)$$

By analogy to polarization, the limits of anisotropy are +1 to -0.5

We can write

$$r = \frac{2}{3} \left(\frac{1}{P} - \frac{1}{3} \right)^{-1} \quad (2.6)$$

Or

$$r = \frac{2P}{3-P} \quad (2.7)$$

For example

P	r
0.50	0.40
0.30	0.22
0.10	0.069

Clearly, the information content in the polarization function and the anisotropy function is identical and the use of one term or the other is dictated by practical consideration.

Small molecules rotate quickly during the excited state, and upon emission, have low polarization values. Large molecules, caused by binding of a second molecule, rotate little during the excited state, and therefore have high polarization values.

Dependence of fluorescence polarization on molecular mobility

Interpretation of the dependence of the fluorescence polarization on molecular mobility is usually based on a model derived in 1926 from the physical theory of Brownian motion by Perrin:

$$r = \left(\frac{1}{P} - \frac{1}{3} \right) = \left(\frac{1}{P_0} - \frac{1}{3} \right) \left(1 + \frac{\tau}{\Phi} \right) \quad (2.8)$$

Where P_0 is the fundamental polarization of the dye (for fluorescein, rhodamine and BODIPY dyes, P_0 is close to the theoretical maximum of 0.5), r is the excited-state lifetime of the dye and Φ is the rotational correlation time of the dye or dye conjugate. These relationships can be expressed in terms of fluorescence anisotropy in an equivalent and mathematically simpler manner. For a hydrodynamic sphere, Φ can be estimated as follows:

$$\Phi = \frac{\eta V}{RT} \quad (2.9)$$

Where η = solvent viscosity, T = temperature, R = gas constant and V = molecular volume of the fluorescent dye or dye conjugate. In turn, V can be estimated from the molecular weight of the dye or dye conjugate with appropriate adjustments for hydration.

Polarizer

The most common polarizers used today are (i) dichroic devices, which operate by effectively absorbing one plane of polarization (e.g. Polaroid type-H sheets based on stretched polyvinyl alcohol impregnated with iodine) and (ii) double refracting calcite (CaCO_3) crystal polarizers which differentially disperse the two planes of polarization (examples of this class of polarizers are Nicol polarizers, Wollaston prisms and Glan-type polarizers such as the Glan-Foucault, Glan-Thompson and Glan-Taylor polarizers).

[1.3] α -Synuclein

[1.3.1] Historical overview

The name 'Synuclein' was first derived from the protein that was found in both **syn**apses and in the **nuclear** envelope [Maroteaux et al., 1988]. The 143-amino acid (aa) long neurone-specific protein was isolated from the electric organ of the fish *Torpedo californica* by expression screening was called synuclein. Independently, NACP, the 140-aa non-A β component of AD amyloid precursor [Ueda et al., 1993], and synelfin [George et al., 1995] were cloned in human and in the zebra finch, respectively. They were found to be orthologs of torpedo fish synuclein and rat brain synuclein [Campion et al., 1995; Maroteaux et al., 1991; Jakes et al., 1994]. When Jakes et al. cloned β -synuclein as a second member of the human synuclein family, they termed the initially isolated family members ' α -synuclein.' All α -synucleins were shown to be extremely well conserved among distantly related species [George et al., 1995; Maroteaux et al., 1991; Jakes et al., 1994]. α -Synuclein was not found in the nucleus in several subsequent studies. It appears therefore to be a purely presynaptic protein [Jakes et al., 1994; Iwai et al., 1995].

[1.3.2] The Synuclein family

Three members of the human synuclein family have been identified: α -, β -, and γ -synuclein (see **Figure 1.6**). The genes are located on chromosome 4q21 [Shibasaki et al., 1995; Spillantini et al., 1995; campion et al., 1995 and Chen et al., 1995], 5q35 [Spillantini et al., 1995], and 10q23 [Lavedan et al., 1998], respectively.

- (i) α -Synuclein (NACP)
- (ii) β -Synuclein (PNP14)
- (iii) γ -Synuclein (BCSG1)

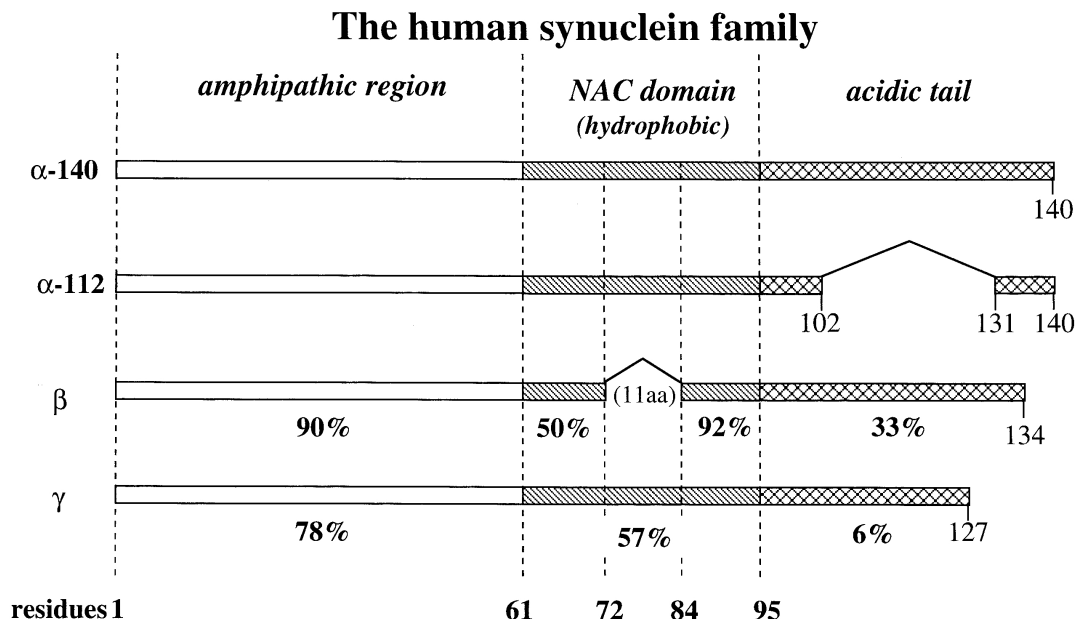


Figure 1.6: The human synuclein family. The different synucleins are represented as a bar. Amino acid positions are indicated at the bottom. The N-terminal amphipathic region, the hydrophobic NAC region, and the acidic tail are separated by vertical dashed lines and are differently hatched. The α -112 splice variants of α -synuclein (lacking 28 amino acids within the acidic tail) as well as β - and γ -synuclein are shown. The NAC region of β -synuclein lacks 11 central amino acids (residues 73–83). The degree of amino acid identity compared to α -synuclein, according to cross-species consensus sequences [Clayton et al., 1998], and is given as a percentage below each domain. [Reproduced from Lucking et al., 2000]

β - and γ -Synucleins

Three different types of synucleins (α , β - and γ -synuclein) have been identified. β - and γ -synuclein are 78% and 60% identical to α -synuclein. They preserve some characteristic features of α -synuclein, while missing others. The α - and β -synucleins share a conserved C-terminus with three identically placed tyrosine residues. However, β -synuclein lacks 11 residues within the specific NAC region [Clayton and George, 1998]. γ -Synuclein specifically lacks the tyrosine rich C-terminal signature of α - and β -synucleins [Clayton and George, 1998]. Comparison of the structural properties of the members of synuclein family by several physicochemical methods revealed that all three synuclein are typical natively unfolded proteins, with some structural differences. β -Synuclein exhibited the properties of a typical random coil, whereas α - and γ -synucleins were slightly more compact and structured [Uversky et al., 2002d]. Both α - and γ -synucleins were shown

to form fibrils, whereas β -synuclein did not fibrillate when incubated under the same conditions [Uversky et al., 2002d]. However, even apparently 'nonamyloidogenic' β -synuclein can be forced to fibrillate in the presence of some metals (Zn^{2+} , Pb^{2+} , and Cu^{2+} ions) or pesticides [Yamin et al., 2005]. Furthermore, the metal-induced fibrillation of β -synuclein was further accelerated by the addition of GAGs or high concentrations of macromolecular crowding agents [Yamin et al., 2005]. Intriguingly, the addition of either β - or γ -synuclein in a 1 : 1 molar ratio to α -synuclein solution substantially increased the duration of the lag-time and dramatically reduced the elongation rate of α -synuclein fibrillation [Uversky et al., 2002d]. Fibrillation was completely inhibited at a 4 : 1 molar excess of β - or γ -synuclein over α -synuclein [Uversky et al., 2002d]. β -Synuclein inhibited α -synuclein aggregation in animal models too [Hashimoto et al., 2001]. This suggests that β - and γ -synucleins may act as regulators of α -synuclein fibrillation *in vivo*, potentially acting as chaperones [Uversky et al., 2002d].

[1.3.3] Structural and conformational aspects of α -Synuclein

Structural and conformational behavior of α -synuclein is crucial to understand the aggregation and fibrilization process α -synuclein. α -Synucleins from different organisms possess a high degree of sequence conservation [Clayton and George, 1998]. α -Synuclein-140 is the best isoform reported out of all three synucleins [Bayer, 2006], which is the whole and major transcript of the protein. Two other isoforms, α -synuclein-126 and α -synuclein-112, are produced by alternative splicing, resulting in an inframe deletion of exons 3 and 5, respectively. Exon 3 encodes for residues towards the N-terminus, residues 41–54, and exon 5 encodes for residues towards the C-terminus, residues 103–130.

On the basis of structural point of view α -synuclein-140 can be divided into three regions: (i) The N-terminal region, residues 1–60, include the sites of three familial PD mutations and contain four 11-amino acid, imperfect repeats with a highly conserved hexameric motif (KTKEGV). The N-terminal region is predicted to form amphipathic α -helices, typical of the lipid-binding domain of apolipoproteins [George et al., 1995; Clayton and George, 1998]. (ii) The central region, residues 61–95, comprises the highly aggregation-prone NAC sequence [Ueda et al., 1993; Han et al., 1995]. (iii) The C-terminal region, residues 96–140, is highly enriched in acidic residues and prolines. Three highly conserved tyrosine residues, which are considered a signature of the α - and β -synuclein family, are located in this region.

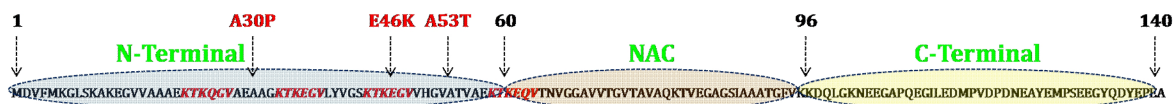


Figure 1.7: Schematic representation of primary structure of α -synuclein.

[1.3.3.1] α -Synuclein as an intrinsically disordered protein

α -Synuclein is a typical intrinsically disordered (or natively unfolded) protein, which possesses disordered structure under physiological conditions *in vitro* [Weinreb et al., 1996; Uversky et al., 2001a]. Intrinsically disordered proteins have recently been recognized as a new protein class, which are gaining considerable attention due to the capability of these proteins to perform numerous biological functions despite the lack of unique structure [Uversky et al., 2000, 2005a; Uversky, 2002a, b, 2003; Fink, 2005]. These proteins exist as dynamic and highly flexible ensembles that undergo a number of distinct interconversions on different time scales. The difference in amino acid composition between ordered and intrinsically disordered proteins created the basis for the development of numerous algorithms that predict disordered proteins or regions.

According to PONDR VL3 [Li et al., 1999; Romero et al., 2001], VSL2 [Obradovic et al., 2005], RONN [Yang et al., 2005], and IUPred [Dosztanyi et al., 2005] revealed that this protein is predicted to be almost completely disordered and its sequence is typical of intrinsically disordered proteins. In agreement with these computational predictions, α -synuclein was shown to possess little ordered structure under physiological conditions by techniques as far-UV circular dichroism and Fourier transform infra red spectroscopy, sedimentation, gel-filtration, dynamic light scattering, and SAXS [Weinreb et al., 1996; Eliezer et al., 2001; Uversky et al., 2001a; Uversky, 2003]. A high-resolution NMR analysis revealed that α -synuclein is largely unfolded in a solution, but exhibits a region between residues 6 and 37 with a preference for helical conformation [Eliezer et al., 2001]. Raman optical activity spectroscopy has revealed that α -synuclein may contain some residues in a helical poly-(L-proline) II-like conformation [Syme et al., 2002].

[1.3.3.2] Conformational equilibria in α -synuclein

The conformational behavior of α -synuclein under a variety of conditions was extensively analyzed [Uversky, 2003]. This analysis found that the structure of α -synuclein is extremely sensitive to its environment and can be easily modulated by a change in conditions. The list of known α -synuclein conformations includes:

(i) The extended state is the intrinsic state of α -synuclein under physiologic conditions *in vitro* [Weinreb et al., 1996; Uversky et al., 2001a; Sandal et al., 2008] and *in vivo* [McNulty et al., 2006].

(ii) The pre-molten globule state is the predominant state of α -synuclein in conditions like a low pH [Uversky et al., 2001a], a high temperature [Uversky et al., 2001a], low concentrations of organic solvents [Munishkina et al., 2003] and trimethylamine N-oxide [Uversky et al., 2001d], various metal ions [Uversky et al., 2001b], various salts [Munishkina et al., 2004], several common pesticides/herbicides [Uversky et al., 2001c, 2002a; Manning-Bog et al., 2002], heparin and other glycosoaminoglycans [Cohlberg et al., 2002], some polycations [Goers et al., 2003a].

(iii) The α -helical membrane bound form: interaction of α -synuclein with synthetic vesicles containing acidic phospholipids is accompanied by a dramatic increase in α -helical content [Davidson et al., 1998; Perrin et al., 2000]. For example, upon addition of small unilamellar vesicles containing 30% phosphatidylserine and 70% phosphatidylcholine, the circular dichroism spectrum of purified α -synuclein shifts from a characteristic random coil pattern with a 195 nm minimum to a typical α -helical pattern with 206 and 222 nm minima [Chandra et al., 2003]. Using NMR, these dramatic changes were attributed to the formation of α -helical conformation in the N-terminal fragment (~100 residues) [Chandra et al., 2003]. A noticeable break in the helical pattern was observed around residues 43 and 44, revealing an interruption of the helical structure in this region [Chandra et al., 2003]. Later, the formation of two curved α -helices (Val3-Val37 and Lys45-Thr92) connected by a well ordered, extended linker was reported [Ulmer et al., 2005].

The acidic glutamate-rich C-terminal region (Asp98-Ala140) was shown to behave as a highly mobile tail and remained unstructured even in the presence of membranes [Jao et al., 2004; Ulmer et al., 2005]. However, it becomes insensitive to protease digestion when the micelle bound α -synuclein is exposed to calcium [de Laureto et al., 2006].

(iv) α -helical and β -structural species in organic solvents: The addition of various alcohols increases the content of ordered secondary structure in α -synuclein [Munishkina et al., 2003]. The type of structural transformation induced by high solvent concentrations was dependent on the type of alcohol used, where simple alcohols induced enrichment in β -sheet and fluorinated alcohols promoted enrichment in α -helix [Munishkina et al., 2003]. Both α -helical and β -sheet species were shown to be initially monomeric, but underwent association over longer times, where β -structure rich conformations were very prone to form amorphous aggregates [Munishkina et al., 2003]. Oligomeric α -helical globular species possibly possessing rigid tertiary structure were induced in α -synuclein by high concentrations of trimethylamine N-oxide [Uversky et al., 2001d].

(v) Dimers: α -Synuclein is able to form morphologically distinct oligomers and aggregates. For example, the prolonged incubation of

this protein at high temperatures results in the progressive aggregation, where dimers are formed first [Uversky et al., 2001e]. The formation of oxidative dimers and higher-order oligomers with dityrosine cross-links under conditions of oxidative stress was also reported [Souza et al., 2000].

(vi) Oligomers: In addition to covalent and non-covalent dimers, α -synuclein was shown to form a series of morphologically different soluble oligomers. Nitrated α -synuclein assembles into oligomeric spheroids [Yamin et al., 2003a]. The incubation of α -synuclein with different metals gave rise to three different classes of oligomers: Cu^{2+} , Fe^{3+} , and Ni^{2+} ions yielded 0.8–4 nm spherical particles, similar to α -synuclein incubated without metal ions; Mg^{2+} , Cd^{2+} , and Zn^{2+} ions gave larger, 5–8 nm spherical oligomers; and Co^{2+} and Cd^{2+} ions produced ring oligomers with diameters of 70–90 nm and 22–30 nm in the case of Co^{2+} ion [Lowe et al., 2004]. Several oligomeric ‘protofibrillar’ species with various morphologies were detected by atomic force microscopy at early stages of fibrillation [Conway et al., 1998, 2000c; Ding et al., 2002; Lashuel et al., 2002a, b]. The earliest form of α -synuclein protofibrils appeared to be predominantly spherical with heights varying between 2.5 and 4.2 nm [Conway et al., 2000b; Ding et al., 2002]. Under the appropriate conditions, these spherical oligomers convert into rings [Ding et al., 2002]. In addition to the complete rings, the partially formed rings (i.e. crescents) were found [Ding et al., 2002]. The incubation of the spherical α -synuclein oligomers with brain derived membranes was shown to also produce pore-like ring-type protofibrils [Ding et al., 2002].

(vii) Insoluble aggregates: Finally, α -synuclein was shown to assemble into large, insoluble aggregates with two distinct morphologies—amorphous aggregates and fibrils. The type of insoluble aggregate is also determined by the solution conditions. For example, α -synuclein precipitated from solutions containing high concentrations of simple alcohols predominantly form amorphous aggregates. In many other cases, the major insoluble species are amyloid-like fibrils. In a few cases, the successful partitioning between these two pathways is observed and α -synuclein is present in both fibrillar and amorphous forms simultaneously. The various studies described above indicate that α -synuclein possesses a remarkable conformational plasticity, being able to adopt structurally unrelated conformations, including a substantially unfolded native state, and fibrillation prone partially folded conformation, and various α -helical and β -sheet species folded to different degrees in both monomeric and oligomeric states [Uversky et al., 2002d; Uversky, 2003]. Furthermore, this protein can form several morphologically different types of aggregates, including oligomers (i.e. spheres or ring), amorphous aggregates, and amyloid-like fibrils [Uversky et al., 2002d; Uversky, 2003]. The various insoluble aggregates observed *in vitro* might represent major building blocks of pathology-related inclusions, such as LBs, LNs, GCIs,

neuronal cytoplasmic inclusions, and axonal spheroids, which have all been found in neurons affected by the synucleinopathies.

[1.3.4] α -Synuclein aggregation

[1.3.4.1] Role of partial folded structure in aggregation or fibril formation

Early stages of fibril formation involve the partial folding of α -synuclein into the highly fibrillation-prone pre-molten globule-like conformation, which represents a key intermediate on the fibrillation pathway [Uversky et al., 2001a]. Hence, factors that shift the equilibrium in favor of this partially folded conformation facilitate fibril formation. Possibilities include point mutations that shift the conformational equilibrium towards these partially folded conformations, non-polar molecules such as some pesticides that might preferentially bind to them. Cations that might mimic over the amino acid residue at the effect of low pH (high proton concentration) in protein solution. Aggregation might be favored by other factors as well that result in an increase in the concentration of α -synuclein itself or into a chemical modification of the protein (e.g. via oxidative damage, etc.). As stated above, a number of environmental factors are able to induce partial folding of α -synuclein. Consequently, it was not surprising to find that all these factors do indeed result in the accelerated α -synuclein fibrillation [reviewed in Uversky 2003].

[1.3.4.2] Mechanism of α -synuclein aggregation

Because of its “natively unfolded” structure, α -synuclein might be especially prone to self-aggregate or to cause the aggregation of other proteins or intracellular structures (**Figure 1.8**). *In vitro*, both full-length WT and mutant α -synuclein (A30P and A53T) when present in supersaturating conditions undergo time-, temperature-, pH- and concentration-dependent self-aggregation into fibrils [Hashimoto et al., 1998; Giasson et al., 1999].

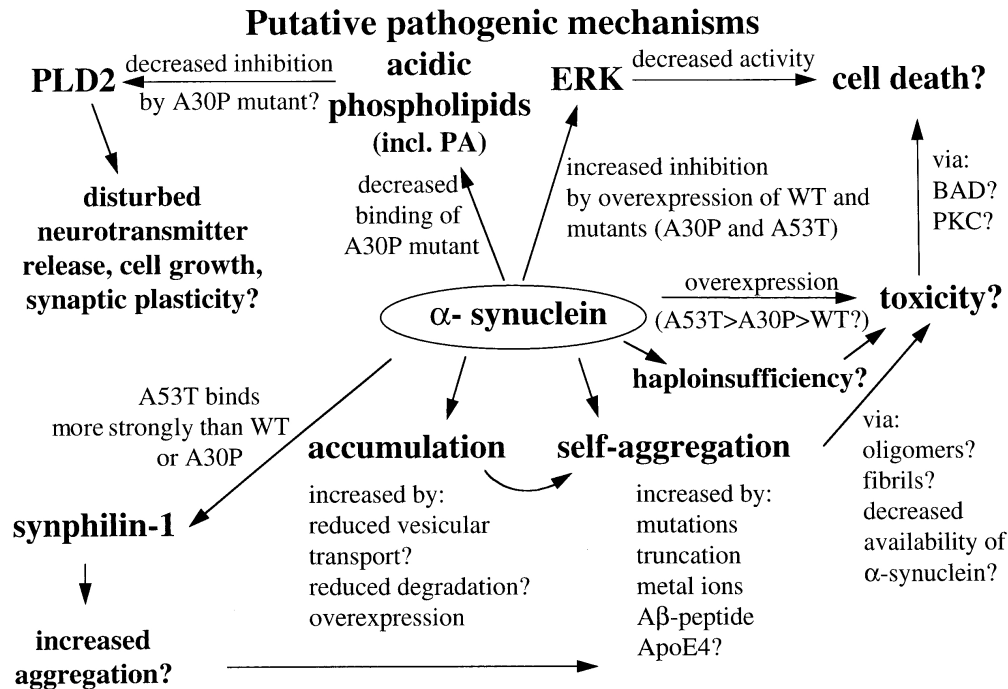


Figure 1.8: Putative pathological mechanisms of α -synuclein. The binding partners and hypothetical steps of the different pathogenic mechanisms are indicated by arrows. PA, phosphatidic acid; PLD2, phospholipase D2; ERK, extracellular regulated kinase; WT, wild type; A30P and A53T, described α -synuclein mutations; >, possibly more toxic than. [Reproduced from Lucking et al., 2000]

These fibrils were similar to those isolated from LBs of patients with PD and DLB, or from the filamentous inclusions characteristic for MSA [Conway et al., 1998]. Fibrillization was accompanied by a change in the secondary structure of α -synuclein from an unfolded random coil to an antiparallel β sheet [Narhi et al., 1999; Conway et al., 2000a; Conway et al., 2000b].

In a similar time-, concentration-, and temperature-dependent manner, the α -synuclein fragment NAC self-aggregated into amyloid like filaments with a thioflavin-positive β -sheet structure [Iwai et al., 1995; Han et al., 1995], residues 1–18 of the NAC peptide being sufficient for this aggregation [El-Agnaf et al., 1998]. Solutions containing aggregated α -synuclein, NAC (1–35) and NAC (1–18) were toxic to SH-SY5Y cells *in vitro* [El-Agnaf et al., 1998]. Fibril formation from wild-type and mutated (A53T and A30P) α -synuclein involves nucleation-dependent elongation [Conway et al., 2000; Wood et al., 1999] in which the protein aggregates into seeds and then accelerates fibril formation in a dose-dependent manner. Heterologous seeding of wild-type α -synuclein by A53T-mutated seeds also occurred, a possible explanation for the dominant effect of this mutation.

Although, it is clear that two mutations (A30P and A53T) in the α -synuclein gene can give rise to an inherited form of PD, the mechanism by which the disease occurs is not very clear. One possibility is that α -synuclein containing these mutations aggregates more rapidly, and indeed, both α -synuclein mutations appear to accelerate the aggregation process [Conway et al., 1998; El-Agnaf et al., 1998a; Giasson et al., 1999; Narhi et al., 1999]. Aggregates formed from wild-type α -synuclein or from either mutant were thioflavin-S positive, indicative of the presence of aggregates with the β -pleated sheet conformation characteristic of amyloid fibrils [Hashimoto et al., 1998; El-Agnaf et al., 1998a]. Anti-parallel β -sheet structure in wild-type and mutant aggregates has been confirmed by Fourier transform infrared spectroscopy [Narhi et al., 1999].

More recently, the kinetic mechanism of α -synuclein aggregation was studied and found to be rate limited by a nucleation step. Addition of preformed fibrils of α -synuclein caused rapid aggregation of a supersaturated solution, bypassing a lag phase that occurred in the absence of seeding. Aggregate growth followed first-order kinetics with respect to α -synuclein concentration, and α -synuclein (A53T) could seed the aggregation of wild-type α -synuclein. In addition, the wild-type and mutant forms of α -synuclein had similar critical concentrations, as measured by peptide remaining in solution after complete aggregation and attainment of equilibrium between peptide in solution and peptide in fibrillar form. These results suggest that the more rapid rate of aggregation of A53T α -synuclein compared to wild-type could not be explained by decreased solubility but was due to an increased nucleation rate [Wood et al., 1999]. Differences in the morphology of fibrils formed by wild-type and mutant α -synucleins under the same conditions have been reported [El-Agnaf et al., 1998a; Giasson et al., 1999].

Goedert and co-workers carried out studies on fibril morphology and staining pattern using antisera of different regional specificity in immunoelectron microscopy of filamentous assemblies isolated from the Sarcosyl-insoluble fraction of brains from patients with PD and dementia with Lewy bodies. They observed 5- and 10-nm filaments and a staining pattern that could be explained by postulating a buried N-terminus of all α -synuclein molecules except the one at the end of each filament; in other words, fibrils were polar structures. They proposed a model in which the α -synuclein molecules in Lewy bodies and Lewy neuritis assembled first to form protofibrils, two of which could associate to produce a variable twisted mature fibril [Spillantini et al., 1998a].

[1.3.4.3] Aggregation of α -synuclein fragments

The discovery of NAC, a hydrophobic peptide that was the second major component in Alzheimer's disease amyloid, led to the suggestion that it might seed amyloid formation in plaques [Ueda et al.,

1993]. Subsequently NAC fragment (amino acid residues 61-95) was found to aggregate *in vitro*. These aggregates have been shown, by thioflavin-S staining, Congo red staining, and Fourier transform infrared spectroscopy, to contain β -sheet structure, indicative of the presence of amyloid-like fibrils. Indeed, the aggregates had distinct fibrillar morphology, as observed by electron microscopy of negatively stained samples. Electron microscopy has revealed the presence of clumps of short irregular fibrils of variable length, mainly of 4–11 nm in diameter, similar in size to those found in neuritic plaques [El-Agnaf et al., 1998b, c; Han et al., 1995; Iwai et al., 1995b]. The transition from totally random structure to predominantly β -sheet like structure upon ageing of NAC in solution may be a general prelude to the formation of toxic fibrils by amyloidogenic peptides [El-Agnaf et al., 1998b, c].



Figure 1.9: Comparison of NAC with A β , PrP, and IAPP sequences. The GAVV sequence in NAC and GAXX sequences in the amyloidogenic regions of three other proteins are shaded. This alignment highlights a number of sequence identities between any pair of the four peptides (underlined). [Reproduced from El-Agnaf et al., 1998c]

Examination of the N-terminal sequence of NAC revealed a degree of similarity to regions crucial for the aggregation and toxicity of three other amyloidogenic proteins; namely, A β , prion protein, and islet amyloid polypeptide (see **Figure 1.9**). A four-residue motif, Gly-Ala-X-X, where X is an amino acid with an aliphatic side chain, that is common to all four peptides is shaded dark grey. The physicochemical characteristics of these sequences determine the similar fibrillogenic tendencies of NAC, islet amyloid polypeptide, A β , and prion protein, so that the amyloidogenic region of NAC lie in its N-terminal half [El-Agnaf et al., 1998c].

[1.3.4.4] α -Synuclein mutants

The term mutation stands for the change in genomic sequence and that changes leads to the different results compared to the parental sequence. There are several mutations in α -synuclein sequence have been reported, but only three mutations (A30P, E46K, and A53T) are leads to the formation of familial parkinson's disease; the A53T mutation in a large Italian-American family,

known as the Contursi kindred [Polymeropoulos et al., 1997]; the A30P mutation in a German family [Kruger et al., 1998]; and the E46K mutation in a Spanish family with autosomal dominant parkinsonism, dementia, and visual hallucinations of variable severity [Zarranz et al., 2004].

Despite of point mutations in α -synuclein genes, we have prepared cystein mutated dimer for the study of α -synuclein aggregation. The cystein mutated dimer is different from the point mutated α -synuclein. Our idea was to understand the aggregation mechanism of α -synuclein and the arrangement of monomeric α -synuclein in beta sheet like structure during aggregation process, by studying cystein mutated α -synuclein dimer.

[1.3.4.5] Seeded growth of α -synuclein

α -Synuclein is a major filamentous constituent of Lewy bodies, a pathological hallmark of Parkinson's disease (PD) [Spillantini et al., 1997; Spillantini et al., 1998]. When incubated *in vitro*, α -synuclein has undergone structural alteration from its natively unfolded state to cross β -sheet conformation, which results in the filamentous aggregate formation. The filamentous aggregate formation of α -synuclein has been considered to be a nucleation dependent process [Wood et al., 1999]. It could be seeded by a previously self-assembled species of α -synuclein acting as a nucleus. Its growth kinetics, therefore, is dependent upon the seed concentration, whereas a critical concentration of the α -synuclein monomer at the stationary phase is independent of the seed [Wood et al., 1999]. During fibril formation, natively unfolded α -synuclein is believed to adopt a partially unfolded intermediate structure and transform into highly ordered fibrils. Under optimized conditions of pH and temperature for this partially unfolded intermediate, the α -synuclein fibril formation could be accelerated [Uversky et al., 2001]. Macromolecular crowding, metal ions, and small chemicals also facilitated the fibril formation [Munishkina et al., 2004; Uversky et al., 2001; Uversky et al., 2001b]. Some chemicals, however, induced α -synuclein to protofibrils instead of the eventual fibril formation [Lee et al., 2006].

[1.3.4.6] Factors affecting α -synuclein aggregation

There are more than hundred factors and thousand compounds have been found to affect α -synuclein aggregation *in vitro* including metal ions, pesticides, herbicides, detergents, drugs, chemicals and particularly proteins like chaperones [reviewed in Uversky 2007].

[1.3.4.7] Proteins inhibiting α -synuclein aggregation

Chaperones

There are some heat shock proteins which have been found to slow down the α -synuclein aggregation. These proteins belong to the family of chaperone proteins. These proteins suppress protein aggregation and participate in protein refolding and/or degradation. Several chaperones, including torsin A, a protein with homology to yeast heat shock protein 104 [Walker et al., 2001], α B-crystallin, a small chaperone that binds to unfolded proteins and inhibits aggregation, molecular chaperones Hsp70 and Hsp40, and several other heat shock proteins [McLean et al., 2002], being prominent components of LBs and/or GCIs, co-localize with α -synuclein. The over-expression of torsin A and heat shock proteins suppressed α -synuclein aggregation in a cellular model [McLean et al., 2002]. *In vitro* analysis revealed that α B-crystallin serves as a potent inhibitor of wild-type, A30P and A53T α -synucleins fibrillation [Rekas et al., 2004]. Directed expression of the molecular chaperone Hsp70 prevented dopaminergic neuronal loss associated with α -synuclein in *Drosophila*, whereas the interference with endogenous chaperone activity accelerated α -synuclein toxicity. These informations suggest a role for chaperones in pathologies involving α -synuclein in humans, such that they may be a critical part of the neuronal arsenal that mitigates α -synuclein toxicity.

[1.3.5] α -Synuclein and neurodegenerative disease

Out of the three synucleins, only α -synuclein is associated with the filamentous inclusions of Lewy body diseases and MSA. Using specific antibodies, β - and γ -synuclein have been shown to be absent from these inclusions [Spillantini et al., 1997; Spillantini et al., 1998]. In addition, there is no genetic evidence linking the β - and γ -synuclein genes to disease. In the context of inherited PD, the immediate question is how missense mutations in the repeat region of the α -synuclein gene can cause degeneration of dopamine nerve cells in the substantia nigra. A related question concerns the relevance of α -synuclein dysfunction to the neurodegenerative process in all cases of Lewy body diseases and MSA. Over the past few years, α -synuclein has become one of only a handful of proteins that are fundamental to the aetiology and pathogenesis of some of the most common neurodegenerative diseases. In particular, the detailed mechanisms by which dysfunction of α -synuclein leads to the degeneration of nerve cells remain to be identified. A crucial question is whether conformationally altered, non-filamentous α -synuclein directly damages nerve cells. Another important question concerns the mechanisms that underlie the assembly of α -synuclein into filaments in idiopathic Lewy body diseases and in MSA. A corollary of this question is how the

presence of α -synuclein filaments in cell bodies and their processes affects the normal function of these cells. Improved experimental animal models will probably be instrumental in providing answers to these questions. This is especially true of transgenic mouse lines that still fall short of replicating many of the most important features of Lewy body diseases.

Native synucleins are unfolded proteins with little ordered secondary structure [Weinreb et al., 1996]. However, on binding to lipid membranes or detergent micelles, α -synuclein undergoes a structural transition to α -helical conformation [Davidson et al., 1998; Jo et al., 2000; Perrin et al., 2000; Eliezer et al., 2001]. Both full-length and carboxy-terminal truncated α -synuclein assemble into filaments that share many of the morphological and ultrastructural characteristics of filaments present in humans [Serpell et al., 2000; Conway et al., 1998; El-Agnaf et al., 1998; Giasson et al., 1999; Narhi et al., 1999; Wood et al., 1999; Conway et al., 2000; Giasson et al., 2001]. Assembly is a nucleation-dependent process and occurs through the repeats in the amino-terminal half. The carboxy-terminal region, in contrast, inhibits assembly. The A53T mutation in α -synuclein increases the rate of filament assembly, indicating that this might be its primary effect. The effect of the A30P mutation on the assembly of α -synuclein is less clear. One study reported an increase in filament assembly, another study found no change, and a third found an inhibitory effect on assembly [Serpell et al., 2000; Narhi et al., 1999; Conway et al., 2000]. The third study showed that the A30P monomer was consumed at a similar rate to wild-type α -synuclein, leading to the suggestion that oligomeric, non-fibrillar α -synuclein species might be detrimental to nerve cells [Conway et al., 2000]. The A30P mutation has also been shown to produce reduced binding of α -synuclein to rat brain vesicles *in vitro*, indicating that this might lead to its accumulation over time, resulting in filament assembly.

The assembly of α -synuclein is accompanied by the transition from random-coil conformation to a β -pleated sheet [Serpell et al., 2000; Conway et al., 2000]. By electron diffraction, α -synuclein filaments have been found to show a conformation characteristic of amyloid fibres [Serpell et al., 2000]. Under the conditions of these experiments, β - and γ -synuclein failed to assemble into filaments, and remained in a randomcoil conformation [Serpell et al., 2000; Giasson et al 2001]. This behaviour is consistent with their absence from the filamentous lesions of the α -synuclein diseases. It provides further evidence in favour of the hypothesis that α -synuclein aggregation is central to the neurodegeneration observed in Lewy body diseases and MSA.

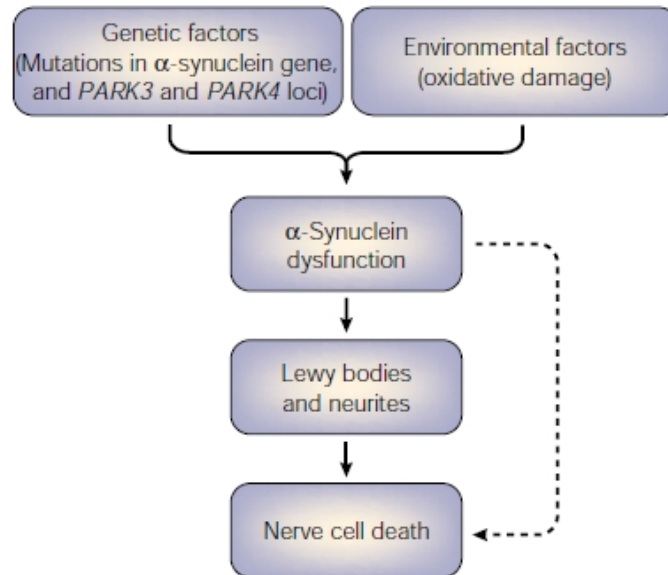


Figure 1.10: Model of disease pathway in Parkinson's disease. Genetic factors (mutations in the α -synuclein gene and mutations at the *PARK3* and *PARK4* loci) or environmental factors (oxidative damage, as exemplified by the experimental effects of rotenone) lead to a dysfunction of α -synuclein, which results in its ordered assembly into the filaments that characterize Lewy bodies and neurites. It is probable that the space-occupying Lewy body pathology contributes directly to nerve cell death. In addition, it is possible that conformationally altered, non-filamentous α -synuclein is toxic to nerve cells. [Reproduced from Goedert et al, 2001]

[1.3.5.1] α -Synuclein and parkinson's disease

PD is one of the most frequent neurodegenerative disorders followed by AD, with prevalence close to 2% after age 65. It is characterized by resting tremor, rigidity, and bradykinesia, which respond well to levodopa treatment. The pathological hallmarks are the presence of Lewy bodies (LBs) and massive loss of dopaminergic neurons in the pars compacta of the SN. The cause of this selective neurodegeneration is still unknown. Genetic factors, although initially underestimated, have become an important issue in PD research. The involvement of susceptibility genes is supported by epidemiological studies that showed a higher frequency of PD in relatives of PD patients than in those of controls and by elevated concordance in monozygotic twins. In addition, the observation that the disease is transmitted in some families as an autosomal dominant or an autosomal recessive trait suggests that mutations in single genes can cause some forms of PD in a monogenic manner [Goedert et al., 2001].

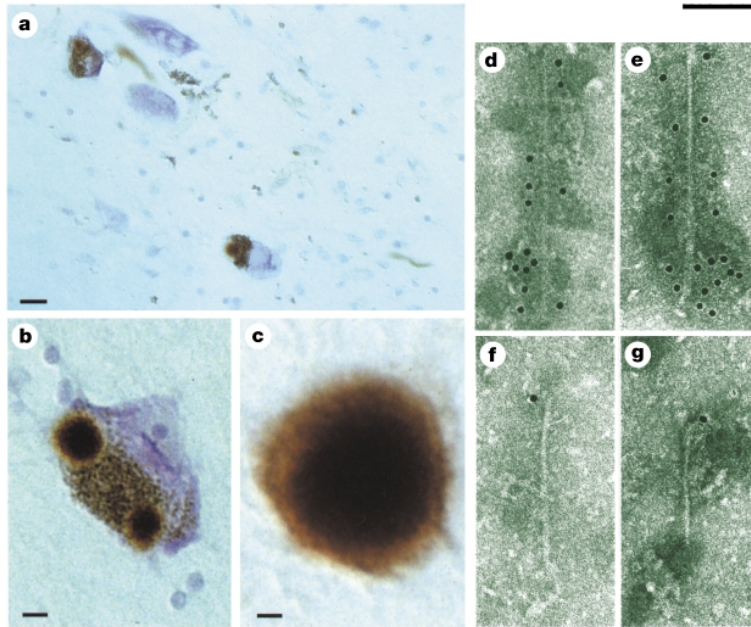


Figure 1.11: The α -synuclein pathology of parkinson's disease. Lewy bodies and Lewy neurites in the substantia nigra and several other brain regions define Parkinson's disease at a neuropathological level. Here, these entities are shown at the light (a–c) and electron microscopic (d–g) levels, labelled by α -synuclein antibodies. (a) Two pigmented nerve cells, each containing α -synuclein-positive Lewy body (red arrows). Lewy neurites (black arrows) are also immunopositive. Scale bar, 20 μ m. (b) Pigmented nerve cell with two α -synuclein-positive Lewy bodies. Scale bar, 8 μ m. (c) α -Synuclein-positive extracellular Lewy body. Scale bar, 4 μ m. (d–g) Isolated filaments from the substantia nigra of patients with Parkinson's disease are decorated with an antibody directed against the carboxy-terminal (d and e) or the amino-terminal (f and g) region of α -synuclein. The gold particles conjugated to the second antibody appear as black dots. Note the uniform decoration in d and e, and the labelling of only one filament end in f and g. Scale bar, 100 nm. [Reproduced from Spillantini et al., 1997 and Crowther et al., 2000]

α -Synuclein was the first 'PD gene' to be discovered. It is also involved in the pathogenesis of Alzheimer's disease (AD) and multiple system atrophy (MSA). Although a coherent view of its role in normal cell function and in neurodegeneration has not yet emerged, important progress has been made, especially through the identification of a number of partners that interact with α -synuclein. In addition, we are beginning to understand how disruption of normal function and/or protein aggregation may result in neuronal cell death.

[1.3.5.2] α -Synuclein toxicity

Though α -synuclein is the major component of the Lewy bodies, but the main cause of cell death is still unclear. It has been found that the aggregate of α -synuclein gets deposited into the nerve terminal, and the secretion of dopamine gets decreased from the deposited cells. While the NAC reason is known to be present in an extracellular location, namely, the plaques of Alzheimer's disease brains [Ueda et al., 1993], there is as yet no evidence to support the presence of α -synuclein

in extracellular form. However, if α -synuclein accumulates in neurons (see **Figure 1.12**), which eventually die, aggregates could leak out of the dead neuron and spread the disease to neighbouring cells [Mezey et al., 1998]. The toxicity of α -synuclein and NAC is sequence specific and increased by ageing in solution, meaning that it is dependent on aggregation and the formation of fibrils similar to the toxicity of other amyloid peptides [reviewed in Lansbury, 1999]. It is also apparent that the amyloidogenic portion of α -synuclein fragment NAC (1–18) mediated the toxic effect of α -synuclein and NAC.

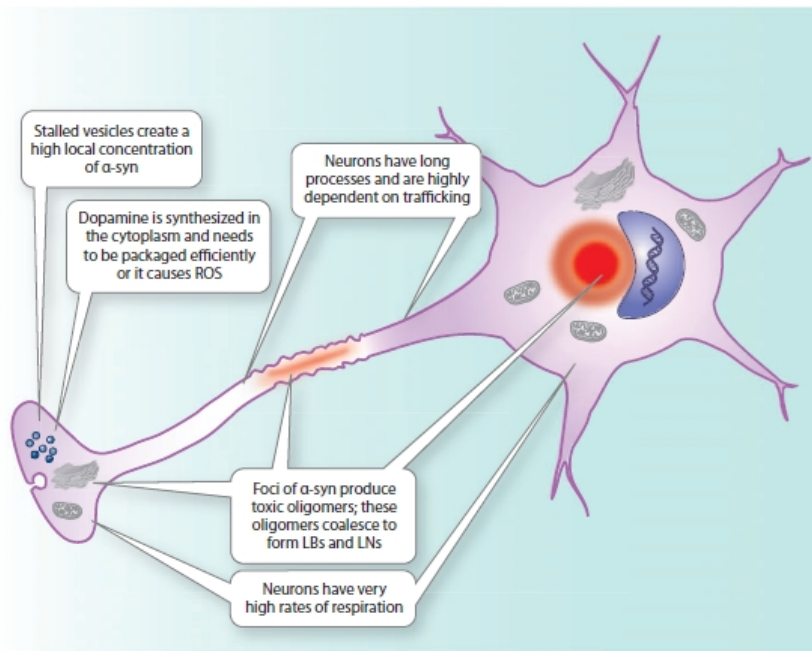


Figure 1.12: Summary schematic of α -synuclein toxicity in a dopaminergic neuron. Lewy bodies, Lewy neuritis, reactive oxygen species. [Reproduced from Auluck et al., 2010]

Recently [Ostrerova et al., 1999] have studied the effects of overexpressing wild-type or mutant α -synucleins in cells. Their interest in α -synuclein arose from its homology to 14-3-3 proteins, a family of protein chaperones expressed in brain. Like 14-3-3, α -synuclein bound to and inhibited protein kinase C and also bound BAD, a protein that regulates cell death. α -Synuclein levels increased during conditions promoting cell stress, while overexpression of α -synucleins induced a dose-dependent increase in toxicity, as measured by trypan blue staining. On the other hand, reduced expression of α -synuclein by transfection with antisense α -synuclein was cytoprotective.

Mutant α -synucleins were more toxic than wild-type α -synuclein, potentiating necrosis. The toxicity associated with overexpression of both mutant α -synucleins was probably due to a mechanism involving BAD. The ability of α -synuclein and related fragments to cause cell death

suggests that intracellular accumulation of α -synuclein in neurons and extracellular accumulation of NAC-containing amyloid might contribute to the synaptic loss and cell death that underlies a number of important neurodegenerative diseases (see **Figure 1.12**).

In general, the toxicity of amyloid proteins is closely associated to the processes of aggregation and fibril formation. It has been shown that different amyloid proteins share the same mechanism of toxicity to cells *in vitro*. This mechanism may involve reactive oxygen species and the elevation of intracellular calcium ion levels [Mattson and Goodman, 1995; Schubert et al., 1995]. Thus it has been proposed that the ability of amyloid proteins to undergo a transition to β -sheet structure is a prerequisite to filament formation and subsequent pathological consequences [reviewed in Lansbury, 1999]. It is not clear whether amyloid fibrils are directly toxic or produce damage by the mechanical disruption of tissue. Alternatively, the toxic state may consist of a soluble conformationally altered fibril precursor, or protofibril (see **Figure 1.12**), that induces cell death directly or indirectly. Accordingly, efforts to elucidate the pathological roles of α -synuclein may lead to improved strategies for the development of novel therapeutic agents for the treatment of these important neurodegenerative disorders.

[1.3.6] α -Synuclein interacting molecules

One of the most fascinating properties of α -synuclein is its ability to react with many other proteins, lipids, drugs and metal ions. α -Synuclein comprises 140 amino acids in two domains, linked via the NAC sequence. The C-terminal domain is rather acidic. The N-terminal domain, which is highly conserved between species, comprises seven repeats of a degenerate 11-amino-acid motif (residues 9–89). This feature is reminiscent of many apolipoproteins that form amphipathic α -helices [George et al., 1995]. α -Synuclein in its native state is unfolded, perhaps explaining its ability to interact with many other proteins [Weinreb et al., 1996]. However, α -synuclein can bind to small acidic phospholipid vesicles, resulting in a marked increase in α -helicity [Davidson et al., 1998]. Fast axonal transport of vesicle-bound α -synuclein is dependent on the integrity of the first N-terminal four of the 11-amino-acid repeats [Jensen et al., 1998]. α -Synuclein (A53T), but not (A30P), was able to bind these vesicles, perhaps because proline residues disrupt α -helical structure and interfere with the conformation required for lipid binding. One of the few definite biological activities ascribed to α -synuclein is its inhibition of phospholipase D2, an effect that was dependent on lipid concentration, suggesting that interaction might occur on membrane surfaces [Jenco et al., 1998]. Synphilin-1 has recently been identified, using a yeast two-hybrid system, as a novel protein that interacts with α -synuclein *in vitro* and *in vivo*. In the brain, synphilin-1 is expressed in many

areas, including the substantia nigra. In cells cotransfected with synphilin-1 and NAC the formation of cytoplasmic inclusions was observed. Cotransfection with full-length α -synuclein wild-type or A53T mutant did not lead to the formation of inclusions [Engelender et al., 1999]. This may be because NAC aggregates faster than full-length α -synuclein [El-Agnaf et al., 1998]. It will be interesting to discover whether synphilin-1 is a component of Lewy bodies and Lewy neurites. Since NAC was discovered as a component of senile plaque amyloid in AD brains, and the similarity in sequence between NAC and A β was noted (see **Figure 1.9**), it was of considerable relevance to investigate its interaction with A β . Preformed NAC fibrils were found to seed the aggregation of A β (1–40) and, vice versa, A β fibrils could seed NAC aggregation [Han et al., 1995]. It has also been reported that α -synuclein can bind A β (25–35) and that the NAC region is crucial to this interaction [Yoshimoto et al., 1995]. Binding of α -synuclein to A β is dependent on two domains in the former protein encompassing residues 1–56 and 57–97, respectively [Jensen et al., 1997].

[1.3.6.1] α -Synuclein shares physical and functional homology with 14-3-3 proteins

α -, β - and γ -synucleins show homology to a region of the 14-3-3 proteins and may be members of this superfamily [Ostrerova et al., 1999]. Like these proteins, α -synuclein binds to extracellular regulated kinase (ERK), dephospho-BAD (a Bcl-2 homolog) and protein kinase C (PKC) in decreasing order of affinity, but also to the 14-3-3 proteins themselves.

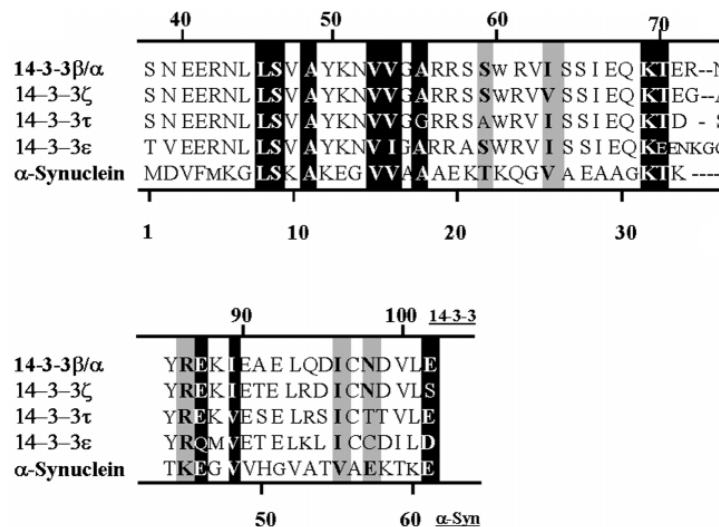


Figure 1.13: Alignment of α -synuclein and the 14-3-3 family of proteins. The alignment was performed using the Multalin program (<http://www.toulouse.inra.fr/multalin.html>). To observe homology, the first 30 amino acids of 14-3-3 proteins were excluded while performing the alignment algorithm. Exact matches are shown as white letters on a black background, and matches of proteins with similar properties are shown as black letters on a gray background. [Reproduced from Ostrerova et al., 1999]

The affinity of membrane-bound α -synuclein for different PKC isoforms also differs ($\alpha = \gamma > \epsilon > \beta = \delta$). Forced expression of wild-type or A53T α -synuclein in human embryonic kidney (HEK) cells inhibited PKC activity. Although α -synuclein and 14-3-3 both bind to BAD, the interactions are independent, the former binding dephospho-BAD, the latter, phospho-BAD [Ostrerova et al., 1999]. Since ERK, BAD, and PKC are involved in the regulation of cell viability, α -synuclein may play a role in the same signaling pathways.

[1.4] Amyloid-beta ($A\beta$)

Amyloid-beta ($A\beta$) is a 36-43 amino acid long peptide that is derived from the Amyloid precursor protein and the aggregation and fibril formation of amyloid-beta peptide are the main cause of pathogenesis and development of AD [Naslund et al., 2000; Selkoe et al., 2001]. There are different isoforms of $A\beta$ have been reported that differ by the number of amino acids at the C terminus [Selkoe et al., 1999]. Specifically, the 40-residue ($A\beta_{40}$) and 42-residue ($A\beta_{42}$) isoforms both have been associated with AD. In particular, $A\beta_{42}$ shows a high propensity to self-assemble and deposit in senile plaques and is highly toxic for neurons [Findeis et al., 2007], and its overproduction has been related to familiar forms of AD [Scheuner et al., 1996].

Aggregation of $A\beta_{42}$ is a complex process that involve in the formation of several soluble intermediate species, including oligomeric and protofibrillar forms, and ends with the deposition of ordered fibrillar architectures whose three-dimensional structure has been recently published [Luhers et al., 2005]. The process of *in vivo* polymerization is poorly understood, and the pathological role of different soluble species is still controversial. For instance, although the amyloid plaques are a major hallmark of AD, they are only part of an array of $A\beta$ aggregate morphologies observed *in vivo* [Walsh et al 2004]. Interestingly, not all of these $A\beta$ assemblies provoke an inflammatory response and are toxic. The detailed pathological mechanism still remains unclear. Considerable evidence suggests that soluble ordered oligomeric intermediates (e.g., soluble oligomers [56 kDa] and protofibrils), rather than insoluble peptide deposits, exert cytotoxic effects and play a crucial role in AD onset and progression [Glabe et al., 2006; Lambert et al., 1998; Walsh et al., 2002]. $A\beta$ deposits may enhance oxidative stress and inflammation, leading to cell injury [Varadarajan et al., 2000].

Despite this acute importance and interest, there are several aspects of amyloid aggregation that conspire against reliable experimental studies and direct comparison of the results. First, the kinetics of $A\beta_{42}$ aggregation is very sensitive to inputs, such as the conformational status of starting material [Sandal et al., 2008] and physicochemical characteristics of the solution

[Hortschansky et al., 2005], and studies are limited by the poor water solubility of A β 42. Indeed, depending on experimental conditions and the detection system, different on- and off-pathway intermediates have been reported, resulting in divergent kinetics and aggregation models [Hortschansky et al., 2005; Necula et al., 2007; Zhu et al., 2004]. Second, the structural polymorphism (i.e., the tendency to aggregate into multiple morphologies, which is a prominent feature of A β aggregation) makes the reliable *in vitro* reproduction of neurotoxicity related assembly difficult, thereby leading to contradictory study outcomes.

[1.4.1] Amyloid-beta in neurodegenerative disease

Amyloid plaques are not only a histopathological hallmark of AD, but the aggregated A β of which they are composed likely play a key role in the pathogenesis of AD [Hardy et al., 2001]. The most direct evidence supporting this hypothesis stems from studies of gene mutations that cause autosomal-dominant inherited forms of AD. As illustrated in **Figure 1.14**, most but not all of these mutations lead to increased production and accumulation of specific A β species (A β 42), either through effects on the amyloid precursor protein (APP) itself [Goate et al., 1991] or through effects on presenilin 1 or 2 [Scheuner et al., 1996], which form part of γ -secretase, one of the proteolytic complexes that cleaves APP to generate A β [Wolfe et al., 1999]. Aggregated amyloid (in the form of oligomers, protofibrils, or fibrils) is toxic to neurons in most but not all culture conditions [Yankner et al., 1996 and Kaye et al., 2003], and in primary neuronal culture and mouse models, A β may act synergistically with neurofibrillary tangle pathology [Rapoport et al., 2002 and Lewis et al., 2001]. These observations have led to the hypothesis that increased production, aggregation, and accumulation of A β initiates a cascade of events leading to neurotoxicity and eventually to clinical symptoms of AD [Hardy et al., 2001], as summarized in **Figure 1.14**. Autopsy studies of patients with genetic forms of AD, Down's syndrome, or mild cognitive impairment (which appears to be a prodromal phase of AD) have shown that accumulation of A β may precede clinical development of AD by as many as 10 years [Mann et al., 1989; Lemere et al., 1996; Smith et al., 2001; Morris et al., 1996]; importantly, the increased presence of A β correlates well with cognitive decline early in the course of the disease [Naslund et al., 2000]. Thus, A β pathology (a) is required for the diagnosis of AD, (b) plays a key role in the pathogenesis of AD, and (c) develops prior to symptomatic manifestations of AD. For these reasons, there has been great interest in developing therapies and diagnostic tools aimed at A β .

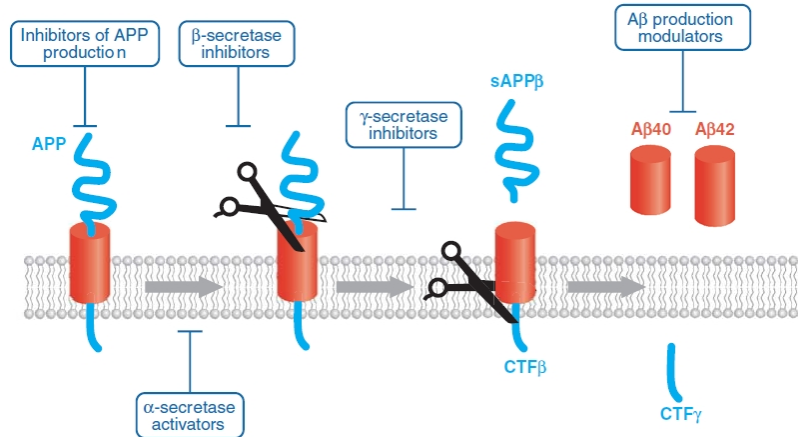


Figure 1.14: A β production. The integral membrane protein amyloid precursor protein (APP) is cleaved by the beta-site APP-cleaving enzyme (BACE, or β -secretase) to yield a secreted fragment of APP (sAPP β) and a C-terminal fragment of APP (CTF β). CTF β is then cleaved by γ -secretase within the membrane to yield a smaller C-terminal fragment (CTF γ) and A β fragments of various lengths (shown in red). An alternate cleavage by α -secretase (not shown) cuts within the A β domain and thus precludes A β production. Potential opportunities for therapeutic intervention are shown in the blue boxes. [Skovronsky et al., 2006]

[1.5] 14-3-3 Proteins

The 14-3-3 proteins were initially described as an acidic, abundant brain protein by Moore & Perez in 1967 [Moore et al., 1967]. The name is derived from the combination of its fraction number on DEAE-cellulose chromatography and its migration position in the subsequent starch-gel electrophoresis. The unique terminology remains while the concept of 14-3-3 has evolved from a brain-specific protein to a family of ubiquitously expressed regulatory molecules of eukaryotic organisms. 14-3-3 has emerged as a group of multifunctional proteins that bind to and modulate the function of a wide array of cellular proteins. More than 50 signaling proteins have been reported as 14-3-3 ligands. This broad range of partners suggests for 14-3-3 a role as a general biochemical regulator, reminiscent of the well-defined regulatory protein calmodulin. Through interaction with its effector proteins, 14-3-3 participates in the regulation of diverse biological processes, including neuronal development, cell growth control, and viral and bacterial pathogenesis. This chapter focuses on recent developments in the understanding of the structural basis of 14-3-3 and α -synuclein interactions and on roles for 14-3-3 on α -synuclein aggregation. The functions of 14-3-3 in neuronal development, signal transduction [Aitken et al., 1996; Morrison et al., 1994; Pawson et al., 1997], and plant biology [Ferl et al., 1996 and Finnie et al., 1999] have recently been reviewed elsewhere.

[1.5.1] General properties

14-3-3 is a family of highly homologous proteins encoded by separate genes. There are seven known mammalian 14-3-3 isoforms, named with Greek letters (β , ϵ , γ , η , σ , τ , ζ) after their elution profile on reversed phase high-performance liquid chromatography [Ichimura et al., 1988 and Martin et al., 1993]. The species initially designated α and δ are actually the phosphorylated forms of β and ζ [Aitken et al., 1995]. The 14-3-3 proteins exist mainly as dimers with a monomeric molecular mass of approximately 30,000 Da and an acidic isoelectric point [Morrison et al., 1994; Pawson et al., 1997].

14-3-3 proteins exhibit a remarkable degree of sequence conservation between species [Wang et al., 1996]. For example, the *Saccharomyces cerevisiae* BMH1 and human ϵ isoforms are approximately 70% similar at the amino acid level. 14-3-3 proteins also share some basic biochemical properties, such as activation of the ExoS ADP-ribosyltransferase [Fu et al., 1993; Zhang et al., 1999] and of tryptophan hydroxylase [Isobe et al., 1991]. These similarities argue strongly for a high degree of functional conservation.

14-3-3 is abundant in the brain, comprising approximately 1% of its total soluble protein [Boston et al., 1982]. It is now clear that 14-3-3 is also present in almost all tissues, including testes, liver, brain and heart [Celis et al., 1990]. Within a eukaryotic cell, 14-3-3 is largely found in the cytoplasmic compartment. However, 14-3-3 proteins can also be detected at the plasma membrane and in intracellular organelles such as the nucleus and the Golgi apparatus [Celis et al., 1990; Freed et al., 1994; Fanger et al., 1998; Leffers et al., 1993; Tang et al., 1998]. Like their high degree of conservation, the ubiquitous nature of 14-3-3 proteins may reflect their fundamental importance in eukaryotic biology. Indeed, recent research on 14-3-3 supports this view.

The frequent isolation of 14-3-3 from many biochemical and genetic screens for different targets must reflect the physiological importance of 14-3-3 in diverse cellular pathways. Depending on its interaction with specific effectors, 14-3-3 participates in many vital regulatory processes, such as cell cycle control, survival signaling, cell adhesion, and neuronal plasticity. The trend of rediscovery of 14-3-3 proteins shows no sign of diminishing and in fact will likely become more common because of an increased understanding of the regulation of 14-3-3–ligand interactions.

[1.5.2] Structural basis

[1.5.2.1] 14-3-3 monomer contains a conserved amphipathic groove

The drive to understand the molecular mechanisms by which 14-3-3 interacts with its ligands led to the solution of the crystal structures of 14-3-3 ζ [Liu et al., 1995] and 14-3-3 τ [Xiao et al., 1995],

revealing strikingly similar dimeric structures. Each monomer consists of a bundle of nine α -helices organized in an antiparallel fashion [Fu et al., 2000]. The molecule has a cup-like shape with a highly conserved, inner, concave surface and a variable outer surface (see **Figure 1.15**). A striking feature of the concave surface is an amphipathic groove in each monomer [Fu et al., 2000]. As revealed from the ζ structure [Liu et al., 1995], on one side of the groove, helices 3 and 5 present a cluster of charged and polar residues. On the other side of the groove, helices 7 and 9 present a patch of hydrophobic residues. It is interesting to note that these residues lining the concave surface of the groove are mostly conserved among different isoforms of the 14-3-3 family [Yaffe et al., 1997; Liu et al., 1995; Xiao et al., 1995; Petosa et al., 1998]. Because many 14-3-3 ligands bind well to all isoforms, it was thought that this conserved amphipathic groove could mediate the binding of 14-3-3 to its target proteins [Liu et al., 1995]. It was further postulated that a basic cluster in the groove, consisting of K49, R56, and R127, may mediate the interaction of 14-3-3 with the phosphoamino acid in its ligands. This model has been unequivocally confirmed by both mutational analysis [Zhang et al., 1997; Wang et al., 1998; Thorson et al., 1998] and co-crystallization studies [Yaffe et al., 1997; Rittinger et al., 1999; Petosa et al., 1998]. 14-3-3 ζ has been co-crystallized in complex with several peptide ligands, providing critical insights into the structural details of 14-3-3–ligand interactions [Yaffe et al., 1997; Rittinger et al., 1999; Petosa et al., 1998].



Figure 1.15: *Crystal structure of 14-3-3 η dimer.*

In the complexes, both phosphorylated and unphosphorylated 14-3-3 binding peptides lie in the conserved amphipathic groove [Fu et al., 2000]. Instead of the α -helical structure originally proposed, 14-3-3 binding peptides adopt an extended conformation. These extended structures may have fewer steric constraints and greater conformational flexibility to sample different residues in the groove for optimal association. This gives 14-3-3 great versatility in the recognition

of a diverse range of ligand sequences. The high-resolution model of 14-3-3 ζ in complex with a mode 1 phosphoserine peptide derived from MT (MARSHpSYPAKK) provides a structural explanation for the 14-3-3-phosphoserine motif interaction [Yaffe et al., 1997; Rittinger et al., 1999]. The phosphoserine contacts 14-3-3 by salt bridges to the side chains of K49, R56, and R127 in the basic cluster and a hydrogen bond to the hydroxyl group of Y128 [Fu et al., 2000]. In support of this interpretation, charge-reversal mutations K49E, R56E, and R127E drastically disrupt the interaction of 14-3-3 ζ with Raf-1 and Bcr. K120 in the charged face of the groove, together with N173 and N224, stabilize an extended ligand conformation by contacting backbone groups of the +1 and -1 residues, which may be important for positioning the phosphoserine to interact with the basic cluster of 14-3-3. All of these interactions were similar for a synthetic peptide based on the mode 2 binding motif [Rittinger et al., 1999], which suggests that diverse ligands use the basic cluster and its accessory residues to bind to 14-3-3. Outside of this cluster, there is considerable variability in 14-3-3-ligand connections, as assessed by comparison of the MT co-crystal structure with that of the mode 2 peptides. For example, E180 forms a hydrogen bond with the -2 Ser in the MT peptide but bonds with the -4 Arg in the mode 2 peptides [Rittinger et al., 1999]. Similarly, several hydrophobic residues, including L172, L216, I217, and L220, are consistently involved in binding, but they interact with different parts of the two ligands. This type of flexible interaction may explain the diversity among 14-3-3 binding sequences from various ligands. The conserved ligand binding groove is also involved in binding unphosphorylated ligands, such as R18 [Fu et al., 2000]. R18 is a peptide selected from a phage display library for its high affinity for 14-3-3 proteins [Wang et al., 1999]. In the 14-3-3 ζ -R18 complex, R18 assumes an extended conformation in the amphipathic groove, similar to phosphorylated peptides [Petosa et al., 1998]. Its core WLDLE sequence is located in the phosphoserine binding site with its two acidic residues, Asp and Glu, next to the basic cluster of 14-3-3. Two Leu of R18 interact with amino acids on the hydrophobic side of the 14-3-3 groove, including L172 and L220. Thus, R18 assumes a true amphipathic structure.

It has been reported that C-terminal fragments of 14-3-3 are capable of ligand binding [Luo et al., 1995; Ichimura et al., 1995; Gu et al., 1998]. For example, the “box-1” region, which spans residues 171–213 of 14-3-3 η , efficiently binds tryptophan hydroxylase, Raf-1, and Bcr [Ichimura et al., 1995; Ichimura et al., 1997]. Although several hydrophobic and polar residues that contribute to the ligand binding groove of 14-3-3 are located in these regions, the exact nature of the stable interaction of these regions with different proteins remains to be clarified.

[1.5.2.2] 14-3-3 dimer can simultaneously bind two ligands

As seen in the various crystal structures, the N-terminal portion of 14-3-3 is involved in dimer formation [Fu et al., 2000; Liu et al., 1995; Xiao et al., 1995]. The dimer interface is formed by the packing of helix $\alpha 1$ from one monomer against $\alpha 3$ and $\alpha 4$ from the other, leaving a 6- to 8-Å hole in the center. Several hydrophobic and polar residues are buried in the dimer interface, including L12, A16, V62, I65, and Y82. These residues are largely conserved among mammalian 14-3-3 isoforms, which raises the possibility that 14-3-3 proteins can form heterodimers between different isoforms [Jones et al., 1995]. The dimeric structure of the 14-3-3 protein allows it to bind two ligands simultaneously (**Figure 1.16 a, b**). In the co-crystal structures of 14-3-3 with peptides, the ligand binding sites are located within the same concave surface, and each site is occupied [Yaffe et al., 1995; Petosa et al., 1998]. The dimer is arranged such that the ligand binding groove runs in opposite directions in each monomer of the molecule (**Figure 1.16b**). Simultaneous binding of a 14-3-3 dimer to two protein ligands would have significant implications.

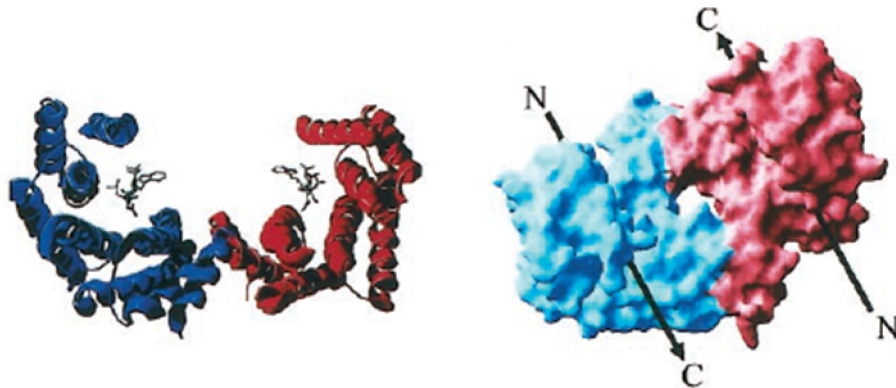


Figure 1.16: Crystal structural model of 14-3-3 ζ . (a) 14-3-3 ζ crystallized with R18 (PDB ID 1A38), rotated 90° relative to (b) Solvent accessible surface of 14-3-3 ζ with bound peptides (represented by arrows). Dimerization forces bound ligands to adopt opposite orientations. [Reproduced from Fu et al., 2000]

In this regard, it is interesting to note that many 14-3-3 ligands, such as Raf-1 and Cbl, have multiple recognition motifs. Dual recognition by 14-3-3 of two weakly interacting motifs, such as those found in Cbl, may promote a more stable interaction. In contrast, 14-3-3 may bind to two high-affinity sites, such as those found in Raf-1, perhaps to promote a regulatory conformational change in Raf-1. Alternatively, 14-3-3 may bring together two different signaling molecules to modulate each other's activity. Some evidence has been provided that 14-3-3 can mediate the association of Raf-1 with Bcr [Braselmann et al., 1995] or A20 [Vincenz et al., 1996], but the physiological significance of these complexes is unclear. It is plausible that this adaptor function of

14-3-3 exists only for specific ligand pairs. Yet another possible role for dimerization of 14-3-3 is in subcellular localization. For example, one monomer could function as a targeting unit by binding an anchored ligand while the other binds a cargo protein. Depending on the site of the anchored ligand, 14-3-3 may localize the cargo protein to distinct intracellular compartments. The recently reported binding of 14-3-3 to CRM1 may serve such a purpose [Rittinger et al., 1999].

Although the exact function of 14-3-3 dimerization is not clear, the importance of this phenomenon is supported by data showing that several ligand binding-defective mutants of 14-3-3 act as dominant negative inhibitors *in vivo* [Thorson et al., 1998; Chang et al., 1997; Zhang et al., 1999a; Zhang et al., 1999b]. The dimeric nature of 14-3-3 may hold the key for many critical roles of 14-3-3 in cells.

[1.5.3] Disease associated with 14-3-3 proteins

Although 14-3-3 has not been directly linked to a specific disease, it has been implicated in a variety of pathological processes. A large number of 14-3-3 ligands are proto-oncogene or oncogene products, which suggests the participation of 14-3-3 in mitogenic signal transduction as well as neoplastic transformation. Indeed, the tumor profile of mice infected with polyomavirus expressing a 14-3-3 binding-defective mutant MT showed a striking deficiency in the induction of salivary gland tumors [Cullere et al., 1998]. Another possible connection of 14-3-3 to tumorigenesis is its involvement in regulating cell survival, for example through its interaction with IGFIR. The IGFIR plays an important role in controlling normal cell survival as well as in tumorigenesis [Baserga et al., 1997]. The major site for 14-3-3 interaction is located within a Ser quartet critical for IGFIR-mediated cell transformation [Craparo et al., 1997; Furlanetto et al., 1997; Li et al., 1996], implying that 14-3-3 participates in this process. Significantly elevated levels of both the IGFIR [Kaiser et al., 1993] and 14-3-3 proteins [Nakanishi et al., 1997] have been detected in all major types of lung cancer. On the other hand, the 14-3-3 ϵ gene is found in a region with frequent loss of heterozygosity in several cancers, which suggests that some 14-3-3 isoforms may be important for suppression of tumorigenesis [McDonald, 1994]. Taken together, these data argue that 14-3-3 may be involved in the development of human cancer.

The abundance of 14-3-3 proteins in brain tissues points to a critical role of 14-3-3 in neuronal function. There are some indications that 14-3-3 is involved in several neurological disorders. 14-3-3 ϵ is located in a chromosomal region, 17p13.3 that contains genes implicated in isolated lissencephaly sequence (ILS) and Miller-Dieker syndrome (MDS) [Chong et al., 1997; Hirotsune et al., 1997]. ILS is a brain malformation malady marked by disorganization of the

cortical layers. MDS causes malformations similar to those of ILS, as well as additional abnormalities, and is associated with larger deletions of 17p13.3. The 14-3-3 ϵ sequence is deleted in some MDS patients, and this loss may contribute to the development of MDS phenotypes [Chong et al., 1997]. 14-3-3 proteins are also found in the neurofibrillary tangles seen in patients with Alzheimer's disease [Layfield et al., 1996]. A possible genetic association of a 14-3-3 η polymorphism with early onset schizophrenia has been reported [Toyooka et al., 1999]. Hsich et al., [1996] noted that 14-3-3 proteins are specifically detected in cerebrospinal fluid from patients with Creutzfeldt-Jakob disease (CJD) and related transmissible spongiform encephalopathies. This observation has allowed the use of 14-3-3 as a biochemical marker for a premortem diagnostic test for CJD and related diseases [Hsich et al., 1996; Moussavian et al., 1997]. It is not known whether 14-3-3 is involved in the pathogenesis of CJD, or whether the presence of 14-3-3 in cerebrospinal fluid is simply the consequence of neuronal cell death in CJD brains.

Table 1.3: Milestones in 14-3-3 research

Year	Function , System, Specific finding	References
1968	Naming; identification as abundant brain proteins	Moore et al., 1967
1980	Purification and axonal transport	Erickson et al., 1980
1982	14-3-3 in cerebro spinal fluid	Boston et al., 1982
1987	Enzyme regulation; activation of tryptophan and tyrosine monoxygenase	Ichimura et al., 1987
1988	Separation by HPLC and naming of brain forms by greek letters; cloning of 14-3-3	Ichimura et al., 1988
1990	Interaction with a kinase (inhibition of PKC)	Aitken et al., 1990
1992	Exocytosis (Exo1)	Morgan et al., 1992
	14-3-3 in other eukaryotes: yeast, plant and <i>Xenopus</i> 14-3-3	Van-Heusden et al., 1992
	G-box binding factor, GF14	Lu et al., 1992
	Phosphorylated forms of 14-3-3	Toker et al., 1992
1993	Exoenzyme S	Fu et al., 1993
1994	AANAT and 14-3-3	Roseboom et al., 1994
	14-3-3 association with Raf kinase	Fantl et al., 1994
	Receptors: fusicoccin receptor/binding protein	Marra et al., 1994
	Association with c-Bcr and Bcr-Abl	Reuther et al., 1994
	Association of polyomavirus middle tumour antigen with 14-3-3	Pallas et al., 1994
	14-3-3 fission yeast homologues and DNA damage checkpoint	Ford et al., 1994
	EF-hand calcium binding motif in sub-class of plant 14-3-3s	Lu et al., 1994
1995	14-3-3 α and δ are the brain phosphorylated 14-3-3 β and ζ	Aitken et al., 1995
	Crystal structures of 14-3-3	Xiao et al., 1995
	Heterodimers	Jones et al., 1995
	Stage-specific expression of 14-3-3 during life cycle of <i>Schistosoma mansoni</i>	Schechtman et al., 1995
	Phosphatidylinositol 3-kinase association	Schechtman et al., 1995b
	14-3-3 association with phosphatase (Cdc25)	Conklin et al., 1995

1996	Neurodegenerative disease: 14-3-3 in neurofibrillary tangles of Alzheimer's brains.	Layfield et al., 1996
	Interaction mediated by phosphoserine interaction motif, RXS ^p XP	Muslin et al., 1996
	Plant function: 14-3-3 is inhibitor of phosphorylated nitrate reductase	Moorhead et al., 1996
	Apoptosis: phosphorylation dependent association of BAD with 14-3-3	Zha et al., 1996
	Leonardo, a <i>Drosophila</i> 14-3-3: function in olfactory bulb	Skoulakis et al., 1996
1997	14-3-3 σ in DNA damage checkpoint: transcriptional regulation by p53	Chan et al., 1997
	Structure of 14-3-3: phosphopeptide complex	Yaffe et al., 1997
	Phosphorylation by CKI and regulation of Raf interaction	Dubois et al., 1997
	Binding to insulin receptor substrate-1	Craparo et al., 1997
	KSR signalling complex	Xing et al., 1997
	Glucocorticoid receptor	Wakui et al., 1997
1998	Interaction of 14-3-3 with a nonphosphorylated protein ligand	Petosa et al., 1998
	Interaction with DNA: 14-3-3 is cruciform binding protein	Todd et al., 1998
	Interaction with specific MEK kinases	Fanger et al., 1998
	ATM activation of p53 involves dephosphorylation and association with 14-3-3	Waterman et al., 1998
1999	GM-CSF, IL-3, IL-5 receptors and haematopoiesis	Stomski et al., 1999
	Trafficking of forkhead transcription factor	Brunet et al., 1999
	G-protein coupled receptors	Prezeau et al., 1999
2000	Hypermethylation at the 14-3-3 σ locus in breast cancer	Ferguson et al., 2000
	Regulation of histone deacetylase 4 and 5	Wang et al., 2000
	Modulation of DNA topoisomerase	Kurz et al., 2000
2001	Crystal co-structure of 14-3-3 with AANAT (serotonin <i>N</i> -acetyltransferase)	Obsil et al., 2001
2002	Phosphorylation of 14-3-3 by AKT	Powell et al., 2002
2003	Structure of fusicocin/14-3-3 complex	Wurtele et al., 2003
	14-3-3 protein functions in left-right patterning during amphibian embryogenesis	Bunney et al., 2003
	Phosphorylation of 14-3-3 by CaM kinase II	Ellis et al., 2003
	Phosphorylation of 14-3-3 may promote monomerisation	Woodcock et al., 2003
2004	Role in AKAPs	Baisamy et al., 2004
	Apoptosis regulation by JNK phosphorylation at S185	Tsuruta et al., 2004
2005	Mode III binding motif	Ganguly et al., 2005
	14-3-3 σ X-ray structure accounts for isoform specificity	Benzinger et al., 2005
	Recognition of phosphoacetylated Histone H3	Macdonald et al., 2005
2006	14-3-3 ζ acts as molecular chaperon	Yano et al., 2006
	Binding of 14-3-3 proteins to diverse proteins of varying size and sequence	Yang et al., 2006
2007	14-3-3 protein FTT-2 regulate DAF-16 transcriptional activities in <i>C. elegans</i>	Li et al 2007
2008	Detection of 14-3-3 ζ in cerebro spinal fluid	Murphy et al., 2008
2009	Interaction between 14-3-3 proteins and N-terminal region of tyrosine hydroxylase	Halskau et al., 2009
2010	14-3-3 proteins binds to LRRK2	Nichols et al., 2010
2011	14-3-3 proteins regulate exonuclease-1	Engels et al., 2011
	Structural mechanism of 14-3-3 dependent inhibition of RGS3-G α interaction	Rezabkova et al., 2011
	Co-localization of 14-3-3 proteins with SOD1 in lewy body	Okamoto et al., 2011

[1.5.4] Co-localization of 14-3-3 protein in Lewy- bodies

Parkinson's disease (PD), one of the most common neurodegenerative diseases, is characterized neuropathologically by the presence of intracytoplasmic inclusions called Lewy bodies (LBs), which mainly contain aggregated α -synuclein [Spillantini et al., 1997]. Point mutations in the α -synuclein genes have been discovered in families afflicted with autosomal dominant inherited PD [Kruger et al., 1998; Polymeropoulos et al., 1997; Zarranz et al., 2004]. α -Synuclein is expressed predominantly in the presynaptic nerve terminals [George et al., 1995]. Under normal conditions, it is thought to have a role in the modulation of synaptic vesicle turnover and synaptic plasticity [Chandra et al., 2005; Clayton et al., 1999]. However, this physiological role of α -synuclein is not essential for nerve terminal function, because α -synuclein knockout mice display only a mild phenotype. Nevertheless, α -synuclein is likely to protect nerve terminals under unusual conditions such as neuronal stress or injuries, since the transgenic expression of α -synuclein has been shown to abolish the lethality and neurodegeneration caused by the deletion of cysteine-string protein-1 (CSP), a co-chaperone protein localized in the synaptic vesicles [Chandra et al., 2005]. Therefore, the loss of functional α -synuclein may predispose dopaminergic neurons to oxidative injury or mitochondrial dysfunction.

Lewy bodies also contain other proteins including ubiquitin [Lowe et al., 1988], parkin [Shimura et al., 2001], cytoskeletal proteins like neurofilaments [Schmidt et al., 1991], and septins [Ihara et al., 2003], 14-3-3 proteins [Kawamoto et al., 2002a], and synphilin-1 [Wakabayashi et al., 2001]. The 14-3-3 proteins, a family of protein chaperones, are abundant in the brain, comprising approximately 1% of the total brain proteins [Boston et al., 1982]. 14-3-3 proteins consist of seven different isoforms [Fu et al., 2000]. 14-3-3 proteins exist mainly as homo- or hetero-dimers consisting of ϵ and ζ , or τ and ζ subunits, and participate in intracellular signal transduction pathways [Aitken et al., 1996]. 14-3-3 Proteins are increased in the cerebrospinal fluid from patients with Creutzfeldt-Jakob disease (CJD), and the detection of 14-3-3 proteins is a marker in the pre-mortem diagnosis of CJD [Hsich et al., 1996]. In recent studies, 14-3-3 proteins were found in abnormal pathological structures, including the neurofibrillary tangles in AD [Layfield et al., 1996], the Pick bodies in Pick's disease [Umahara et al., 2004], the Lewy bodies in PD [Kawamoto et al., 2002b], the Lewy body-like hyaline inclusions in amyotrophic lateral sclerosis [Kawamoto et al., 2004], the glial cytoplasmic inclusions in multiple system atrophy [Kawamoto et al., 2002a], the nuclear inclusions in spinocerebellar ataxia-1 [Chen et al., 2003], the prion plaques in sporadic CJD, and the florid plaques in variant CJD [Richard et al., 2003]. Ostrerova et al. [Ostrerova et al., 1999] showed that regions of α -synuclein and 14-3-3 proteins share over 40% homology, and bind to

each other. These proteins were found to oppositely regulate parkin activity [Sato et al., 2006], suggesting important roles for 14-3-3 and α -synuclein together with parkin in the pathogenesis of PD.

On the other hand, Engelender et al. [Engelender et al., 1999] identified synphilin-1, a novel protein which also interacts with α -synuclein to form cytoplasmic inclusions *in vitro*. The C-terminus of synphilin-1 is closely associated with the C-terminus of α -synuclein [Kawamata et al., 2001]. The function of synphilin-1 is not fully understood yet; however, it is enriched in the presynaptic terminals, possibly mediating the synaptic function attributed to α -synuclein [Ribeiro et al., 2002]. Synphilin-1 is enriched in the central cores of LBs, and is presumed to play a role in LB formation *in vivo* [Wakabayashi et al., 2000]. Recently, Eyal et al. [Eyal et al., 2006] identified synphilin-1A, an isoform of synphilin-1, which has enhanced aggregatory properties and causes neurotoxicity. Synphilin-1A is also observed in LBs. Synphilin-1 and synphilin-1A differs in their exon organization, and is translated from different start codons. Therefore, the N-terminus of synphilin-1A is different from that of synphilin-1. In addition, a mutation of the synphilin-1 gene has been detected in two German PD patients. Collectively, clarifying the roles of α -synuclein, 14-3-3, and synphilin-1 in the process of LB formation may shed some light on the pathogenesis of PD. In this study, we examined A53T-Tg mice, which overexpress mutated human A53T α -synuclein under the control of a prion promoter, using immunohistochemistry for α -synuclein, the seven 14-3-3 isoforms, and synphilin-1. α -Synuclein has a tendency to selfaggregate and form fibrils in the presence of the familial PD-linked A53T mutation of α -synuclein [Conway et al., 1998], and the A53T-Tg mice show numerous α -synuclein-based aggregates in the brain [Giasson et al., 2002]. We determined the distribution of the seven 14-3-3 isoforms and synphilin-1 in the aggregates from these mice to uncover the roles of 14-3-3 proteins and synphilin-1 in the pathogenesis of PD.

[1.5.5] Sequence similarity between 14-3-3 η and α -synuclein

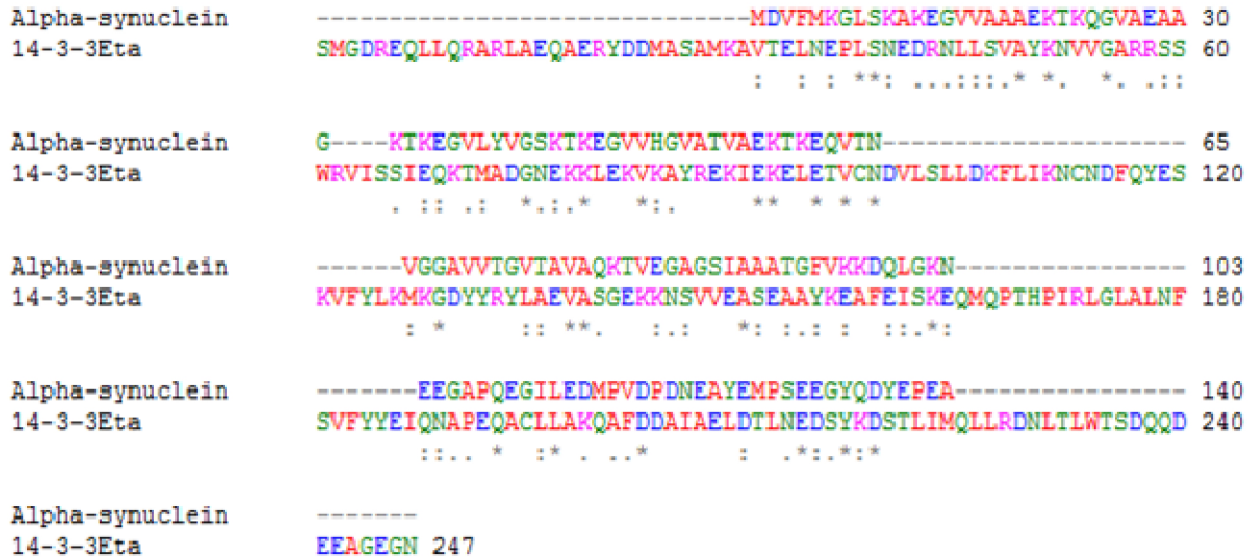


Figure 1.17: Multiple sequence alignment of α -synuclein and 14-3-3 η showing alignment score 47.

Single letter: amino acids, **Red:** small, hydrophobic, aromatic, **Blue:** acidic, **Magenta:** basic, **Green:** hydroxyl, amine, amide

"*": Identical

": Conserved substitution (similar color group)

": Semi conserved substitution (similar shapes)

Score: 47

[1.5.6] Sequence similarity between 14-3-3 η and 14-3-3 γ

14-3-3 γ belongs to the 14-3-3 family of proteins which mediate signal transduction by binding to phosphoserine-containing proteins. It is induced by growth factors in human vascular smooth muscle cells, and is also highly expressed in skeletal and heart muscles, suggesting an important role for this protein in muscle tissue.

```

14-3-3gamma      MVDREQLVQKARLAEQAERYDDMAAAMKNVTELNEPLSNEERNLLSVAYKNVVGARRSSW 60
14-3-3eta       MGDREQLLQARLAEQAERYDDMASAMKAVTELNEPLSNEDRNLLSVAYKNVVGARRSSW 60
*  ****:*:*****:*** *****:*****:*****

14-3-3gamma      RVISSIEQKTSADGNEKKIEMVRAYREKIEKELEAVCQDVLSELLDNYLIKNCSETQYESK 120
14-3-3eta       RVISSIEQKTMADGNEKKLEKVKAYREKIEKELETVCNDVLSLLDKFLIKNCNDFQYESK 120
*****  *****:*  *:*****:*.*****:*****:*****

14-3-3gamma      VFYLMKMGDYRYRLAEVATGKRAIVVESSEKAYSEAHEISKEHMQPTHPIRLGLALNYS 180
14-3-3eta       VFYLMKMGDYRYRLAEVASGEKKNVVEASEAAYKEAFEISKEQMPTHPIRLGLALNFS 180
*****:***:  ***:*  **.*.*****:*****:*****

14-3-3gamma      VFYYEIQNAPEQACHLAKTAFDDAIAELDTLNEDSYKDSTLIMQLLRDNLTLWTSDQQDD 240
14-3-3eta       VFYYEIQNAPEQACLLAKQAFDDAIAELDTLNEDSYKDSTLIMQLLRDNLTLWTSDQQDE 240
*****  *** *****:*****:*****:*****

14-3-3gamma      DGGEENN 247
14-3-3eta       EAGEGN- 246
:.*.****

```

Figure 1.18: Multiple sequence alignment of 14-3-3 γ and 14-3-3 η .

Single letter: amino acids, **Red:** small, hydrophobic, aromatic, **Blue:** acidic, **Magenta:** basic, **Green:** hydroxyl, amine, amide

****:** Identical

":": Conserved substitution (similar color group)

":": Semi conserved substitution (similar shapes)

14-3-3 γ and 14-3-3 η shows more than 95% sequence similarity. Nevertheless, 14-3-3 η does not interact with α -synuclein.

Chapter-2

(Results and Discussion)

Morphological Analysis of Proteins

[2.1] α -Synuclein

[2.1.1] Monomer

α -Synuclein is a 140 aa long polypeptide chain that acquires partially unfolded state when it comes in contact with solution. It is very difficult to see α -synuclein monomer by AFM Probe being their end radius of curvature of the order of 10 nm.

[2.1.2] Oligomers

α -Synuclein acquires different conformations in solution state which leads to the formation of different kind of oligomers. These oligomers are considered as a most toxic species in PD. There are several factors (e.g. temperature, metal ions, pesticides, herbicides, chaperone protein etc.) that influence the α -synuclein aggregation, and leads to the formation of morphologically distinct oligomers [Uversky et al., 2007].

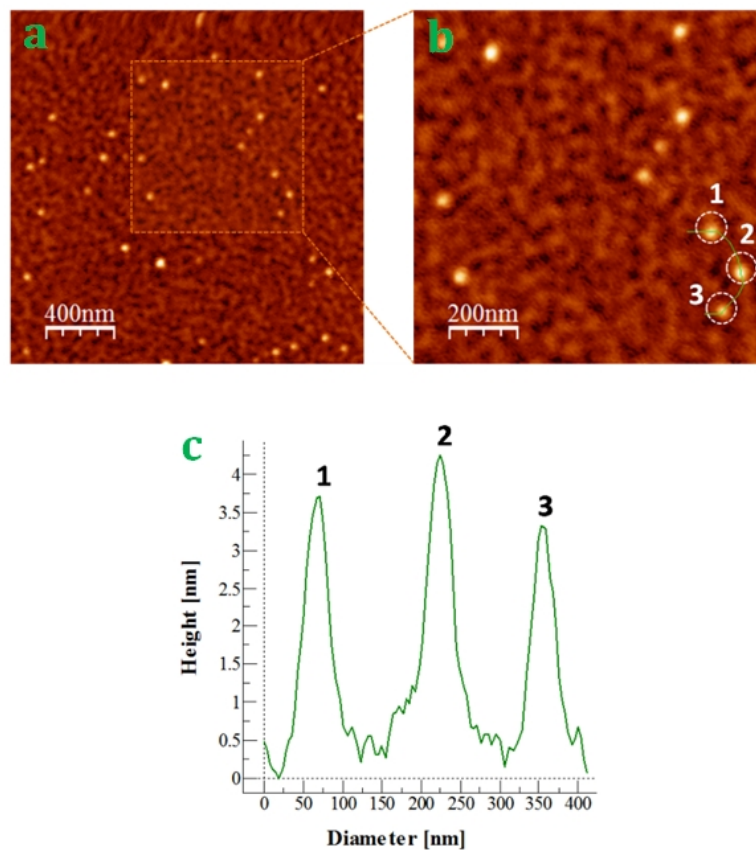


Figure 2.1: AFM image analysis of early-formed α -synuclein oligomers. (a) Early-formed α -synuclein oligomers ($2\mu\text{m}\times 2\mu\text{m}$), (b) Early-formed α -synuclein oligomers ($1\mu\text{m}\times 1\mu\text{m}$), (c) Height profile of early-formed α -synuclein oligomers (heights were measured between 2.5–5 nm).

α -Synuclein forms oligomers of height between 2–8 nm [Lowe et al., 2004]. There are several other factors that stimulate α -synuclein aggregation and leads to the formation of morphologically distinct and bigger oligomers. In case of adding metal ions (e.g., Co^{2+} , Cd^{2+} , Ca^{2+} ions) in α -synuclein solution, α -synuclein forms oligomers of 30–50 nm in diameter [Lowe et al., 2004]. We observed oligomers which supports the data which has been reported previously.

The early formed oligomers were observed by incubating α -synuclein (80 μM) in 200 μl of PBS buffer (50 mM, pH 7.4) at 37 $^{\circ}\text{C}$ for 2–6 h with continuous shaking at 1000 rpm (see section 3.2.1 in detail for protein aggregation). Images were taken in tapping mode AFM, and analyzed by Scanning probe microscopy software, WSxM 5.0 (see section 3.2.4 in detail for image analysis). The image analysis was based on the shapes and heights of oligomers. In fact their lateral dimension observed by AFM is expected to be much larger than the real one due to the well known tip-broadening effect, contrary to their height that is correctly reproduced in the AFM images, instead. Heights of the oligomers were measured between 2.5–5 nm which is compatible with the expected height of early formed oligomers.

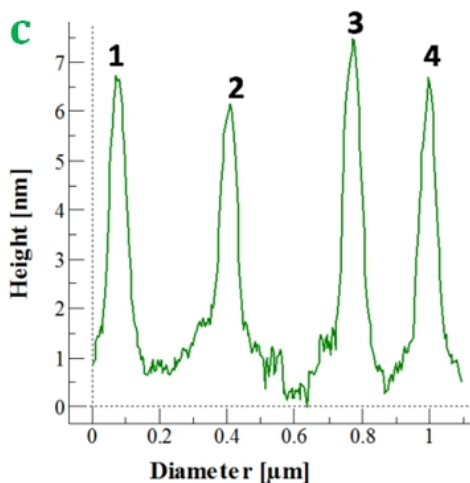
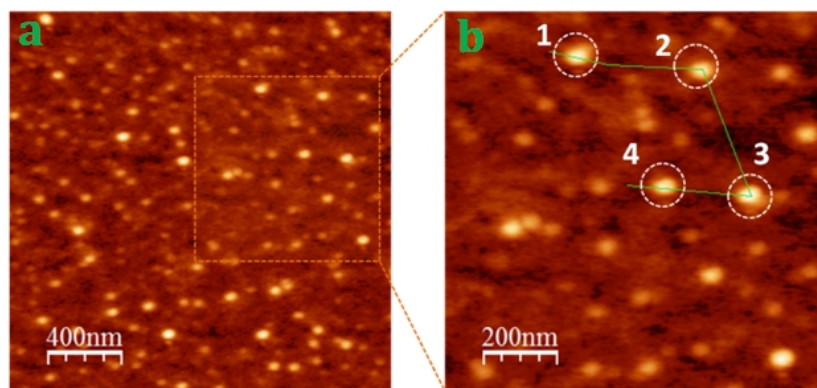


Figure 2.2: AFM image analysis of belatedly-formed α -synuclein oligomers. (a) Belatedly-formed α -synuclein oligomers ($2\mu\text{m}\times 2\mu\text{m}$), (b) Belatedly-formed α -synuclein oligomers ($1\mu\text{m}\times 1\mu\text{m}$), (c) Height profile of belatedly-formed α -synuclein oligomers (heights were measured between 5–8 nm).

Also heights between 5–8 nm were measured at 6–12 h. These values are compatible with the height of belatedly-formed mature oligomers, instead [Conway et al., 2000a].

[2.1.3] Morphologically distinct oligomers

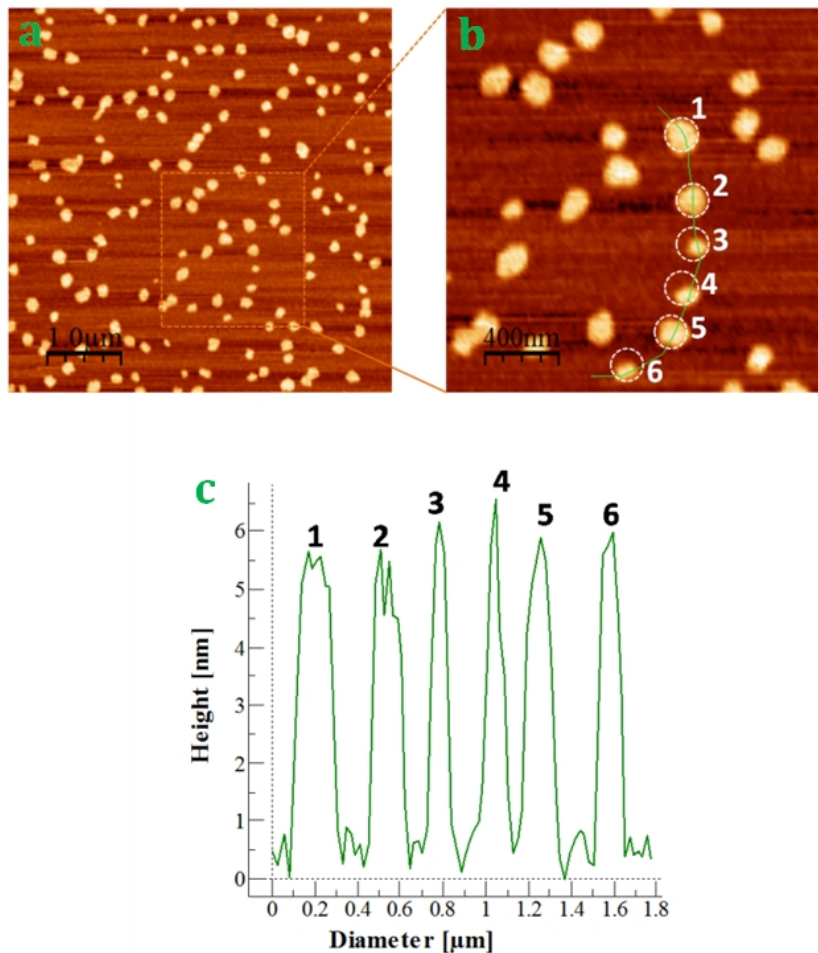


Figure 2.3: AFM image analysis of non-spherical α -synuclein oligomers. (a) α -Synuclein oligomers ($5\mu\text{m}\times 5\mu\text{m}$), (b) α -Synuclein oligomers ($2\mu\text{m}\times 2\mu\text{m}$), (c) Height profile of α -synuclein oligomers (heights were measured between 5–7 nm and diameters were measured between 30–70 nm).

Diverse morphological shapes of α -synuclein oligomers were observed. The average height of non-spherical (angular shaped) oligomers were measured was ~ 5.5 nm and diameters were measured between 30–70 nm. It is expected that the morphological appearance of oligomers depends on the

conformations of the α -synuclein monomer which participates in protein aggregation [Uversky et al., 2007].

[2.1.4] Protofilaments

Protofilaments were observed after 12–13 days long incubation of α -synuclein (80 μ M) in 200 μ l of PBS buffer (50 mM, pH 7.4) at 37°C with continuously shaking at 1000 rpm (see section 3.2.1 in detail for protein aggregation). Images were taken in tapping mode AFM, and analyzed by Scanning probe microscopy software, WSxM 5.0 (see section 3.2.4 in detail for image analysis).

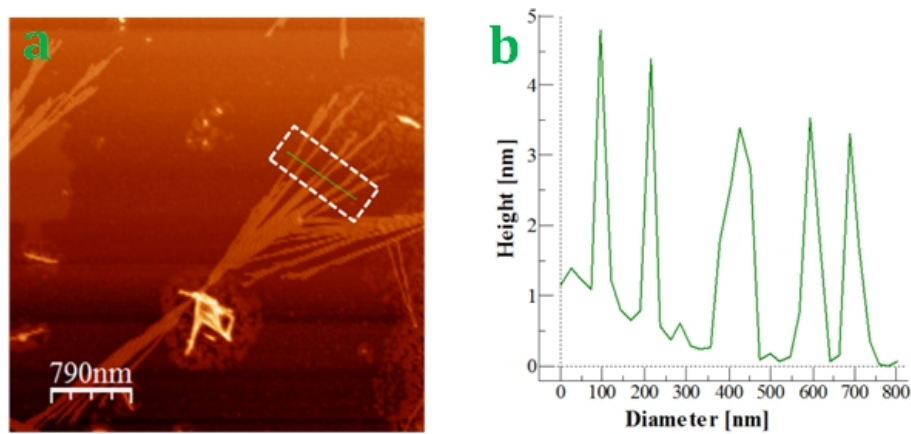


Figure 2.4: AFM image analysis of α -synuclein protofilaments. (a) Bundles of protofilaments, (b) Height profile of protofilaments (height measured between 2.5–3.5 nm).

We observed bundles of α -synuclein mature fibrils only after 5–6 days of incubation at 37°C with continuously shaking at 1000 rpm. The observation of α -synuclein protofilaments after forming α -synuclein mature fibrils show that the formation of protofilaments was initiated by mature fibrils. Heights of the protofilaments were measured between 2.5–4.5 nm. These values are compatible with the heights of protofilaments reported previously [Conway et al., 2000b; Ding et al., 2002].

[2.1.5] Protofibrils

Protofibrils were observed after 13–15 days long incubation of α -synuclein (80 μ M) in 200 μ l of PBS buffer (50 mM, pH 7.4) at 37°C with continuously shaking at 1000 rpm (see section 3.2.1 in detail for protein aggregation). Images were taken in tapping mode AFM, and analyzed by Scanning probe microscopy software, WSxM 5.0 (see section 3.2.4 in detail for image analysis).

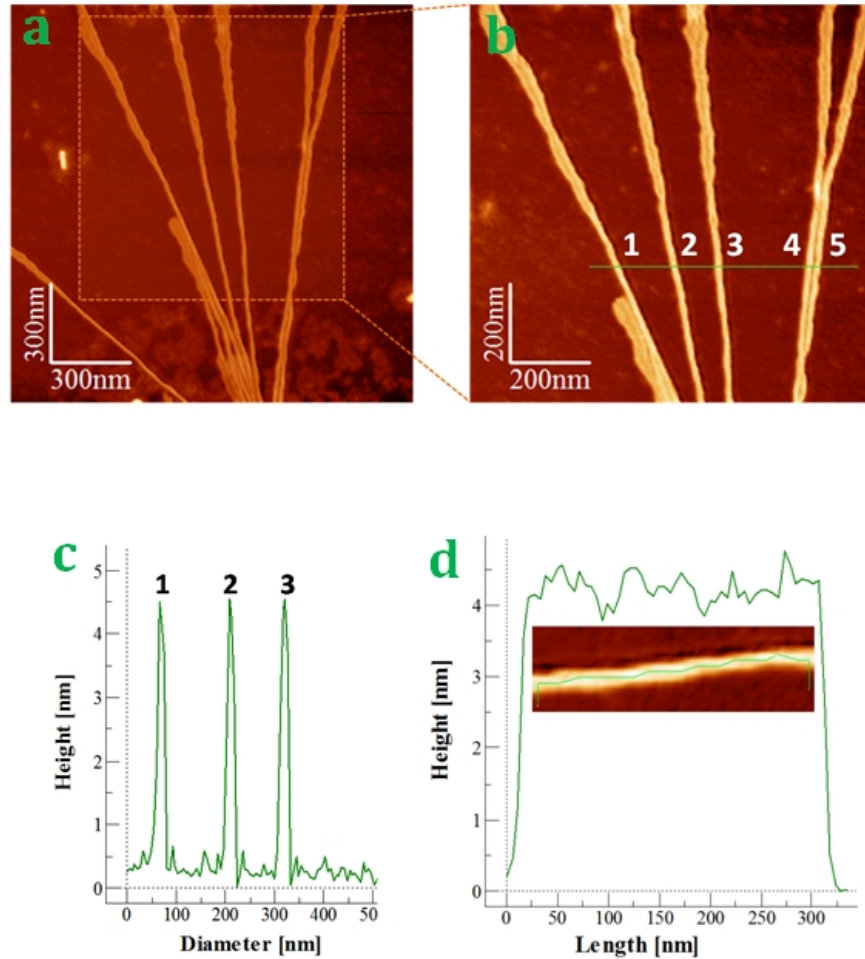


Figure 2.5: AFM image analysis of α -synuclein protofibrils. (a) α -Synuclein protofibrils ($1.5\mu\text{m}\times 1.5\mu\text{m}$), (b) α -Synuclein protofibrils ($1\mu\text{m}\times 1\mu\text{m}$), (c) Height profile of α -Synuclein protofibrils (height was measured between 4 nm – 6 nm), (d) Height profile of single α -synuclein protofibril (~ 4.5 nm).

We observed bundles of α -synuclein mature fibrils only after 5–6 days. The observation of α -synuclein protofibrils after forming α -synuclein mature fibrils shows that the formation of protofibrils was initiated by mature fibrils. Heights of the protofibrils were measured between 4–6 nm. These values are compatible with the heights of protofibrils reported previously [Conway et al., 2000b; Ding et al., 2002].

[2.1.6] Mature fibrils

Apart from studying oligomers, protofilaments and protofibrils we also studied two different kinds of mature fibrils, mature fibrils with twist and mature fibrils without twist. Those fibrils were observed after incubating α -synuclein ($80\ \mu\text{M}$) in $200\ \mu\text{l}$ of PBS buffer ($50\ \text{mM}$, pH 7.4) at $37\ ^\circ\text{C}$ for 3–6 days with continuous shaking at 1000 rpm (see section 3.2.1 in detail for protein aggregation).

Images were taken in tapping mode AFM, and analyzed by Scanning probe microscopy software, WSxM 5.0 (see section 3.2.4 in detail for image analysis).

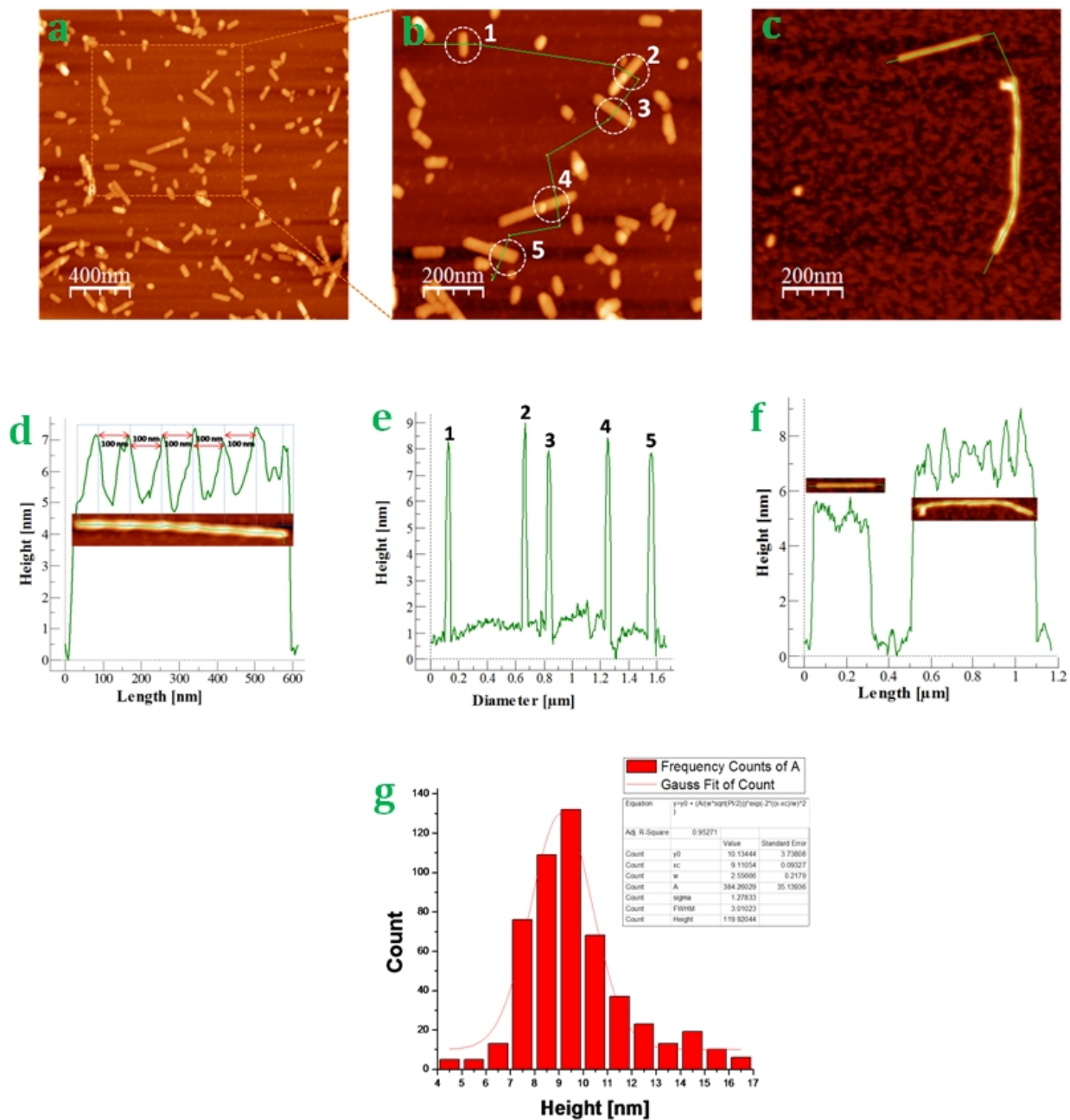


Figure 2.6: AFM image analysis of α -synuclein mature fibrils. (a) α -Synuclein mature fibrils ($2\mu\text{m}\times 2\mu\text{m}$), (b) α -Synuclein mature fibrils ($1\mu\text{m}\times 1\mu\text{m}$), (c) Both twisted and untwisted α -synuclein mature fibrils ($1\mu\text{m}\times 1\mu\text{m}$), (d) Height profile of a single left handed twisted α -synuclein mature fibrils (height was measured between 5–7 nm). The periodical arrangement of twist in the mature fibrils (measured ~ 2 nm depth and ~ 100 nm width), (e) Height profile of α -synuclein mature fibrils (measured between 7–9 nm), (f) Height profile of twisted (~ 8.5 nm) and untwisted (~ 5.5 nm) α -synuclein mature fibrils, (g) Kinetics measurement of α -synuclein mature fibrils. The average height of fully formed mature fibrils was measured around ~ 9 nm.

The height of twisted α -synuclein mature fibrils was measured around 8 nm and height of untwisted α -synuclein mature fibrils was measured around 6 nm. There are several hypothesis have been proposed about the fibrils assembly, which suggest that the protofibrils are formed by the combination of 2–3 protofilaments, furthermore diameter of mature fibrils depends on the formation of protofibrils and protofilaments [Uversky et al., 2002d; Uversky, 2003; Qin et al., 2007].

The processes of formation of protofilaments and protofibrils are not very well understood. There are some studies show that β -strands of the fibrils runs orthogonal to the fibril direction and are hydrogen-bonded, 4.7 Å apart, to form β -sheet parallel to the axis of the fibril [Quin et al., 2007]. X-ray and electron diffraction studies of the α -synuclein fibrils show similar structure [Serpell et al., 2000]. For short peptides the arrangement of the molecules perpendicular to the fibril axis may be fully extended [Makin et al., 2005], or, in larger peptides such as Alzheimer's A β , include a hairpin loop [Fraser et al., 1992].

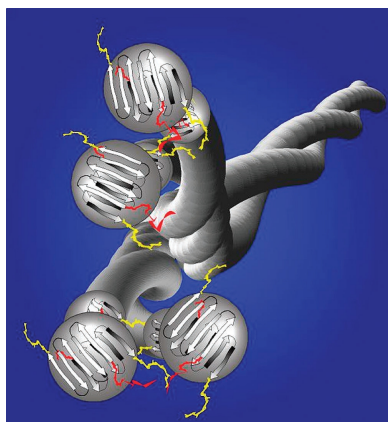


Figure 2.7: Model of the hierarchical structure and the roles of the terminal regions in the assembly of α -synuclein fibril. Two protofilaments are shown interacting via their N- and/or C-terminal regions to form a protofibril. Subsequently, two protofibrils assemble by the interaction of C-terminal fragments to form a mature fibril. [Reproduced from Qin et al., 2007]

Eisenberg and co-workers proposed eight classes of steric zippers, in which the β -strands differ in their arrangement with respect to orientation of their faces, direction, and whether parallel or antiparallel [Sawaya et al., 2007]. Given the 3.5 Å axial distances between adjacent amino acids in an extended β -strand, the length of the β -strands of α -synuclein calculated in this way exceeds the narrowest fiber dimension [Serpell et al., 2000]. Thus, models of the arrangement of α -synuclein molecules with several turn and bend or loop regions were proposed [Der-Sarkissian et al., 2003]. The smallest cross dimension of protofilaments to be ~ 28 Å from both protease-resistant filaments of trypsin digested fibrils and the protofilaments derived from synuclein 30-103 [Qin et al., 2007]. A potential model for α -synuclein protofilaments has been proposed by Qin et al. 2007, given that the protofilament assembled from a polypeptide of ~ 70 amino acid residues, assuming 3.5 Å axial distances between adjacent amino acids in an extended β -strand, with 4.8 Å for the interstrand

distance in a β -sheet, and that the length of the β -strands should not exceed eight amino acids (connected by β -turns), and the maximum number of strands would be seven, assuming all the strands are arranged in a β -sheet plane which in turn assemble into fibrils in-register, although it cannot be eliminated the possibility of only five or six strands [Qin et al., 2007]. The model is shown in **Figure 2.7**, with five strands for clarity. Thus, the fibrillar core of the protofilaments of α -synuclein consists of two β -sheets in which the β -strands are connected by β -turns with seven strands per molecule [Qin et al., 2007].

[2.2] Seeded growth of α -synuclein

Seeds were prepared by the ultrasonication of fully formed α -synuclein mature fibrils, by applying electrical current for total 4 min with intervals of 5 sec. The average height of the seeds was measured around 5 nm; moreover the mature fibrils formed by the initiation of seeds were not so diversified. We measured the heights of α -synuclein mature fibrils initiated by seeds were between 5–7 nm. α -Synuclein aggregation into mature fibrils is very fast when seeds are added to the protein solution. The exposed living ends of the seeds contains hydrophobic surface [Kim et al., 2007], which show strong binding affinity with partially unfolded monomer. That could be the reason why seeds promote α -synuclein aggregation.

Mature fibrils were observed after incubating α -synuclein (80 μ M) and α -synuclein seeds (16 μ M) (4:1 molar ratio) in 200 μ l of PBS buffer (50 mM, pH 7.4) at 37 °C for 3–6 days with continuous shaking at 1000 rpm (see section 3.2.1 in detail for protein aggregation). Images were taken in tapping mode AFM, and analyzed by Scanning probe microscopy software, WSxM 5.0 (see section 3.2.4 in detail for image analysis).

We observed the constant height pattern of α -synuclein mature fibrils induced by seeds by increasing incubation time. The height of α -synuclein mature fibrils induced by seeds was measured around 7 nm. Fibrils growth in a constant height show that the accretion of the α -synuclein monomer to the living ends of the seeds was not random process. Monomeric α -synuclein attach to the living ends of the seeds in a regular pattern. We never observed this kind of regular fibrils growth pattern with constant height in the case of α -synuclein aggregation. The measured height of the fibrils around 7 nm was constant by increasing incubation period of α -synuclein in the presence of seeds. Only lengths of the fibrils were increased by increasing incubation period of α -synuclein in the presence of seeds. These observations suggest that the mature fibrils form directly by attaching at the living ends of the seeds.

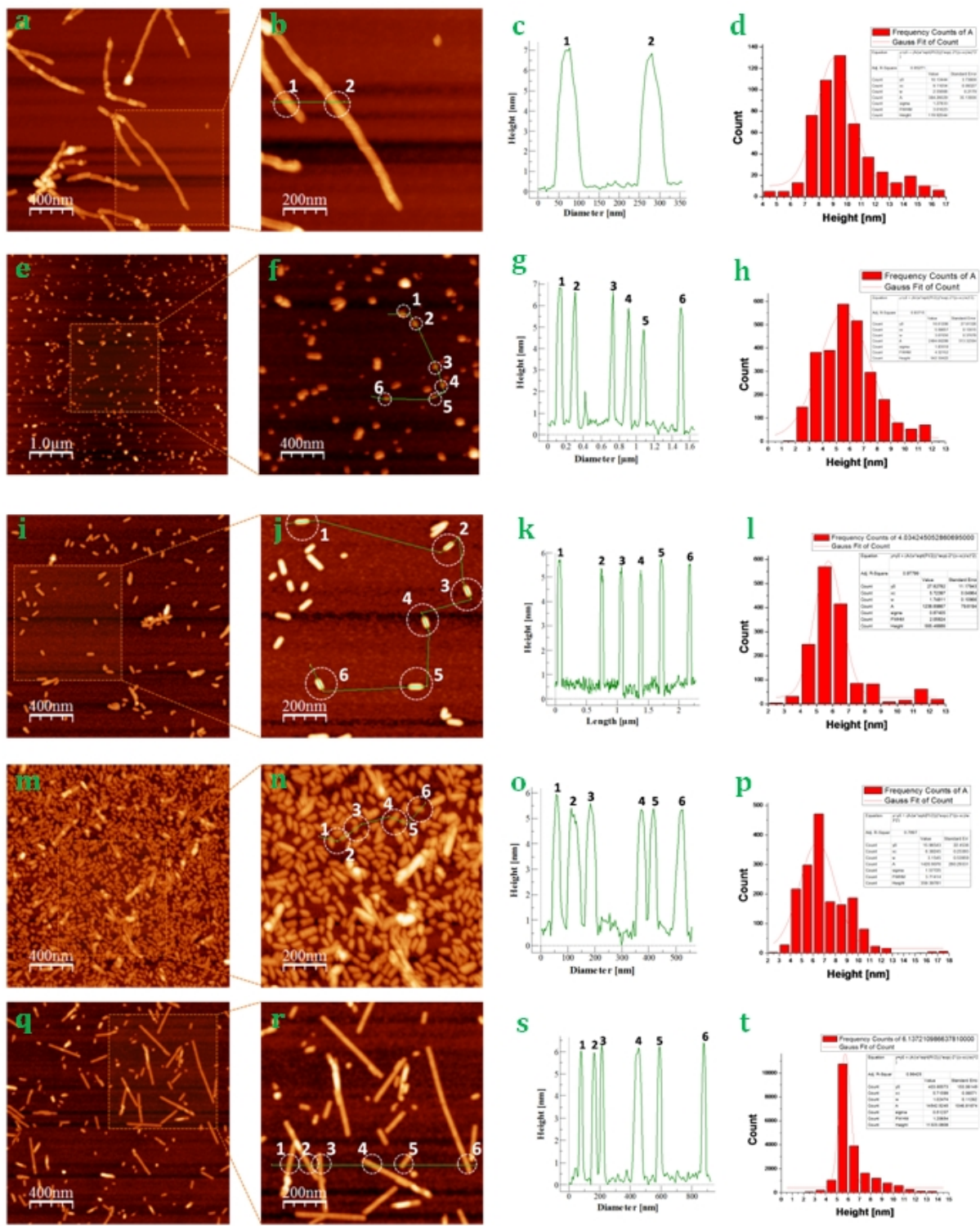


Figure 2.8: AFM image analysis of α -synuclein mature fibrils induced by seeds. (a) α -Synuclein mature fibrils ($2\mu\text{m}\times 2\mu\text{m}$), (b) α -Synuclein mature fibrils ($1\mu\text{m}\times 1\mu\text{m}$), (c) Height profile of α -synuclein mature fibrils (height measured between 6–8 nm), (d) Kinetics measurement of α -synuclein mature fibrils. The average height of mature fibrils was measured around ~ 9 nm, (e) α -Synuclein fragmented fibrils (seeds) ($5\mu\text{m}\times 5\mu\text{m}$), (f) α -

Synuclein fragmented fibril (seeds)($2\mu\text{m}\times 2\mu\text{m}$), (g) Height profile of α -synuclein fragmented fibrils (seeds) (height measured between 3–9 nm), (h) Kinetics measurement of α -synuclein fragmented fibrils (seeds). The average height of fragmented fibrils was measured around ~ 5.5 nm, (i) α -Synuclein mature fibrils initiated by seeds ($2\mu\text{m}\times 2\mu\text{m}$), (j) α -Synuclein mature fibrils initiated by seeds ($1\mu\text{m}\times 1\mu\text{m}$), (k) Height profile of α -synuclein mature fibrils initiated by seeds (height was measured around ~ 5.5 nm), (l) Seed dependent aggregation kinetics of α -synuclein mature fibrils. The average height of mature fibrils was measured around ~ 5.5 nm, (m) α -Synuclein mature fibrils initiated by seeds ($2\mu\text{m}\times 2\mu\text{m}$), (n) α -Synuclein mature fibrils initiated by seeds ($1\mu\text{m}\times 1\mu\text{m}$), (o) Height profile of α -synuclein mature fibrils initiated by seeds (height was measured between 5–6 nm), (p) Seed dependent aggregation kinetics of α -synuclein mature. The average height of mature fibrils was measured around ~ 6.5 nm, (q) α -Synuclein mature fibrils initiated by seeds ($2\mu\text{m}\times 2\mu\text{m}$), (r) α -Synuclein mature fibrils initiated by seeds ($1\mu\text{m}\times 1\mu\text{m}$), (s) Height profile of α -synuclein mature fibrils initiated by seeds (height was measured between 6–7 nm), (t) Seed dependent aggregation kinetics of α -synuclein mature. The average height of mature fibrils was measured around ~ 6 nm.

[2.3] α -Synuclein dimers and constructs

[2.3.1] NN-terminal dimer

NN-terminal dimers were formed by adding two cystein mutated α -synuclein at N-terminal region. The cystein mutated α -synuclein at N-terminal region joined together through disulfide bond and it formed NN-terminal dimer.

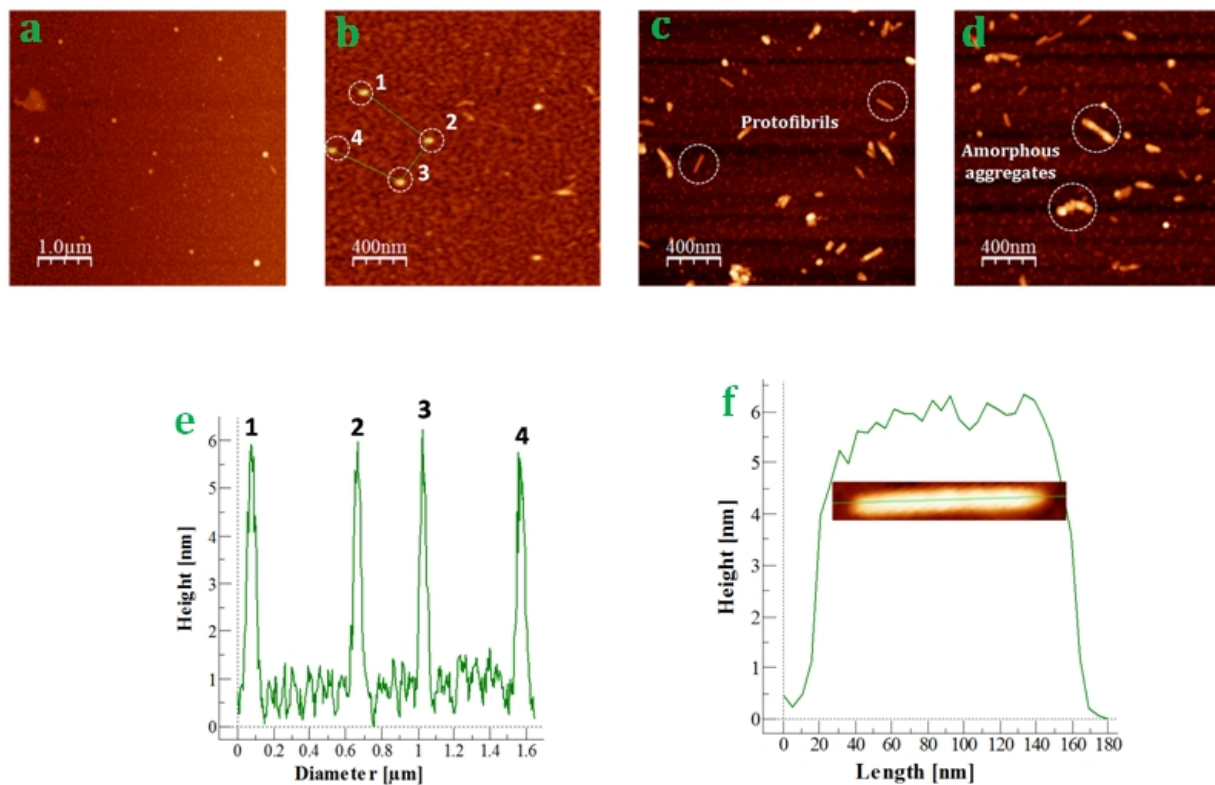


Figure 2.9: AFM image analysis of NN-terminal dimer. (a) Oligomers of NN-terminal dimer ($5\mu\text{m}\times 5\mu\text{m}$), (b) Oligomers of NN-terminal dimer ($2\mu\text{m}\times 2\mu\text{m}$), (c, d) AFM image of NN-terminal dimer, oligomers, protofibrils and amorphous aggregates: (c) NN-terminal dimer protofibrils ($2\mu\text{m}\times 2\mu\text{m}$), (d) NN-terminal dimer amorphous

aggregates (2 μ m \times 2 μ m), (e) Height profile of NN-terminal dimer oligomers (height was measured between 5–6 nm), (f) Height profile of single protofibril of NN-terminal dimer (~6 nm).

NN-terminal dimer aggregates were observed by incubating **NN**-terminal dimer (80 μ M) in 200 μ l of PBS buffer (50 mM, pH 7.4) at 37°C with continuously shaking at 1000 rpm (see section 3.2.1 in detail for protein aggregation). Images were taken in tapping mode AFM, and analyzed by Scanning probe microscopy software, WSxM 5.0 (see section 3.2.4 in detail for image analysis).

The oligomers formed by **NN**-terminal dimer have height between 5–6 nm. The height of the very short protofibrils formed by **NN**-terminal dimer was around 6 nm.

Our studies show that the **NN**-terminal dimer aggregates to form globules, protofibrils and amorphous aggregates. We did not observe mature fibrils in the case of **NN**-terminal dimer aggregation. It formed globular oligomers of height around 5 nm and very short protofibrils of height around 5–6 nm, and then it formed amorphous aggregates. In normal aggregation condition α -synuclein forms long and mature fibrils of average height around 8 nm. The formation of amorphous aggregates of **NN**-terminal dimer indicates that the oligomers and protofibrils formation does not influenced by disulfide bond present in the **NN**-terminal dimer, whereas the mature fibrils formation influenced by the disulfide bond present in the **NN**-terminal dimer. The free N- and C-terminal of the α -synuclein plays an important role in the formation of mature fibrils. This is the reason why we never observed mature fibrils of **NN**-terminal dimer. This indicates that the NAC region of **NN**-terminal dimer plays an important role in the formation of oligomers, protofilaments and protofibrils but not in the formation of mature fibrils.

[2.3.2] CC-terminal dimer

CC-terminal dimers were formed by adding two cystein mutated α -synuclein at C-terminal region. The cystein mutated α -synuclein at C-terminal region joined together through disulfide bond and it formed **CC**-terminal dimer.

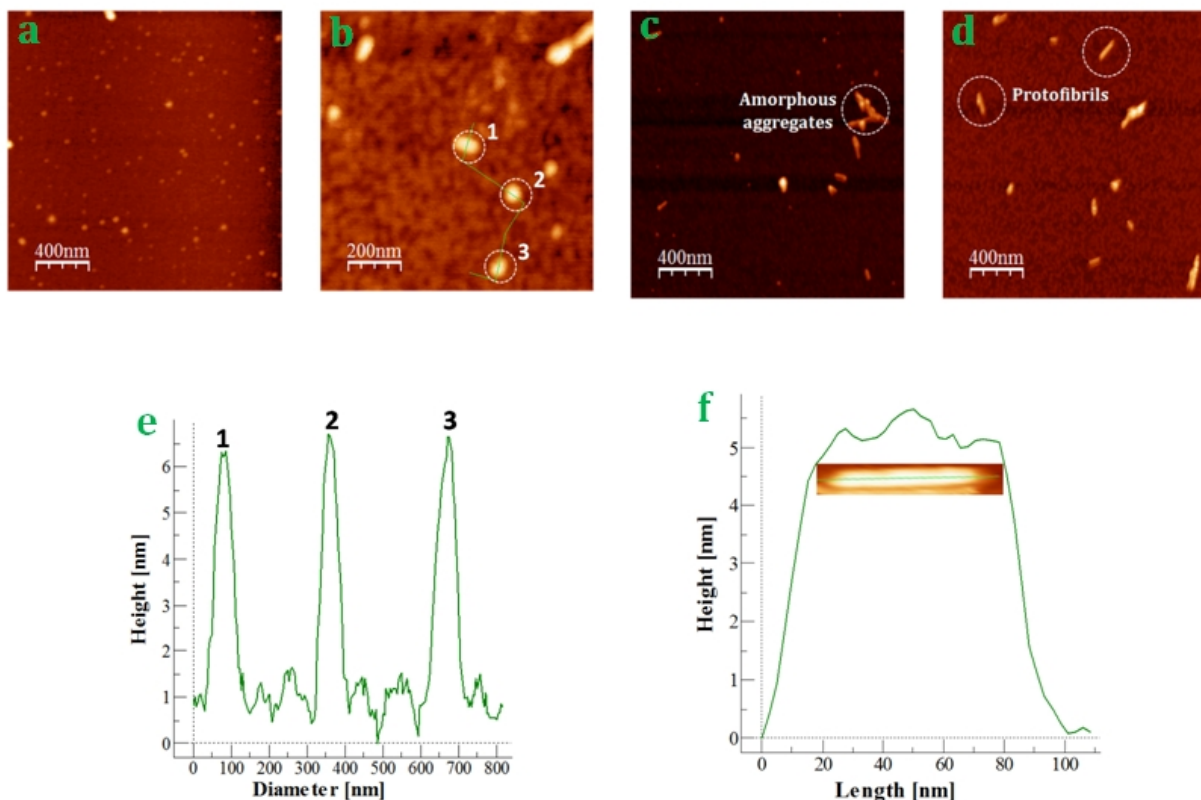


Figure 2.10: AFM image analysis of CC-terminal dimer. (a) Oligomers of CC-terminal dimer ($2\mu\text{m}\times 2\mu\text{m}$), (b) Oligomers of CC-terminal dimer ($1\mu\text{m}\times 1\mu\text{m}$), (c, d) AFM image of oligomers, protofibrils and amorphous aggregates of CC-terminal dimer: (c) Amorphous aggregates of CC-terminal dimer ($2\mu\text{m}\times 2\mu\text{m}$), (d) Protofibrils of CC-terminal dimer ($2\mu\text{m}\times 2\mu\text{m}$), (e) Height profile of oligomers of CC-terminal dimer (height was measured between 5–6 nm), (f) Height profile of single protofibril of CC-terminal dimer (height was measured around ~5 nm).

CC-terminal dimer aggregates were observed by incubating CC-terminal dimer ($80\ \mu\text{M}$) in $200\ \mu\text{l}$ of PBS buffer ($50\ \text{mM}$, pH 7.4) at 37°C with continuously shaking at 1000 rpm (see section 3.2.1 in detail for protein aggregation). Images were taken in tapping mode AFM, and analyzed by Scanning probe microscopy software, WSxM 5.0 (see section 3.2.4 in detail for image analysis).

The oligomers formed by CC-terminal dimer have height between 5–6 nm. The height of the very short protofibrils formed by CC-terminal dimer was around 6 nm.

Our studies show that the CC-terminal dimer aggregates to form globules, protofibrils and amorphous aggregates. We did not observe mature fibrils in the case of CC-terminal dimer aggregation. It formed globular oligomers of height around 5 nm and very short protofibrils of height around 5–6 nm, and then it formed amorphous aggregates. In normal aggregation condition α -synuclein forms long and mature fibrils of average height around 8 nm. The formation of amorphous aggregates of CC-terminal dimer indicates that the oligomers and protofibrils formation

does not influenced by disulfide bond present in the **CC**-terminal dimer, whereas the mature fibrils formation influenced by the disulfide bond present in the **CC**-terminal dimer. The free N- and C-terminal of the α -synuclein plays an important role in the formation of mature fibrils. This is the reason why we never observed mature fibrils of **CC**-terminal dimer. This indicates that the NAC region of **CC**-terminal dimer plays an important role in the formation of oligomers, protofilaments and protofibrils but not in the formation of mature fibrils.

[2.3.3] NC-terminal dimer

NC-terminal dimers were formed by adding α -synuclein through N- and C-terminal region. Methionine of N-terminal region covalently attached through peptide bond with the alanine of C-terminal region.

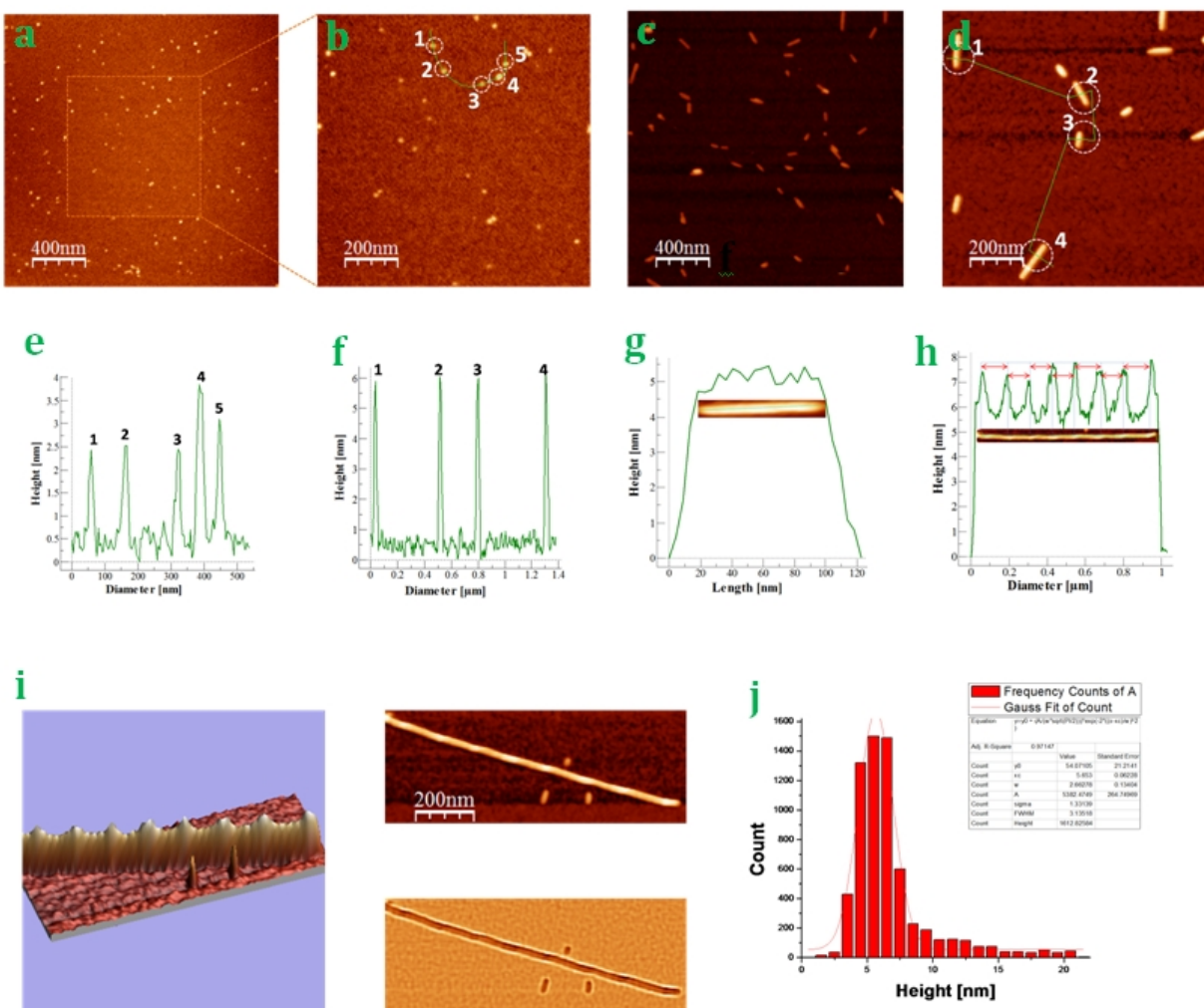


Figure 2.11: AFM image analysis of NC-terminal dimer. (a) Oligomers of NC-terminal dimer ($2\mu\text{m}\times 2\mu\text{m}$), (b) Oligomers of NC-terminal dimer ($1\mu\text{m}\times 1\mu\text{m}$), (c) Protofibrils of NC-terminal dimer ($2\mu\text{m}\times 2\mu\text{m}$), (d) Protofibrils of NC-terminal dimer ($1\mu\text{m}\times 1\mu\text{m}$), (e) Height profile of oligomers of NC-terminal dimer (height was

measured between 2–4 nm), (f) Protofibrils height profile of NC-terminal dimer (height was measured ~6 nm), (g) Height profile of single protofibril of NC-terminal dimer (height was measured around ~5 nm), (h) Height profile of a single left handed twisted NC-terminal dimer mature fibrils (height was measured between 5.5–7.5 nm). The periodical arrangement of twist in the mature fibrils showed ~2 nm depth and ~130 nm width of the twisted fibrils. (i) 3D topography of mature fibrils of NC-terminal dimer (height was measured between 5.5–7.5 nm). (j) Kinetics measurement of mature fibrils of NC-terminal dimer. The average height of fully formed mature fibrils was around ~6 nm.

NC-terminal dimer aggregates were observed by incubating **NC-terminal dimer** (80 μ M) in 200 μ l of PBS buffer (50 mM, pH 7.4) at 37°C with continuously shaking at 1000 rpm (see section 3.2.1 in detail for protein aggregation). Images were taken in tapping mode AFM, and analyzed by Scanning probe microscopy software, WSxM 5.0 (see section 3.2.4 in detail for image analysis).

In the case of **NC-terminal dimer** we observed microns long untwisted mature fibrils of height around 6 nm and twisted mature fibrils of height around 7 nm. The periodicity of twisted fibrils in **NC-terminal dimer** was longer than the periodicity of α -synuclein mature fibrils. We have observed around 130 nm long twists in **NC-terminal dimer** mature fibrils compared to 100 nm twists in α -synuclein mature fibrils.

We observed that the aggregation process of **NC-terminal dimer** was faster than that of α -synuclein, and it leads to spherical oligomers of height between 2–4 nm. The oligomers of **NC-terminal dimer** formed faster but smaller than in the case of the α -synuclein. **NC-terminal dimer** formed microns long mature fibrils that we never observed in the case of α -synuclein. These observations suggest that only one N-terminal region and only one C-terminal region in **NC-terminal dimer** participates in the formation of protofilaments and protofibrils. This is the reason why **NC-terminal dimer** formed microns long mature fibrils of height around 5 nm.

[2.3.4] Synucle-Nuclein constructs

Synucle-Nuclein constructs were prepared by adding end to end C-terminal region of Synucle (α -synuclein without N-terminal) with N-terminal region of Nuclein (α -synuclein without C-terminal). Synucle-nuclein is a mutated construct of α -synuclein. This construct was prepared by adding two mutated α -synuclein; one α -synuclein with deleted N-terminal region another α -synuclein with deleted C-terminal region. As the name Synucle-nuclein indicates that synucle does not contains N-terminal region and Nuclein does not contains C-terminal region.

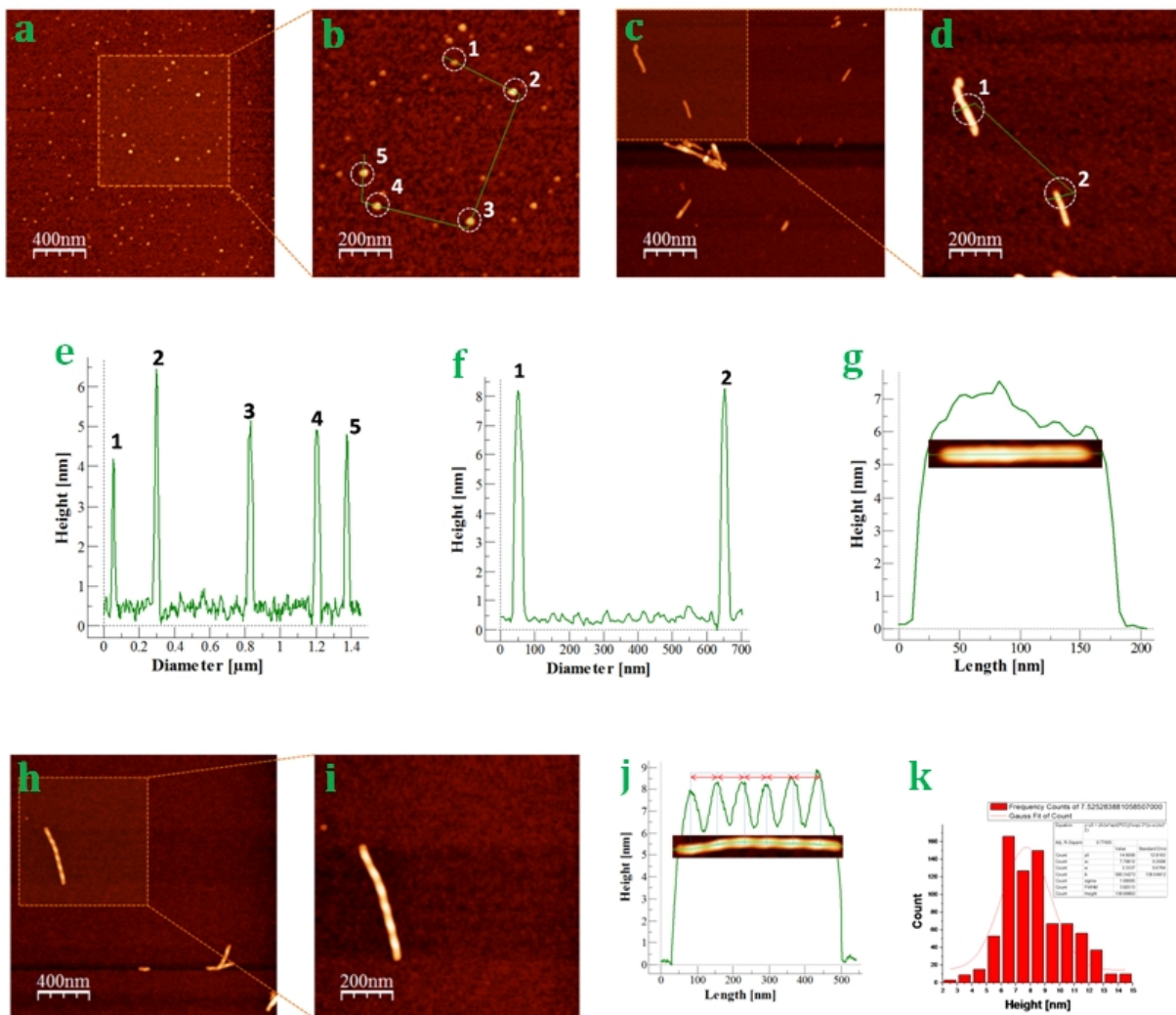


Figure 2.12: AFM image analysis of Synucle-Nuclein construct. (a) Oligomers of Synucle-Nuclein construct ($2\mu\text{m}\times 2\mu\text{m}$), (b) Oligomers of Synucle-Nuclein construct ($1\mu\text{m}\times 1\mu\text{m}$), (c) Mature fibrils of Synucle-Nuclein construct ($2\mu\text{m}\times 2\mu\text{m}$), (d) Mature fibrils of Synucle-Nuclein construct ($1\mu\text{m}\times 1\mu\text{m}$), (e) Height profile of oligomers of Synucle-Nuclein construct (height was measured between 3–6 nm), (f) Height profile of mature fibrils of Synucle-Nuclein construct (height of the oligomers varying between 6–8 nm). (g) Height profile of single fibril of Synucle-Nuclein construct (height was consistent around ~ 7 nm), (h) Twisted mature fibrils of Synucle-Nuclein construct ($2\mu\text{m}\times 2\mu\text{m}$), (i) Twisted mature fibrils of Synucle-Nuclein construct ($1\mu\text{m}\times 1\mu\text{m}$), (j) Height profile of single left handed twisted mature fibril of Synucle-Nuclein construct (height was measured between 6–9 nm), (k) Kinetics measurement of Synucle-Nuclein construct. The average height of fully formed mature fibrils was measured around ~ 7.5 nm.

Synucle-Nuclein aggregates were observed by incubating Synucle-Nuclein construct ($80\ \mu\text{M}$) in $200\ \mu\text{l}$ of PBS buffer ($50\ \text{mM}$, pH 7.4) at 37°C with continuously shaking at 1000 rpm (see section 3.2.1 in detail for protein aggregation). Images were taken in tapping mode AFM, and analyzed by Scanning probe microscopy software, WSxM 5.0 (see section 3.2.4 in detail for image analysis).

Synucle-Nuclein construct also formed oligomers and mature fibrils; however the aggregation process was slower than the α -synuclein. Synucle-Nuclein aggregate to formed spherical oligomers of height between 3–6 nm. It formed protofilaments and mature fibrils of height between 6–8 nm. Synucle-Nuclein construct formed untwisted mature fibrils of height around 6 nm. There are some twists we have observed in Synucle-Nuclein mature fibrils and the length of twist was smaller than the α -synuclein mature fibrils. In case of Synucle-Nuclein mature fibrils we observed twist around 70 nm in length which was less than the twist in α -synuclein (100 nm).

As it have been reported previously that the NAC region of the α -synuclein only plays an important role in the formation of beta sheet (fibrillar core) like structure, and N- and C-terminal regions play an important role in the formation of outer part of the mature fibrils [Qin et al., 2007]. In case of Synucle-nuclein construct, two NAC region forms more beta sheet like structure (core part of the fibril) and thicker fibrils compare to the single NAC region in α -synuclein. This is the reason why Synucle-Nuclein constructs forms mature fibrils of short in length compare to mature fibrils of α -synuclein.

[2.4] Amyloid-beta (A β) aggregation

We also studied the aggregation and characterization of A β protein. Mature fibrils were generated by incubating A β (80 μ M) in 200 μ l of PBS buffer (50 mM, pH 7.4) at 37 °C for 3–6 days with continuous shaking at 1000 rpm (see section 3.2.1 in detail for protein aggregation). Images were taken in tapping mode AFM, and analyzed by Scanning probe microscopy software, WSxM 5.0 (see section 3.2.4 in detail for image analysis).

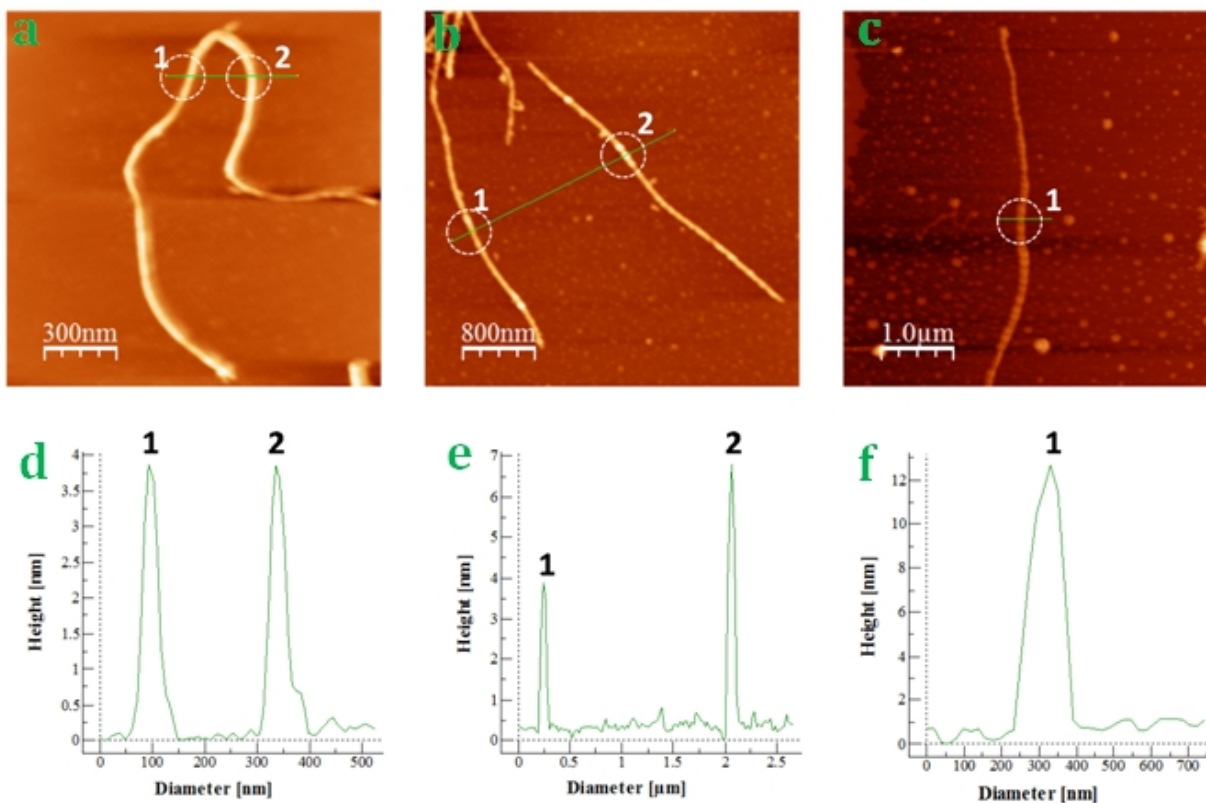


Figure 2.13: AFM image analysis of A β mature fibrils. (a) A β mature fibrils of height ~ 4.5 nm ($1.5\mu\text{m}\times 1.5\mu\text{m}$), (b) A β mature fibrils of height ~ 6 nm ($4\mu\text{m}\times 4\mu\text{m}$), (c) A β mature fibrils of height ~ 11 nm ($5\mu\text{m}\times 5\mu\text{m}$), (d, e, f) Height profile of different kind of mature fibrils measured by nanoscope.

It is well known that amyloid-beta aggregates to form insoluble fibrillar object which is normally associated with the Alzheimer's disease. We observed three different heights of mature fibrils during A β aggregation. First, we measured height of the mature fibrils around 4 nm in 2–3 days. Second, we measured height of the mature fibrils around 6 nm in 3–4 days. Third, the very wide and twisted mature fibrils of height around 11 nm were observed in 6–7 days.

[2.5] Effect of 14-3-3 η on α -synuclein aggregation

[2.5.1] Interaction between 14-3-3 η and α -synuclein monomer

In this case we tried to monitor any possible interaction of 14-3-3 η with α -synuclein monomer by NMR and SPR. We did not get any evidence of interaction between monomeric form of α -synuclein and 14-3-3 η .

NMR experiments were performed in PBS buffer (pH 7.4), with 10% D₂O (v/v), 0.02% NaN₃ (w/v) and 5 mM DTT. [¹H-¹⁵N]-HSQC spectra were recorded at 283K on a 600 MHz Bruker spectrometer equipped with a triple resonance probe. All NMR data were processed and analyzed

using NMRPipe (Delaglio F) and Sparky (T. D. Goddard and D. G. Kneller, University of California, San Francisco) software packages.

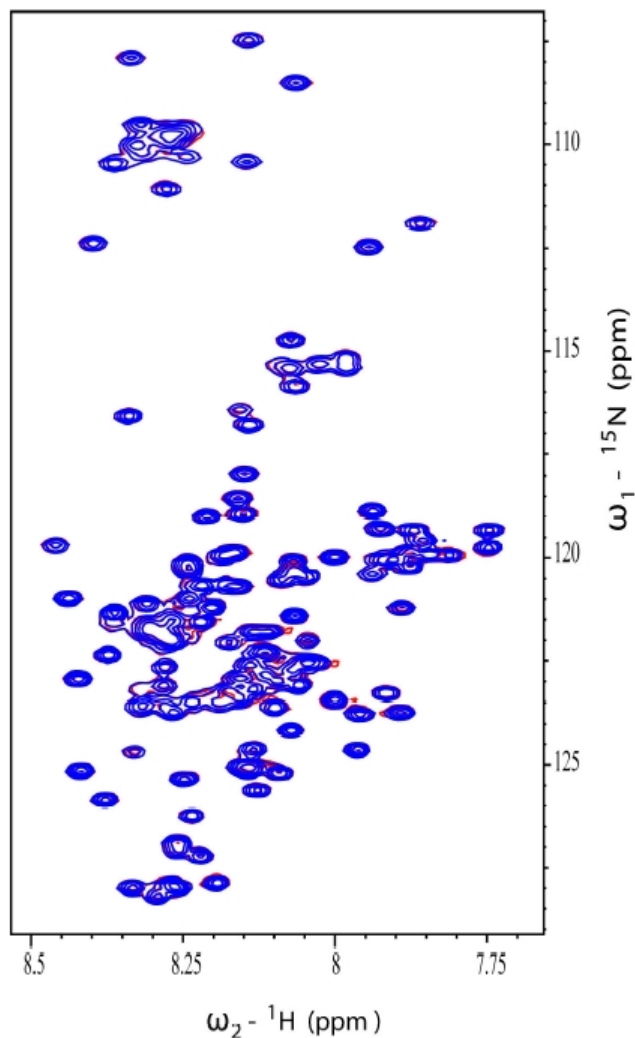


Figure 2.14: NMR analysis of interaction between α -synuclein and 14-3-3 η . Overlay of ^{15}N -labeled α -syn $[^1\text{H}-^{15}\text{N}]$ HSQC spectra recorded with (red) or w/o (blue) 3-fold molar excess of 14-3-3 η . Marginal difference in spectra. [Courtesy from Bubacco's lab Padova]

In **Figure 2.14**, the blue spectra of α -synuclein (without 14-3-3 η) are overlapped with the red spectra of α -synuclein (with 3 fold excess of 14-3-3 η). Very marginal differences appeared between these two spectra. This indicates that α -synuclein monomer does not interact with 14-3-3 η .

We also investigated this interaction by SPR. SPR analyses were carried out in a Biacore X instrument (GE Healthcare), with the technical assistance of Dr. Stefania Sarno and Dr. Maria Ruzzene (Dipartimento di Chimica Biologica, Universita degli Studi di Padova). The Running Buffer used for experiments on Ni-NTA Sensor Chip was composed of 10 mM HEPES, 150 mM NaCl, 50 μM EDTA, pH 7.4. Chip functionalization was made firstly injecting Ni $^{2+}$ solution (10 mM HEPES, 150 mM NaCl, 50 μM EDTA, 500 μM NiCl $_2$, pH 7.4) to create Ni $^{2+}$ -NTA complex selectively in analysis cell, then 2 $\mu\text{g/ml}$ HT 57-102 or 2.4 $\mu\text{g/ml}$ HT α -synuclein, solubilized in Running Buffer. For binding analysis, increasing amount of analyte was injected as required for the calculation of K_d ,

spanning from 1/10 to 10 times the molar concentration of ligand bounded to analysis cell. Regeneration was performed with Regeneration Buffer (10 ml HEPES, 150 mM NaCl, 350mM EDTA, pH 8.3).

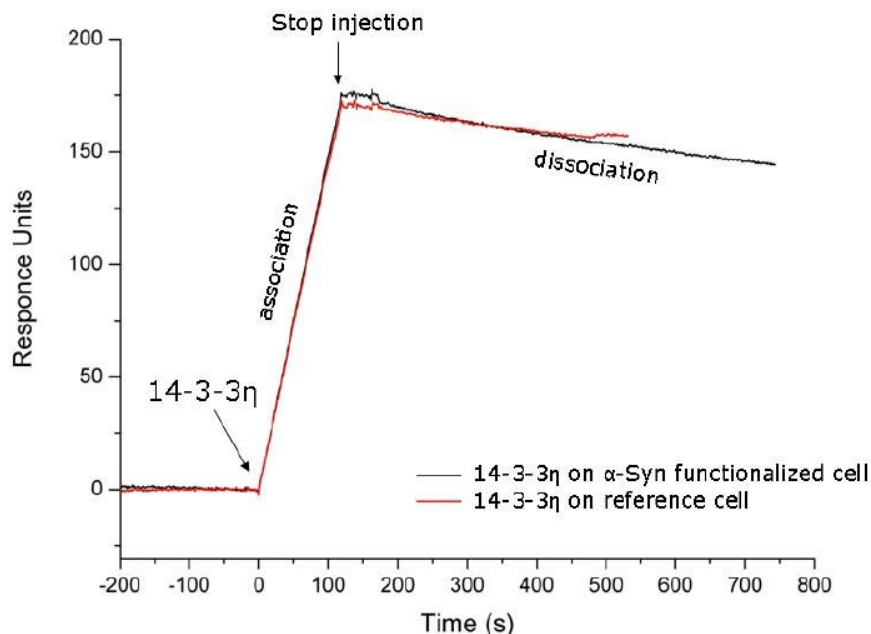


Figure 2.15: SPR analysis of interaction between α -synuclein and 14-3-3 η . SPR signal of 1.3 μ M 14-3-3 η injection (black arrow) on α -syn functionalized biacore chip (black line) or reference empty cell (red line). No differences between these two signals can be detected. [Courtesy from Bubacco's lab Padova]

In **Figure 2.15**, the red signal of 14-3-3 η on reference cell is completely overlapped with the black signal of 14-3-3 η on α -synuclein functionalized cell. This also indicates that α -synuclein monomer does not interact with 14-3-3 η . Both results from NMR and SPR suggest that α -synuclein monomer in the experimental conditions does not have any binding affinity with 14-3-3 η .

[2.5.2] Effect of 14-3-3 η on α -synuclein mature fibrils

α -Synuclein mature fibrils were generated by incubating α -synuclein (80 μ M) in 200 μ l of PBS buffer (50 mM, pH 7.4) at 37 $^{\circ}$ C for 3–6 days with continuous shaking at 1000 rpm. Fully formed mature fibrils of α -synuclein (80 μ M) were incubated with 14-3-3 η (20 μ M) (4:1 molar ratio) at 37 $^{\circ}$ C for 72 h with continuous shaking at 1000 rpm. Images were taken in tapping mode AFM, and analyzed by Scanning probe microscopy software, WSxM 5.0 (see section 3.2.4 in detail for image analysis). The morphological data for the fibril species were obtained by the averaging a large number of individual fibrils ($n > 200$).

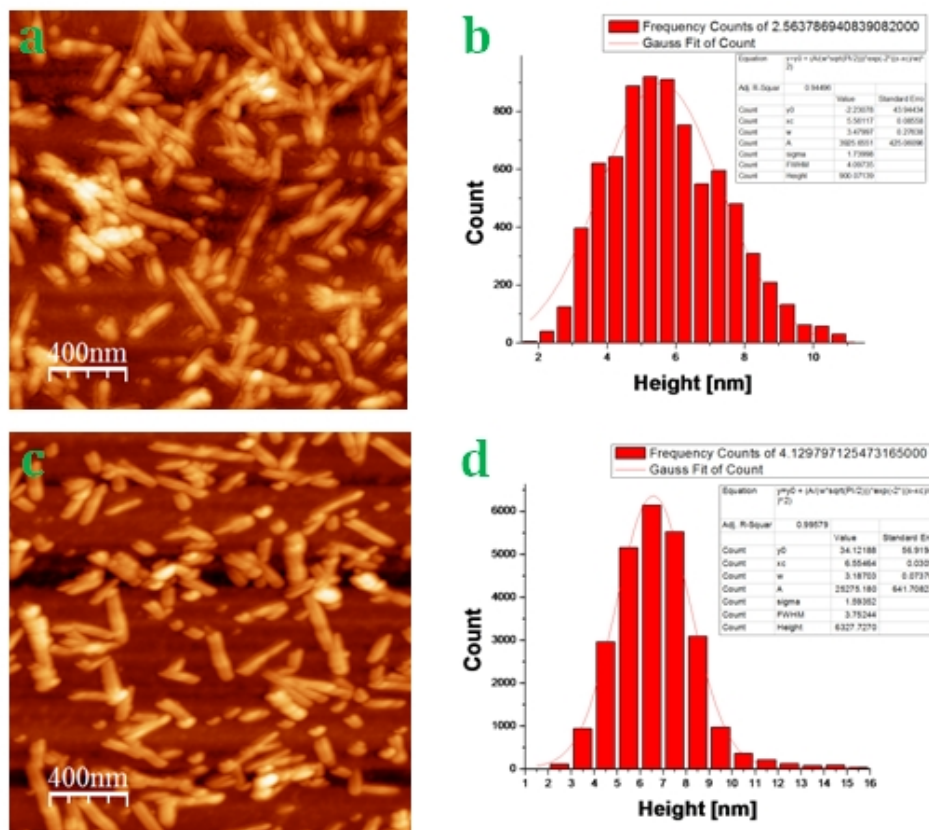


Figure 2.16: AFM image analysis of α -synuclein mature fibrils obtained in the presence and absence of 14-3-3 η . (a) Homogeneous appearance of α -synuclein mature fibrils ($2\mu\text{m}\times 2\mu\text{m}$), (b) Kinetics measurement of α -synuclein mature fibrils of height ~ 6 nm, (c) Homogeneous appearance of α -synuclein mature fibrils after incubation with 14-3-3 η at 37°C and 1000 rpm for 72 h ($2\mu\text{m}\times 2\mu\text{m}$), (d) Kinetics measurement of normal normal α -synuclein mature fibrils of height ~ 6 nm.

The average height of the α -synuclein mature fibrils was measured around 6 nm. We did not observe any significant change in morphology and kinetics of the α -synuclein mature fibrils even after incubating with 14-3-3 η . The height of α -synuclein mature fibrils measured after incubation with 14-3-3 η was around 6 nm. This observation suggests that 14-3-3 η does not have any effect also on mature fibrils; moreover 14-3-3 η does not interact with α -synuclein mature fibrils.

[2.5.3] Effect of 14-3-3 η on α -synuclein oligomers

Protein aggregates were generated by incubating 14-3-3 η (20 μM) and α -synuclein (80 μM) following different stoichiometric ratio (1:1, 1:4, 1:7, 1:12, 1:20, 1:24, 1:30) in PBS buffer (50 mM, pH 7.4) at 37°C for 12–24 h with continuous shaking at 1000 rpm. Images were taken in tapping mode AFM, and analyzed by Scanning probe microscopy software, WSxM 5.0 (see section 3.2.4 in

detail for image analysis). The morphological data for the fibril species were obtained by the averaging a large number of individual fibrils ($n > 200$).

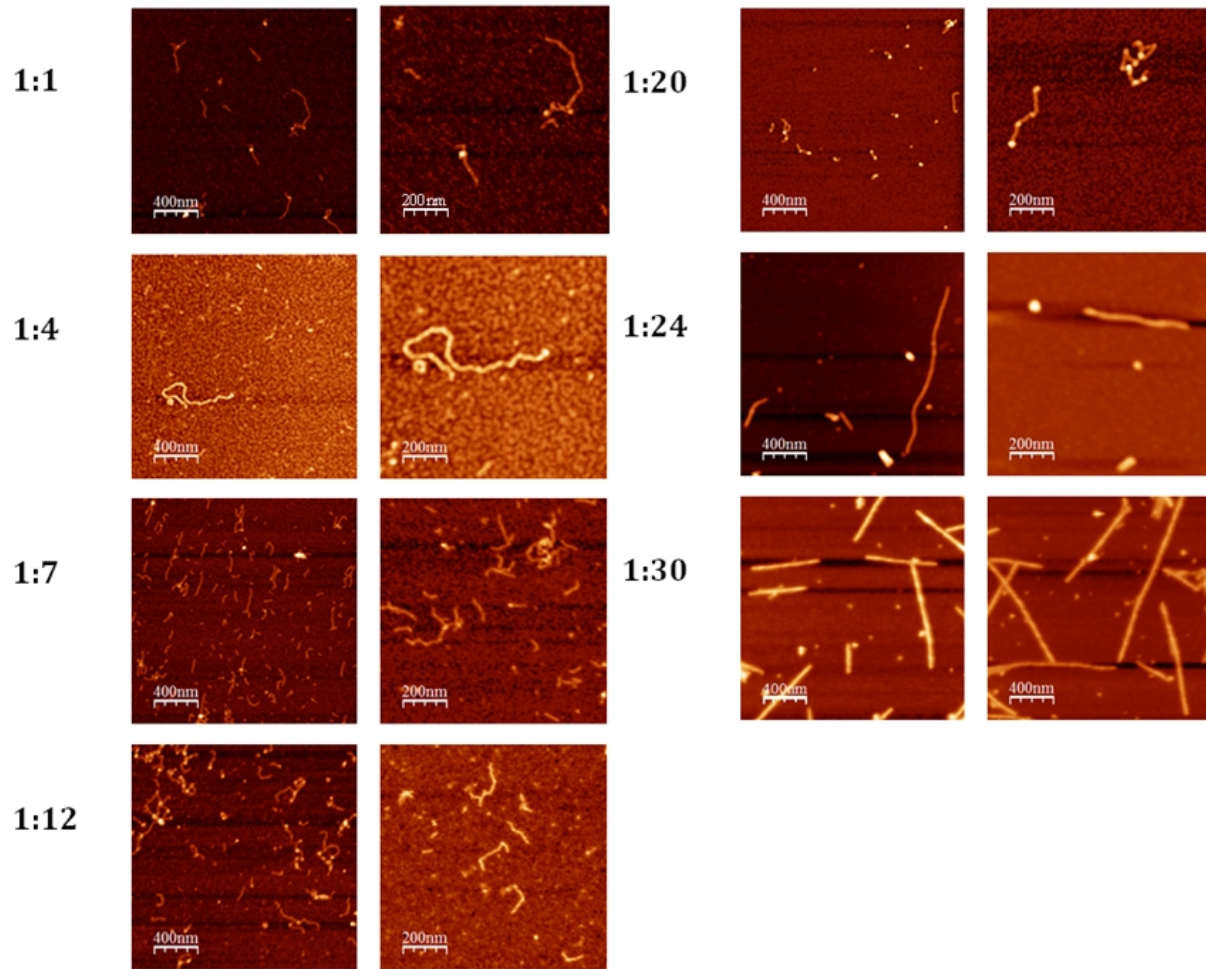
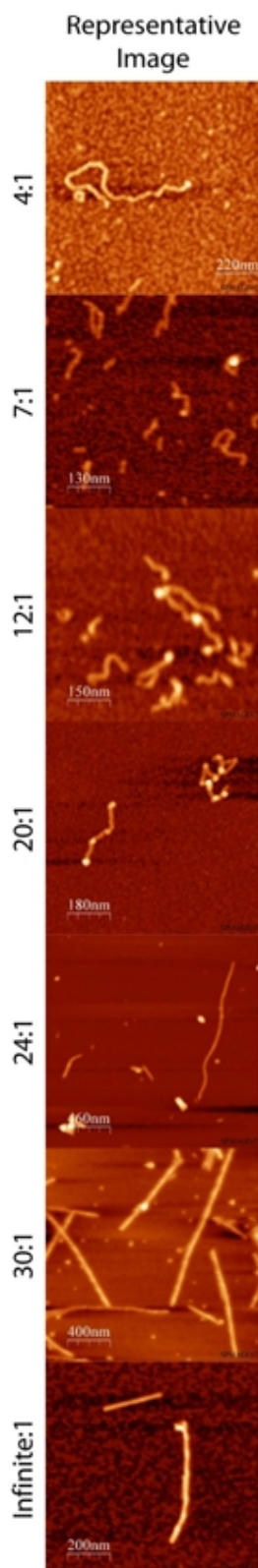
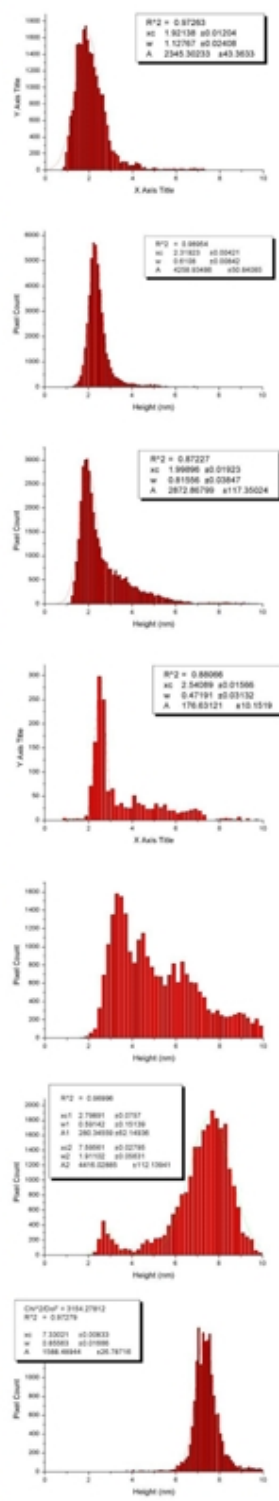


Figure 2.17: AFM image of curved object obtained during α -synuclein aggregation in the presence 14-3-3 η by following different stoichiometric ratio (1:1, 1:4, 1:7, 1:12, 1:20, 1:24, 1:30) of 14-3-3 η and α -synuclein modulate the aggregation process of α -synuclein.



Local Height Distribution



Local Curvature Distribution

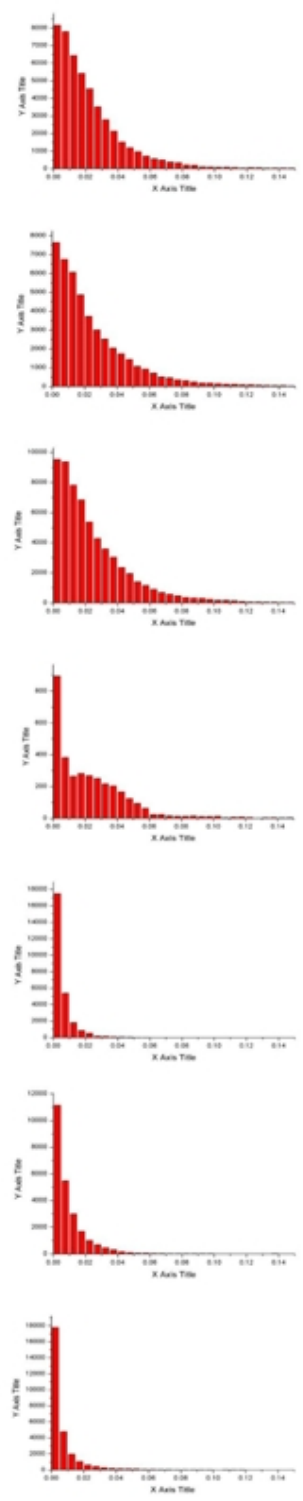


Figure 2.18: Height and curvature distribution of curved object following different stoichiometric ratio of 14-3-3 η and α -synuclein (1:1, 1:4, 1:7, 1:12, 1:20, 1:24, 1:30 1: ∞).

These images show that 14-3-3 η interacts only with the α -synuclein oligomers. 14-3-3 η modulates the aggregation pathway of α -synuclein. We observed flexible curved object of height around 2 nm in the presence of 14-3-3 η instead of mature and rigid fibrils of height around 8 nm of α -synuclein. All through the study of α -synuclein aggregation in the presence of 14-3-3 η proteins, we found that 14-3-3 η modulates the aggregation pathway of α -synuclein by acting on its aggregation intermediates. We have used different stoichiometric ratio of 14-3-3 η and α -synuclein to study the effect of 14-3-3 η on α -synuclein aggregation. By using 1:4 stoichiometric ratios of 14-3-3 η and α -synuclein we observed flexible curved and circular objects of height around 2 nm. At 1:20 stoichiometric ratio of 14-3-3 η and α -synuclein we observed flexible and segmented objects which are different from the curved objects. At this level of 14-3-3 η in α -synuclein aggregation, α -synuclein forms segmented objects of height between 2–4 nm because of low molar concentration of 14-3-3 η . At 1:24 stoichiometric ratio of 14-3-3 η and α -synuclein we observed banana shaped objects of height between 2–6 nm. At 1:30 stoichiometric ratio of 14-3-3 η and α -synuclein we observed straight and mature fibrils of height around 7 nm.

We observed that the different stoichiometric ratio of 14-3-3 η and α -synuclein plays an important role in aggregation and modulation of aggregation pathway. Higher concentration of 14-3-3 η in α -synuclein solution forms more flexible and curved object of height around 2 nm than the lower 14-3-3 η concentrated solution. In normal aggregation condition α -synuclein aggregates to form very long and mature fibrils of height around 8 nm. By decreasing concentration of 14-3-3 η in α -synuclein aggregation, α -synuclein forms less curved and more rigid object. Moreover, we observed that by using 1:24 stoichiometric ratio of 14-3-3 η and α -synuclein, the curvature and flexibility of the intermediate object shifted into the rigid and straight mature fibrils.

Immunogold labeling experiment with curved objects

AFM analysis of curved objects suggests that 14-3-3 η influence the α -synuclein aggregation at oligomeric stage. We studied immunogold labeling experiment with α -synuclein and 14-3-3 η to understand exactly how 14-3-3 η influences the α -synuclein aggregation. First, we prepared immunogold labeled 14-3-3 η specific antibodies, and then we incubated immunogold labeled 14-3-3 η specific antibodies with α -synuclein and 14-3-3 η in PBS buffer (50 mM, pH 7.4) at

37 °C for 12–24 h with continuous shaking at 1000 rpm. Curved object with immunogold labeled 14-3-3 η specific antibody were analyzed by AFM and TEM.

AFM analysis of immunogold labeled curved object of α -synuclein with 14-3-3 η

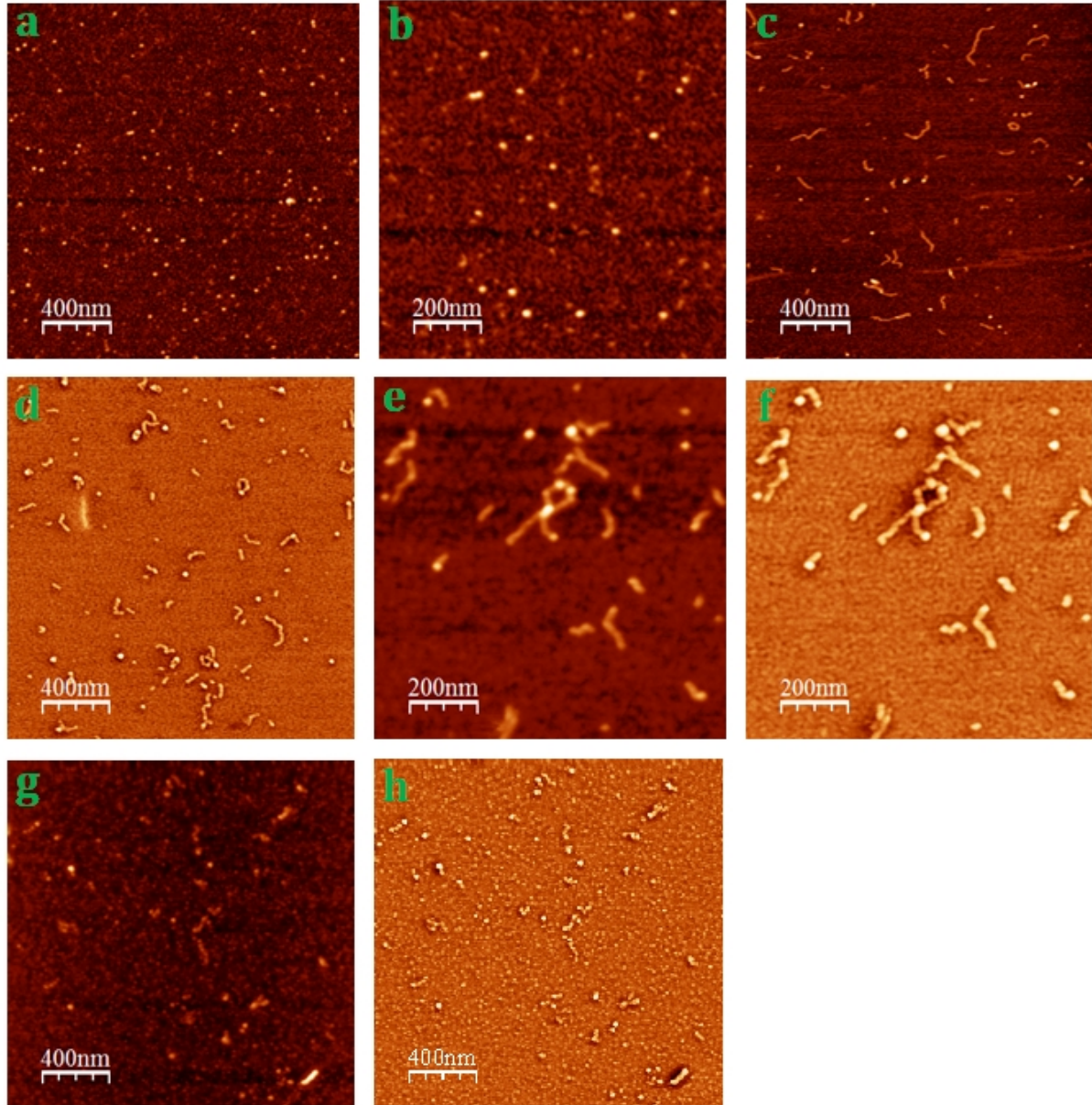


Figure 2.19: AFM image of immunogold labeled curved object α -synuclein with 14-3-3 η in the presence of 14-3-3 η specific antibody. (a, b) 14-3-3 η specific antibody (a; $2\mu\text{m}\times 2\mu\text{m}$, b; $1\mu\text{m}\times 1\mu\text{m}$), (c, d) Curved object in the presence of 14-3-3 η specific antibody ($2\mu\text{m}\times 2\mu\text{m}$), (e, f) Curved object in the presence of 14-3-3 η specific antibody ($1\mu\text{m}\times 1\mu\text{m}$), (g, h) Antibody added to the dried curved surface ($2\mu\text{m}\times 2\mu\text{m}$).

TEM analysis of immunogold labeled curved object of α -synuclein with 14-3-3 η

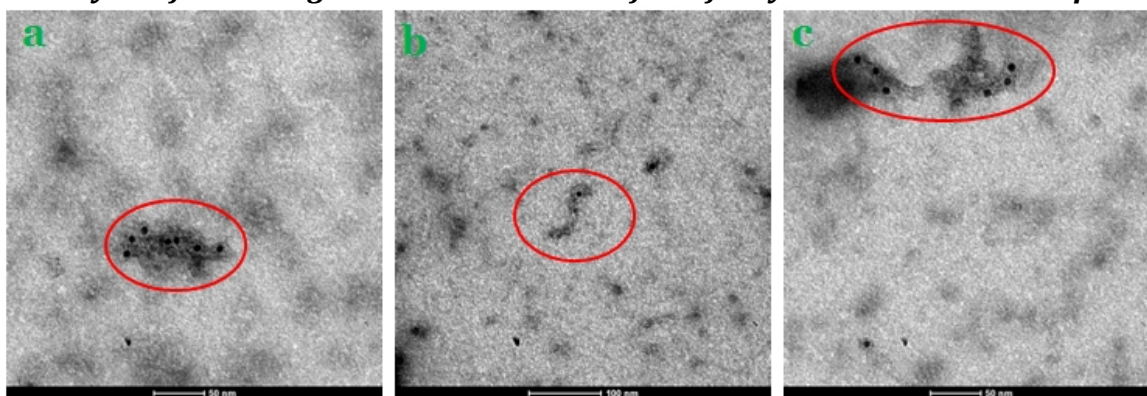


Figure 2.20: TEM image analysis of immunogold labeled curved objects in the presence of 14-3-3 η specific antibody. (a, b, c) Immunogold labeled 14-3-3 η into the curved objects.

We analyzed black spot of immunogold labeled 14-3-3 η antibody into the curved objects formed by the incubation of immunogold labeled 14-3-3 η specific antibodies with α -synuclein and 14-3-3 η . These observations suggest that 14-3-3 η enters into the curved object during α -synuclein aggregation.

Fluorescence emission experiment

We also performed Fluorescence emission experiment to understand intrusion of 14-3-3 η into the curved object. Fluorescence emission experiments were performed to analyze Oregon green labeled α -synuclein and Oregon green labeled 14-3-3 η into the curved object. Curved objects were observed by the incubation of 1:4 ratios of 14-3-3 η and α -synuclein at 37 °C with continuous shaking at 1000 rpm 1–2 days.

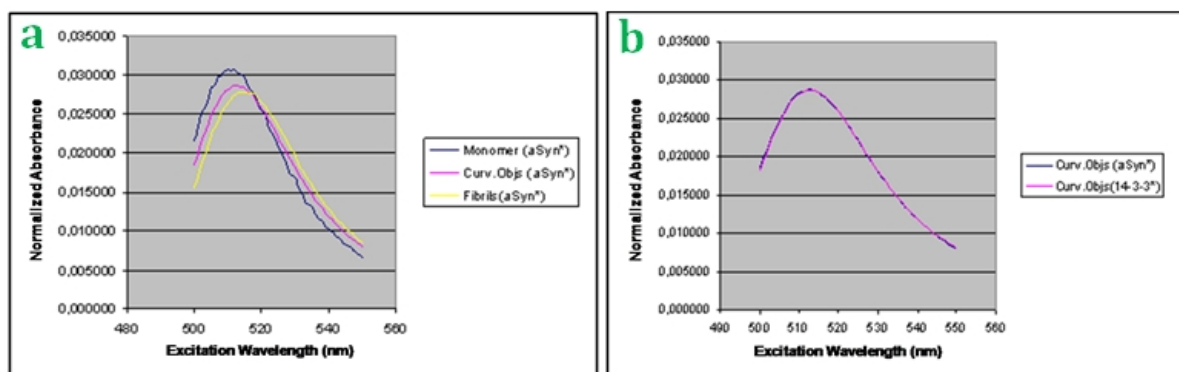


Figure 2.21: Fluorescence emission spectra of α -synuclein aggregates. (a) Fluorescence emission of monomer (blue), curved object (pink), mature fibrils (yellow), (b) Fluorescence emission of fluorescent labeled (α -synuclein+14-3-3 η) curved object, overlapped with each other.

We diluted curved objects in 1 ml of PBS buffer (50 mM, pH 7.4), then we placed curved objects in a cuvette inside the fluorescence spectrometer. Then the emission spectrums of curved objects were measured separately. First, with Oregon green labeled α -synuclein. Second, with Oregon green labeled 14-3-3 η . Both emission spectrums overlapped with each other after normalizing the spectrum.

This result suggests that the curved object contains the labeled 14-3-3 η and labeled α -synuclein, and in both cases Oregon green labeled 14-3-3 η and Oregon green labeled α -synuclein goes along the length of the curved objects.

ThT assay of curved object

2.5 mM solutions of ThT in 1X PBS were added with 1 μ l of ThT solution in 99 μ l of curved object for fluorescence spectroscopy experiment. Blank solution was also prepared by adding 1 μ l of ThT in 99 μ l of 1X PBS. Both samples were diluted up to 1 ml in MilliQ to perform fluorescence spectroscopy experiment.

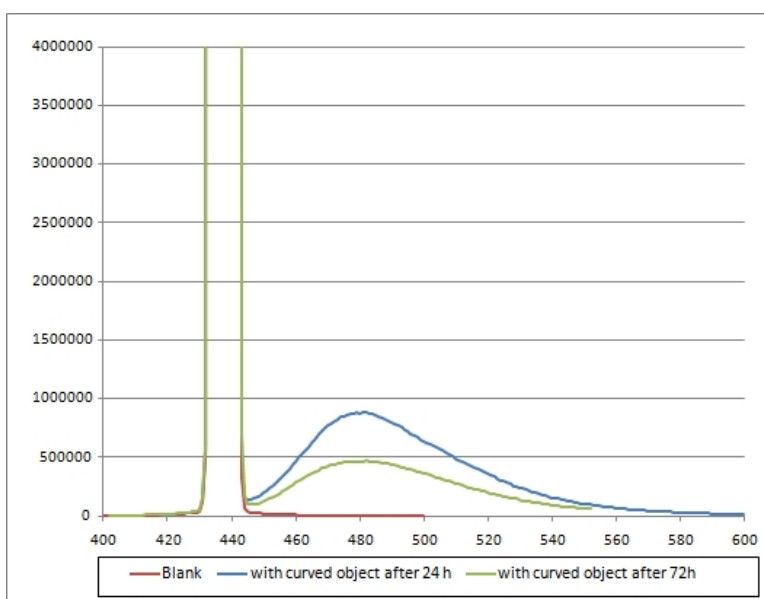


Figure 2.22: Fluorescence spectra of curved object binding with ThT.

Both blank and curved objects were placed in a cuvette one by one into the spectrometer. ThT fluorescence emission was measured with excitation at 450 nm and recorded the spectrum between 465 nm and 565 nm. The excitation spectra were collected by setting the emission wavelength to 482 nm. Emission spectra between 440 nm and 565 nm were collected upon excitation at 450 nm. Excitation and emission spectra in the presence of amyloid fibrils were measured with constant ThT and constant curved object concentrations. The decrease in ThT

fluorescence emission with increasing incubation time of curved object indicates that protein solution decrease amyloid like fibrillar structure. Normally, amyloid fibril enhances the ThT fluorescence emission by increasing amyloid fibrils concentration in protein solution.

[2.5.4] Effect of 14-3-3 η on seeded growth of α -synuclein aggregation

Protein aggregates were generated by incubating α -synuclein (80 μ M), 14-3-3 η (20 μ M), α -synuclein seeds (16 μ M) (4:1:1) in PBS buffer (50 mM, pH 7.4) at 37 $^{\circ}$ C for 3–6 days with continuous shaking at 1000 rpm. Images were taken in tapping mode AFM, and analyzed by Scanning probe microscopy software, WSxM 5.0 (see section 3.2.4 in detail for image analysis).

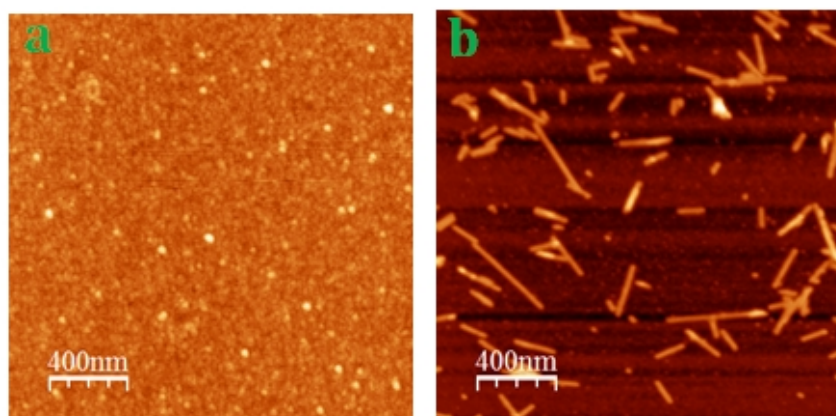


Figure 2.23: AFM image of seeded growth of α -synuclein aggregation suppressed by 14-3-3 η . (a) 14-3-3 η inhibited the aggregation process of α -synuclein ($2\mu\text{m}\times 2\mu\text{m}$), (b) In the absence of 14-3-3 η α -synuclein and seeds formed bundles of long and mature fibrils ($2\mu\text{m}\times 2\mu\text{m}$).

By studying α -synuclein aggregation in the presence of seeds and 14-3-3 η , we observed a very interesting capability of 14-3-3 η . 14-3-3 η would stop/inhibit seeded growth of α -synuclein by acting/binding at the living ends of the seeds. We observed that 14-3-3 η interacted with the living/exposed ends of the seeds, and it stopped further addition of monomeric α -synuclein to the living ends of seeds. In normal aggregation condition seeds promote aggregation and it forms microns long mature fibrils in a very short period of time. When we added 14-3-3 η together with α -synuclein in the presence of seeds, we never observed mature and long fibrils. This observation suggests that 14-3-3 η binds with the living ends of the seeds and it further stops the addition of α -synuclein monomer or oligomers to the living ends of the seeds. By adding at the living ends of seeds 14-3-3 η stops the aggregation process of α -synuclein.

[2.5.5] Effect of 14-3-3 η on NC-terminal dimer

Curved objects were generated by incubating NC-terminal α -synuclein dimer (80 μ M) and 14-3-3 η (20 μ M) in PBS buffer (50 mM, pH 7.4) (following 4:1 molar ratio) at 37 $^{\circ}$ C for 12–24 h with continuous shaking at 1000 rpm. Images were taken in tapping mode AFM, and analyzed by Scanning probe microscopy software, WSxM 5.0 (see section 3.2.4 in detail for image analysis).

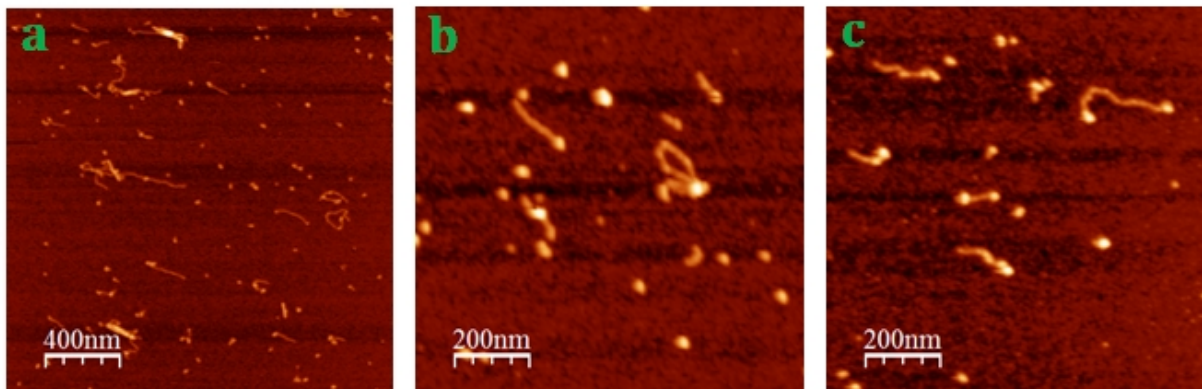


Figure 2.24: AFM image of curved object obtained during the NC-terminal dimer aggregation in the presence 14-3-3 η (a; 2 μ m \times 2 μ m, b&c; 1 μ m \times 1 μ m)

14-3-3 η also modulated the aggregation pathway of NC-terminal α -synuclein dimer, and it formed curved objects instead of mature fibrils. Like α -synuclein, 14-3-3 η modulates the aggregation pathway of NC-terminal α -synuclein dimer. In both cases we observed curved objects of height around 2 nm. This observation strongly suggests that the acting sight of the 14-3-3 η during aggregation is an intermediate object (oligomers).

[2.5.6] Effect of 14-3-3 η on A β aggregation

Curved objects were generated by incubating A β (80 μ M) and 14-3-3 η (4:1) in PBS buffer (50 mM, pH 7.4) at 37 $^{\circ}$ C for 12–24 h with continuous shaking at 1000 rpm. Images were taken in tapping mode AFM, and analyzed by Scanning probe microscopy software, WSxM 5.0 (see section 3.2.4 in detail for image analysis).

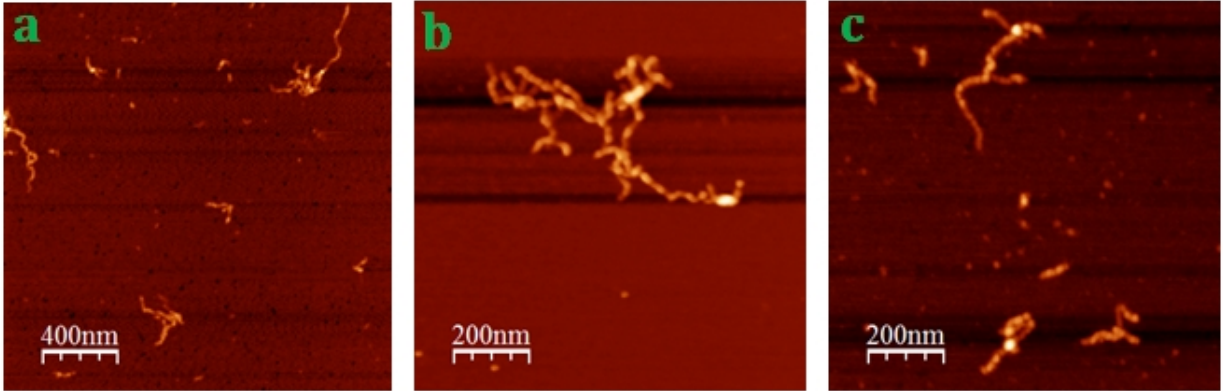


Figure 2.25: AFM image of curved object obtained during the amyloid-beta aggregation in the presence 14-3-3 η (a; 2 μm ×2 μm , b&c; 1 μm ×1 μm).

14-3-3 η also modulated the aggregation process of A β . Like α -synuclein and NC-terminal dimer, 14-3-3 η modulated the aggregation pathway of A β proteins. In this case also we observed curved objects of height around 2 nm. This observation strongly suggests that the acting sight of the 14-3-3 η during aggregation is an intermediate object (oligomers).

[2.6] Effect of 14-3-3 γ on α -synuclein aggregation

[2.6.1] Effect of 14-3-3 γ on α -synuclein aggregation

We did experiments also with 14-3-3 γ , because it belongs to the family of 14-3-3 group and it shows more than 95% sequence similarity with 14-3-3 η . The experiments were carried out in the presence α -synuclein. Protein aggregates were generated by incubating α -synuclein (80 μM) and 14-3-3 γ (20 μM) in PBS buffer (50 mM, pH 7.4) at 37 $^{\circ}\text{C}$ for 3–6 days with continuous shaking at 1000 rpm. Images were taken in tapping mode AFM, and analyzed by Scanning probe microscopy software, WSxM 5.0 (see section 3.2.4 in detail for image analysis).

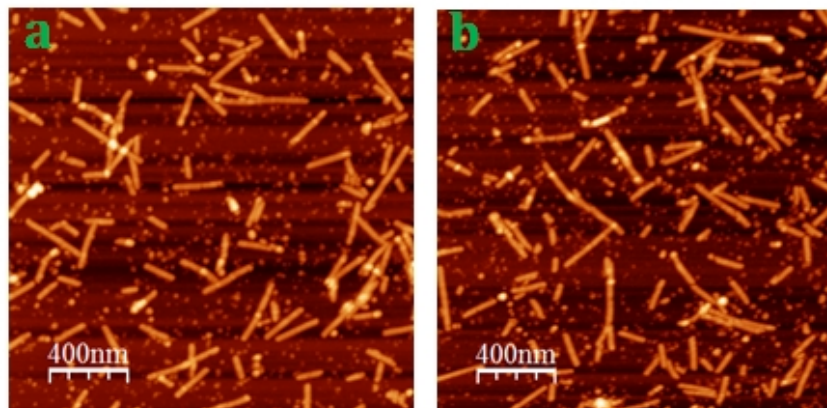


Figure 2.26: AFM image of α -synuclein aggregation unaffected by 14-3-3 γ dimer. (a, b) α -Synuclein formed long and mature fibrils of height ~ 8 nm in the presence of 14-3-3 γ ($2\mu\text{m}\times 2\mu\text{m}$). 14-3-3 γ did not show any effect on α -synuclein aggregation.

By studying the effect of 14-3-3 γ on α -synuclein aggregation we observed that 14-3-3 γ does not influence the aggregation process of α -synuclein. The height and diameter of the mature fibrils observed by adding 14-3-3 γ overlapped with the height and diameter of α -synuclein mature fibrils. We observed height of the α -synuclein mature fibrils in both cases (presence and absence of 14-3-3 γ) around 8 nm. This observation suggests that 14-3-3 γ does not interact with the α -synuclein.

[2.6.2] Effect of 14-3-3 γ on seeded growth of α -synuclein aggregation

Protein aggregates were generated by incubating α -synuclein (80 μM), 14-3-3 γ , α -synuclein seeds (4:1:1) in PBS buffer (50 mM, pH 7.4) at 37 $^{\circ}\text{C}$ for 3–6 days with continuous shaking at 1000 rpm. Images were taken in tapping mode AFM, and analyzed by Scanning probe microscopy software, WSxM 5.0 (see section 3.2.4 in detail for image analysis).

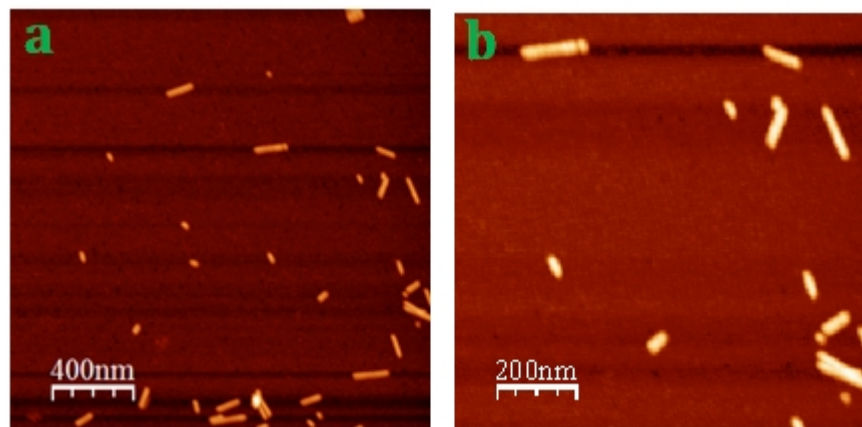


Figure 2.27: AFM image of seeded growth of α -synuclein aggregation unaffected by 14-3-3 γ . (a, b) 14-3-3 γ did not inhibit the aggregation process of α -synuclein in the presence of seeds (a; $2\mu\text{m}\times 2\mu\text{m}$, b; $1\mu\text{m}\times 1\mu\text{m}$).

We did not observe any change in α -synuclein aggregation by adding 14-3-3 γ during seeded growth. This observation suggests that 14-3-3 γ does not interact with the α -synuclein seeds during aggregation.

Chapter-3

(Materials and Methods)

[3.1] Cloning, expression and purification

All the purified proteins (Recombinant α -Synuclein, α -Synuclein mutant and 14-3-3 protein) were provided by Bubacco's lab padova. I was not involved in this work.

[3.2] Atomic force microscopy

Tapping mode (Imaging) AFM was used for the characterization of all kind of aggregates discussed in this thesis (we have discussed in detail about the mode of action and principle of tapping mode AFM in section 1.2).

[3.2.1] Protein aggregation

There are several ways to get aggregated protein *in vitro*. In our case, human recombinant α -synuclein (supplied from Bubacco's lab padova, Italy) was dissolved in double distilled water (Milli-Q, H₂O). After dissolution, it was aliquoted in small eppendorf tube and evacuated to preserve protein samples for long time period. α -Synuclein aggregates were generated by incubating α -synuclein (80 μ M) in 200 μ l of PBS buffer (50 mM, pH 7.4) with 0.05% sodium azide to avoid bacterial growth during protein aggregation at 37 °C for 2–15 days with continuous shaking at 1000 rpm.

[3.2.2] Sample preparation

The samples for AFM imaging were initiated by depositing 10 μ l of α -synuclein aggregates on the freshly cleaved mica (RubyRed Mica Sheets, Electron Microscopy Sciences, Fort Washington, USA) at room temperature (\sim 25 °C). After adsorption for 5 min, the mica surface was gently washed with the 20–30 drops (1–1.5 ml) of double distilled water (Milli-Q H₂O), to remove excess salts and unbounded proteins from the surface. The sample was dried by condensed nitrogen gas by blowing over the mica surface and stored at room temperature (\sim 25 °C) for imaging.

[3.2.3] AFM imaging

All the images for characterizing α -synuclein aggregates were obtained by Multimode AFM facility (Nanoscope III, Veeco/Digital Instruments, Santa Barbara, CA) with scanner 2795E in a tapping mode. Slandered etched silicon cantilevers (Ultra sharp NSC15/AlBS silicon probes with tip apex radius of \sim 10 nm, resonant frequency range of AFM cantilever 325 Hz, and number of pixels 512 \times 512) were used for imaging in air. All the images were taken at room temperature (\sim 25 °C) and

~50% humid environment. In order to obtain the images of real height for the aggregates, the force between tips and samples was slightly reduced by increasing the set point value to a maximum. The scanner parameters were calibrated with Drive amplitude 37.40mV, Drive phase 101.9°, Drive frequency 337.615 kHz, Z-limit 3.0806 μM , Integral gain 0.5000 and Proportional gain 1.000. Each sample was imaged in at least five different regions to avoid experimental error.

In most experiments, the samples were diluted ~10 times with PBS then equilibrated at RT for 10' prior to deposition in an attempt to minimize overlap of individual α -synuclein aggregates. Multiple images from successive depositions were then recorded and digitalized to obtain statistically significant morphological measurements.

[3.2.4] AFM image analysis

The resulting images were processed off-line with free available Scanning probe microscopy software (WSxM 5.0 Develop 4.2) [reviewed in Horcas et al., 2007]. The heights and diameters were measured with the section profile program.

Overview of WSxM

WSxM is a freeware application that is able to read most of the SPM file formats [WSXM free software at www.nanotec.es]. In addition Horcas et al. have developed a tool that is called heuristic open that opens files with unknown format in a semi automated way, including those files that due to the lack of a common identifier are not suitable to be recognized as a specific file format. If we have no information at all about the file that we are trying to open we can simply drag and drop the file from the Windows explorer into the "heuristic open" window and WSXM will suggest us some parameter/s to open the image using an expert system.

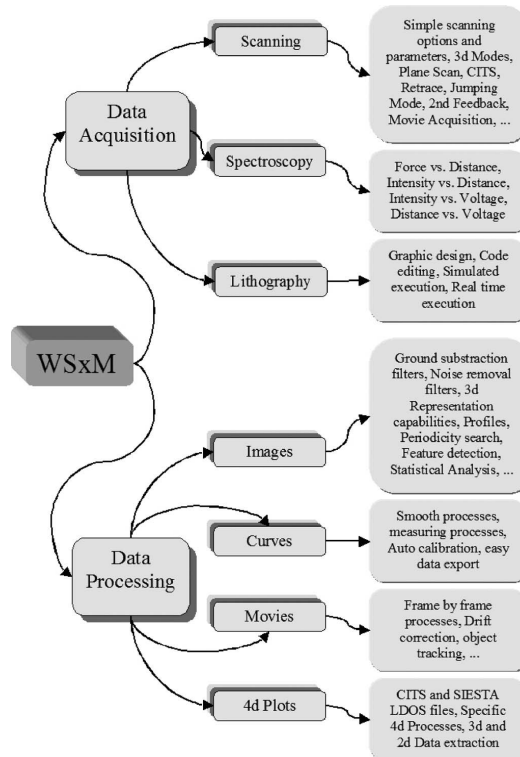


Figure 3.1: General scheme of WSxM showing the most representative process. [Reproduced from Horcas et al., 2007]

The algorithm tries to determine parameters such as the number of points, header size, and number of images in the files based only on the file size. Almost every known information can be fed to the system to improve the reading capabilities including fixed positions for the most important fields in the file header such as number of rows/columns or the real axis amplitudes. The aim of this work is to briefly describe the structure and performances of WSxM by remarking some of its most outstanding features. **Figure 3.7** shows a general scheme of the possibilities of the software.

WSxM has been designed to work under MS-Windows; hence all the common features of this operating system are naturally included in this software: multiple windows, clipboard copy and paste, memory management, etc. WSxM is divided into two clearly different parts: image processing and data acquisition (see **Figure 3.7** for an overview); while the first part runs in all Windows versions since MS-Windows 95, the second part only works under MS-Windows NT, 2000, and XP; in this respect we have sacrificed generality to gain stability in data acquisition where system crash must be avoided as much as possible. WSxM code has been written in C++ using Microsoft Foundation Classes, a C++ library that allows easy handling of the complex Windows programming.

C++ is a well-known object oriented programming language with clear advantages in large codes (WSxM has now about half a million code lines).

[3.2.5] Fibril formation and preparation for ultrasonication experiment

In the routinely α -synuclein aggregation experiment we have used 80 μM α -synuclein concentrations in 200 μl volume of 50 mM PBS with 0.05% sodium azide. After getting mature fibrils of α -synuclein we have diluted it to the 20 μM in 1ml volume of PBS for the ultrasonication experiment.

Seeds preparation

α -Synuclein seeds were prepared by the ultrasonication of fully formed mature fibrils (20 μM) for total 4 min at the intervals of 5 seconds in ice-cold sample reservoir.

Chapter-4

(Conclusions)

[4.1] Conclusions

In my PhD thesis work, I tried to increase our understanding on the amyloidogenic processes of intrinsically unstructured proteins (e.g., α -Synuclein, α -Synuclein dimers (NN-terminal, CC-terminal, NC-terminal dimer and Synucle-Nuclein construct) and Amyloid-beta protein) and the effect of 14-3-3 η on its aggregation.

In order to understand the organization of α -Synuclein monomer during its aggregation and the formation of mature fibrils, I studied the AFM imaging of α -Synuclein, α -Synuclein dimers and Amyloid-beta protein aggregation. The aggregation mechanism of α -Synuclein dimers has provided a strong indication that only NC-terminal dimer aggregates like that of α -synuclein does and it assembles in an N-C-terminal relative orientation during aggregation. From the aggregation of Synucle-Nuclein construct has confirmed that NAC region of α -synuclein plays an important role in the packaging of core part (beta sheet like structure) of mature fibrils. Whereas, Synucle-Nuclein construct of α -synuclein formed wider in diameter mature fibrils than the mature fibrils of α -synuclein. This observation of mature fibrils suggest that the double NAC region of Synucle-Nuclein construct forms more beta sheet like structure to fill the core part of mature fibrils than that of α -synuclein mature fibrils.

The aggregation studies of α -synuclein in the presence of 14-3-3 η lead us to their main conclusion. First, 14-3-3 η does not bind to α -synuclein in its monomeric state, and also does not affect the mature fibers already formed, but targets the most toxic oligomeric species. Second, it affect the aggregation process of α -Synuclein and NC-terminal dimer by interacting with the growing oligomers thus leading to curved and flexible objects, that are most likely off the α -synuclein aggregation pathway. Third, it is able to affect the aggregation process at concentration as low as those at which are chaperons able to act.

In order to understand the effect of 14-3-3 η on α -synuclein aggregation, I studied the *in vitro* aggregation of α -synuclein in the presence of 14-3-3 η by using different biophysical techniques. First, I studied by NMR and SPR the monomeric interaction of α -synuclein with 14-3-3 η . The NMR and SPR observations show that 14-3-3 η does not interact with monomeric form of α -synuclein. To understand the effect of 14-3-3 η on α -synuclein mature fibrils, I incubated 14-3-3 η with α -synuclein mature fibrils. The results from AFM imaging on the α -synuclein mature fibrils in the presence of 14-3-3 suggest that 14-3-3 η does not interact with mature fibrils. These observations suggest that 14-3-3 η does not interact with monomeric form of α -synuclein and even not with mature fibrils.

In order to understand the effect of 14-3-3 η on aggregation intermediates of α -synuclein, I studied α -synuclein aggregation in the presence of different molar concentration of 14-3-3 η . By AFM imaging at 1:1 stoichiometric ratio of 14-3-3 η and α -synuclein, I observed curved and flexible objects of α -synuclein instead of spherical oligomers and mature fibrils. At different stoichiometric ratio of 14-3-3 η and α -synuclein (1:4, 1:7, 1:12, 1:20, 1:24, 1:30, 1: ∞), I found that by lowering the molar concentration of 14-3-3 η in an α -synuclein solution, curvature and flexibility of the curved objects decreases. At the 1:24 molar ratio of 14-3-3 η and α -synuclein, curvature and flexibility of the curved objects shifted into the rigid and straight fibrils. At this point, the single molecule of 14-3-3 η modulates the aggregation pathway of 24 molecules of α -synuclein. Being so small the amount of 14-3-3 η able to modulate the aggregation behavior of α -synuclein. On the basis of these observations, I can infer that 14-3-3 η behaves like a chaperone protein.

At this point, it is clear that 14-3-3 η interacts only with intermediate objects of α -synuclein. Now the question is exactly where and how 14-3-3 η modulates the aggregation pathway of α -synuclein? To answer this question, I performed Fluorescence spectroscopy experiment and Immunogold labeling experiment of 14-3-3 η with α -synuclein. The fluorescence spectroscopy study showed that the 14-3-3 η went inside the growing oligomers and protofibrils and it formed curved object; this observation was confirmed by the immunogold labeling experiment of 14-3-3 η and α -synuclein. These studies then suggest that the 14-3-3 η does not interact both with the monomers of α -synuclein and with mature fibrils. Somehow, 14-3-3 η target is in between these two stages of α -synuclein aggregation. I was able to monitor the stage at which 14-3-3 η enters into the α -synuclein aggregation, and how in this way it can slow down the aggregation process of α -synuclein and modulates its whole pathway.

The experiments carried out on the α -synuclein aggregation in the presence of fragmented α -synuclein mature fibrils (seeds) also catalyzed by 14-3-3 η . It has demonstrated that 14-3-3 η slows down the accretion of monomeric α -synuclein to the fragmented fibrils of α -synuclein by sticking at the living ends of fragmented fibrils. In this way 14-3-3 η inhibits the seeded growth of α -synuclein. This way a very enlightening experiment that greatly increased our understanding on the mechanism of action of these proteins that is present in the Lewy bodies, and whose function and role was not known.

Bibliography

- Aitken A (1996). 14-3-3 and its possible role in co-ordinating multiple signaling pathways. *Trends Cell Biol.* 6, 341–347.
- Arimon M, Diez-Perez I, Kogan MJ, Durany N, Giralt E, Sanz F, Fernandez-Busquets X (2005). Fine structure study of A β 1-42 fibrillogenesis with atomic force microscopy. *FASEB J.* 19, 1344–1346.
- Auluck PK et al. (2010). α -Synuclein: Membrane Interactions and Toxicity in Parkinson's disease. *Annual Review of Cell and Developmental Biology.* Vol. 26, 211–233.
- Baserga R, Hongo A, Rubini M, Prisco M, Valentinis B (1997). The IGF-I receptor in cell growth, transformation and apoptosis. *Biochim. Biophys. Acta.* 1332, F105–126.
- Bayer TA, Jakala P, Hartmann T, Havas L, McLean C, Culvenor JG et al. (1999). Alpha-synuclein accumulates in Lewy bodies in Parkinson's disease and dementia with Lewy bodies but not in Alzheimer's disease beta-amyloid plaque cores. *Neurosci. Lett.* 266, 213–216.
- Blackley HK, Sanders GH, Davies MC, Roberts CJ, Tendler SJ, Wilkinson MJ (2000). In situ atomic force microscopy study of β -amyloid fibrillization. *J. Mol. Biol.* 298, 833–840.
- Boston PF, Jackson P, Thompson RJ (1982) Human 14-3-3 protein: radioimmunoassay, tissue distribution, and cerebrospinal fluid levels in patients with neurological disorders. *J. Neurochem.* 38, 1475–1482.
- Brasemann S, McCormick F (1995). Bcr and Raf form a complex in vivo via 14-3-3 proteins. *EMBO J.* 14, 4839–4848.
- Brookmeyer R, Gray S, Kawas C (1998). Projections of Alzheimer's disease in the United States and the public health impact of delaying disease onset. *Am. J. Public Health.* 88, 1337–1342.
- Buxbaum JN, Tagoe CE (2000). The genetics of the amyloidoses. *Annu Rev Med.* 51, 543–569.
- Campion D, Martin C, Heilig R, Charbonnier F, Moreau V, Flaman JM et al. (1995). The NACP/synuclein gene: chromosomal assignment and screening for alterations in Alzheimer disease. *Genomics.* 26, 254–257.
- Caughey B, Lansbury PT (2003). Protofibrils, pores, fibrils, and neurodegeneration: separating the responsible protein aggregates from the innocent bystanders. *Annu. Rev. Neurosci.* 26, 267–298.
- Celis JE, Gesser B, Rasmussen HH, Madsen P, Leffers H et al. (1990). Comprehensive two-dimensional gel protein databases offer a global approach to the analysis of human cells: the transformed amnion cells (AMA) master database and its link to genome DNA sequence data. *Electrophoresis.* 11, 989–1071.
- Chandra S, Gallardo G, Fernandez-Chacon R, Schluter OM, Sudhof TC (2005). Alpha-synuclein cooperates with CSP α in preventing neurodegeneration. *Cell.* 123, 383–396.
- Chang HC, Rubin GM (1997). 14-3-3 epsilon positively regulates Ras-mediated signaling in Drosophila. *Genes Dev.* 11, 1132–1139.
- Chen HK, Fernandez-Funez P, Acevedo SF, Lam YC, Kaytor MD, Fernandez MH, Aitken A, Skoulakis EM, Orr HT, Botas J, Zoghbi HY (2003). Interaction of Akt-phosphorylated ataxin-1 with 14-3-3 mediates neurodegeneration in spinocerebellar ataxia type 1. *Cell.* 113, 457–468.

- Chen X, Silva HA de, Pettenati MJ, Rao PN, St. George-Hyslop P, Roses AD et al. (1995). The human NACP/alpha-synuclein gene: chromosome assignment to 4q21.3-q22 and TaqI RFLP analysis. **Genomics**. 26, 425-427.
- Chong SS, Pack SD, Roschke AV, Tanigami A, Carrozzo R et al. (1997). A revision of the lissencephaly and Miller-Dieker syndrome critical regions in chromosome 17p13.3. **Hum. Mol. Genet.** 6, 147-155.
- Clayton DF and George JM (1998). The synucleins: a family of proteins involved in synaptic function, plasticity, neurodegeneration and disease. **Trends Neurosci.** 21, 249-254.
- Clayton DF, George JM (1999). Synucleins in synaptic plasticity and neurodegenerative disorders. **J Neurosci Res.** 58, 120-129.
- Cohlberg JA, Li J, Uversky VN, Fink AL (2002). Heparin and other glycosaminoglycans stimulate the formation of amyloid fibrils from alpha-synuclein in vitro. **Biochemistry.** 41, 1502-1511.
- Conway KA, Harper JD, Lansbury PT (1998). Accelerated in vitro fibril formation by a mutant alpha-synuclein linked to early-onset Parkinson disease. **Nat. Med.** 4, 1318-1320.
- Conway KA, Harper JD, Lansbury PT Jr (2000). Fibrils formed in vitro from alpha-synuclein and two mutant forms linked to Parkinson's disease are typical amyloid. **Biochemistry.** 39, 2552-2563.
- Conway KA, Lee SJ, Rochet JC, Ding TT, Harper JD, Williamson RE, Lansbury PT Jr (2000c). Accelerated oligomerization by Parkinson's disease linked alpha-synuclein mutants. **Ann. NY Acad. Sci.** 920, 42-45.
- Conway KA, Lee SJ, Rochet JC, Ding TT, Williamson RE, Lansbury PT Jr (2000a). Acceleration of oligomerization, not fibrillization, is a shared property of both alpha-synuclein mutations linked to early-onset Parkinson's disease: implications for pathogenesis and therapy. **Proc. Natl. Acad. Sci. USA,** 97, 571-576.
- Conway KA, Harper JD, Lansbury PT (2000b). Fibrils formed in vitro from α -synuclein and two mutant forms linked to Parkinson's disease are typical amyloid. **Biochemistry.** 39, 2552-2563.
- Craparo A, Freund R, Gustafson TA (1997). 14-3-3 (epsilon) interacts with the insulin-like growth factor I receptor and insulin receptor substrate I in a phosphoserine-dependent manner. **J. Biol. Chem.** 272, 11663-69.
- Crowther RA, Daniel SE, Goedert M (2000). Characterisation of isolated α -synuclein filaments from substantia nigra of Parkinson's disease brain. **Neurosci. Lett.** 292, 128-130.
- Cullere X, Rose P, Thathamangalam U, Chatterjee A, Mullane KP et al. (1998). Serine 257 phosphorylation regulates association of polyomavirus middle T antigen with 14-3-3 proteins. **J. Virol.** 72, 558-563.
- Davidson WS, Jonas A, Clayton DF, George JM (1998). Stabilization of alpha-synuclein secondary structure upon binding to synthetic membranes. **J. Biol. Chem.** 273, 9443-9449.
- de Laureto PP, Tosatto L, Frare E, Marin O, Uversky VN, Fontana A (2006). Conformational properties of the SDS-bound state of alpha-synuclein probed by limited proteolysis: unexpected rigidity of the acidic C-terminal tail. **Biochemistry.** 45, 11523-11531.
- DeArmond SJ, Prusiner SB (1995). Prion protein transgenes and the neuropathology in prion diseases. **Brain Pathol.** 5, 77-89.

- Der-Sarkissian A, Jao CC, Chen J, Langen R (2003). Structural organization of α -synuclein fibrils studied by site-directed spin labeling. *J Biol Chem* 278: 37530–37535.
- Ding TT, Lee SJ, Rochet JC, Lansbury PT Jr (2002). Annular alpha-synuclein protofibrils are produced when spherical protofibrils are incubated in solution or bound to brain-derived membranes. *Biochemistry*. 41, 10209–10217.
- Dosztanyi Z, Csizmok V, Tompa P, Simon I (2005). IUPred: web server for the prediction of intrinsically unstructured regions of proteins based on estimated energy content. *Bioinformatics*. 21, 3433–3434.
- Duyckaerts C, Potier MC, Delatour B (2008). Alzheimer disease models and human neuropathology: similarities and differences. *Acta Neuropathol*. 115, 5–38.
- El-Agnaf OM, Jakes R, Curran MD, Middleton D, Ingenito R, Bianchi E et al. (1998). Aggregates from mutant and wild-type alpha-synuclein proteins and NAC peptide induce apoptotic cell death in human neuroblastoma cells by formation of beta-sheet and amyloid-like filaments. *FEBS Lett*. 440, 71–75.
- El-Agnaf OMA, Bodles AM, Guthrie DJS, Harriott P, Irvine GB (1998c). The N-terminal region of non-A β component of Alzheimer's disease amyloid is responsible for its tendency to assume β -sheet and aggregate to form fibrils. *Eur. J. Biochem*. 258, 157–163.
- El-Agnaf OMA, Bodles AM, Guthrie DJS, Walsh DM, Irvine GB (1998d). The influence of the central region containing residues 19-25 on the aggregation properties and secondary structure of Alzheimer's β -amyloid peptide. *Eur. J. Biochem*. 256, 560–569.
- El-Agnaf OM, Jakes R, Curran MD, Wallace A (1998a). Effects of the mutations Ala30 to Pro and Ala53 to Thr on the physical and morphological properties of α -synuclein protein implicated in Parkinson's disease. *FEBS Lett*. 440, 67–70.
- El-Agnaf OM, Jakes R, Curran MD, Middleton D, Ingenito R, Bianchi E et al. (1998b). Aggregates from mutant and wild-type α -synuclein proteins and NAC peptide induce apoptotic cell death in human neuroblastoma cells by formation of β -sheet and amyloid-like filaments. *FEBS Lett*. 440, 71–75.
- Eliezer D, Kutluay E, Bussell R Jr, Browne G (2001). Conformational properties of α -synuclein in its free and lipid-associated states. *J. Mol. Biol*. 307, 1061–1073.
- Engelender S, Kaminsky Z, Guo X, Sharp AH, Amaravi RK, Kleiderlein JJ, Margolis RL, Troncoso JC, Lanahan AA, Worley PF, Dawson VL, Dawson TM, Ross CA (1999). Synphilin-1 associates with alpha-synuclein and promotes the formation of cytosolic inclusions. *Nat Genet*. 22, 110–114.
- Engelender S, Ross CA, Berger K, Schols L, Schulz JB, Riess O, Kruger R (2003). Identification and functional characterization of a novel R621C mutation in the synphilin-1 gene in Parkinson's disease. *Hum Mol Genet*. 12, 1223–1231.
- Eyal A, Szargel R, Avraham E, Liani E, Haskin J, Rott R, Engelender S (2006). Synphilin-1A: an aggregation-prone isoform of synphilin-1 that causes neuronal death and is present in aggregates from alpha-synucleinopathy patients. *Proc Natl Acad Sci. USA*, 103, 5917–5922.
- Fanger GR, Widmann C, Porter AC, Sather S, Johnson GL et al. (1998). 14-3-3 proteins interact with specific MEK kinases. *J. Biol. Chem*. 273, 3476–3483.
- Ferl R (1996). 14-3-3 proteins and signal transduction. *Annu. Rev. Plant Physiol. Plant Mol. Biol*. 47, 49–73

- Findeis MA (2007). The role of amyloid beta peptide 42 in Alzheimer's disease. *Pharmacol. Ther.* 116, 266–286.
- Fink AL (2005). Natively unfolded proteins. *Curr. Opin. Struct. Biol.* 15, 35–41.
- Finnie C, Borch J, Collinge DB (1999). 14-3-3 proteins: eukaryotic regulatory proteins with many functions. *Plant Mol. Biol.* 40, 545–54.
- Florin E-L, Rief M, Lehmann H, Ludwig M, Dornmair C, Moy VT, and Gaub HE (1995). Sensing specific molecular interactions with the atomic force microscope. *Biosensors and Bioelectronics.* 10, 895–901.
- Freed E, Symons M, Macdonald SG, McCormick F, Ruggieri R (1994). Binding of 14-3-3 proteins to the protein kinase Raf and effects on its activation. *Science.* 265, 1713–1716.
- Fu H, Coburn J, Collier RJ (1993). The eukaryotic host factor that activates exoenzymes of *Pseudomonas aeruginosa* is a member of the 14-3-3 protein family. *Proc. Natl. Acad. Sci. USA,* 90, 2320–2324.
- Fu H, Subramanian RR, Masters SC (2000). 14-3-3 proteins: structure, function, and regulation. *Annu Rev Pharmacol Toxicol.* 40, 617–647.
- Fukuma T, Mostaert AS, and Jarvis SP (2006). Explanation for the mechanical strength of amyloid fibrils. *Tribology Letters.* 22, 233–237.
- Furlanetto RW, Dey BR, Lopaczynski W, Nissley SP (1997). 14-3-3 proteins interact with the insulin-like growth factor receptor but not the insulin receptor. *Biochem. J.* 327, 765–771.
- Garcia R, Perez R (2002). Dynamic atomic force microscopy methods. *Surf. Sci. Rep.* 47, 197–301.
- Garcia-Guzman M, Dolfi F, Russello M, Vuori K (1999). Cell adhesion regulates the interaction between the docking protein p130(Cas) and the 14-3-3 proteins. *J. Biol. Chem.* 274, 5762–5768.
- George JM, Jin H, Woods WS, Clayton DF (1995). Characterization of a novel protein regulated during the critical period for song learning in the zebra finch. *Neuron.* 15, 361–372.
- Giasson BI, Uryu K, Trojanowski JQ, Lee VM (1999). Mutant and wild type human alpha-synucleins assemble into elongated filaments with distinct morphologies in vitro. *J. Biol. Chem.* 274, 7619–7622.
- Giasson BI, Duda JE, Quinn SM, Zhang B, Trojanowski JQ, Lee VM (2002). Neuronal alpha-synucleinopathy with severe movement disorder in mice expressing A53T human alpha synuclein. *Neuron.* 34, 521–533.
- Giasson BI, Forman MS, Higuchi M, Golbe LI, Graves CL et al. (2003). Initiation and synergistic fibrillization of tau and alpha-synuclein. *Science.* 300, 636–640.
- Glabe CG, Kaye R (2006). Common structure and toxic function of amyloid oligomers implies a common mechanism of pathogenesis. *Neurology.* 66, S74–S78.
- Goate A, Chartier-Harlin MC, Mullan M, Brown J, Crawford F et al. (1991). Segregation of a missense mutation in the amyloid precursor protein gene with familial Alzheimer's disease. *Nature.* 349, 704–706.
- Goedert M (2001). Alpha-synuclein and neurodegenerative diseases. *Nature Reviews Neuroscience.* 2, 492–501

- Goers J, Uversky VN, Fink AL (2003a). Polycation-induced oligomerization and accelerated fibrillation of human alpha-synuclein in vitro. *Protein Sci.* 12, 702–707.
- Goldsbury CJ, Kistler U, Aebi T, Arvinte, Cooper GJ (1999). Watching amyloid fibrils grow by time-lapse atomic force microscopy. *J. Mol. Biol.* 285, 33–39.
- Gu M, Du X. (1998). A novel ligand-binding site in the zeta-form 14-3-3 protein recognizing the platelet glycoprotein Ib alpha and distinct from the c-Raf binding site. *J. Biol. Chem.* 273, 33465–33471.
- Han H, Weinreb PH, Lansbury PT Jr (1995). The core Alzheimer's peptide NAC forms amyloid fibrils which seed and are seeded by beta-amyloid: is NAC a common trigger or target in neurodegenerative disease? *Chem. Biol.* 2, 163–169.
- Hardy J (2001). Genetic dissection of primary neurodegenerative diseases. *Biochem Soc Symp.* 51–57.
- Harper JD, Wong SS, Lieber CM, Lansbury Jr PT (1999). Assembly of A-beta amyloid protofibrils: an in vitro model for a possible early event in Alzheimer's disease. *Biochemistry.* 38, 8972–8980.
- Hartley DM, Walsh DM, Ye CP, Diehl T, Vasquez S, Vassilev PM et al. (1999). Protofibrillar intermediates of amyloid-beta protein induces acute electrophysiological changes and progressive neurotoxicity in cortical neurons. *J Neurosci.* 19, 8876–8884.
- Hashimoto M, Hsu LJ, Sisk A, Xia Y, Takeda A, Sundsmo M et al. (1998). Human recombinant NACP/alphasynuclein is aggregated and fibrillated in vitro: relevance for Lewy body disease. *Brain Res.* 799, 301–306.
- Hebert LE, Beckett LA, Scherr PA, Evans DA. (2001). Annual incidence of Alzheimer disease in the United States projected to the years 2000 through 2050. *Alzheimer Dis. Assoc. Disord.* 15, 169–173.
- Hebert LE, Scherr PA, Bienias JL, Bennett DA, Evans DA (2003). Alzheimer disease in the US population: prevalence estimates using the 2000 census. *Arch. Neurol.* 60, 1119–1122.
- Higgins MJ, Riener CK, Uchihashi T, Sader JE, McKendry R, Jarvis SP (2005). Frequency modulation atomic force microscopy: A dynamic measurement technique for biological systems. *Nanotech.* 16, S85–S89.
- Higgins MJ, Sader JE, Jarvis SP (2006). Frequency modulation atomic force microscopy reveals individual intermediates associated with each unfolded I27 titin domain. *Biophys. J.* 90, 640–647.
- Hirotsune S, Pack SD, Chong SS, Robbins CM, Pavan WJ et al. (1997). Genomic organization of the murine Miller-Dieker/lissencephaly region: conservation of linkage with the human region. *Genome Res.* 7, 625–34.
- Horcas I et al. (2007). WSXM: A software for scanning probe microscopy and a tool for Nanotechnology. *Rev. Sci. Instrum.* 78, 013705–013708.
- Hortschansky P, Schroeckh V, Christopeit T, Zandomenighi G, Fandrich M (2005). The aggregation kinetics of Alzheimer's beta-amyloid peptide is controlled by stochastic nucleation. *Protein Sci.* 14, 1753–1759.
- Hoyer W, Cherny D, Subramaniam V, Jovin T (2004). Rapid self-assembly of alpha-synuclein observed by in situ atomic force microscopy. *J. Mol. Biol.* 340, 127–139.
- Hsich G, Kenney K, Gibbs CJ, Lee KH, Harrington MG (1996). The 14-3-3 brain protein in cerebrospinal fluid as a marker for transmissible spongiform encephalopathies. *N Engl J Med.* 335, 924–930.

- Huang TH, Yang DS, Plaskos NP, Go S, Yip CM et al. (2000). Structural studies of soluble oligomers of the Alzheimer beta-amyloid peptide. *J. Mol. Biol.* 297, 73–87.
- Hutter JL, Bechhoefer J (1993). Calibration of atomic-force microscope tips. *Review of Scientific Instruments.* 64, 1868-1871.
- Ichimura T, Isobe T, Okuyama T, Takahashi N, Araki K et al. (1988). Molecular cloning of cDNA coding for brain specific 14-3-3 protein, a protein kinase dependent activator of tyrosine and tryptophan hydroxylases. *Proc. Natl. Acad. Sci. USA*, 85, 7084–7088.
- Ichimura T, Ito M, Itagaki C, Takahashi M, Horigome T et al. (1997). The 14-3-3 protein binds its target proteins with a common site located towards the C-terminus. *FEBS Lett.* 413, 273–276.
- Ichimura T, Uchiyama J, Kunihiro O, Ito M, Horigome T et al. (1995). Identification of the site of interaction of the 14-3-3 protein with phosphorylated tryptophan hydroxylase. *J. Biol. Chem.* 270, 28515–28518.
- Ihara M, Tomimoto H, Kitayama H, Morioka Y, Akiguchi I, Shibasaki H, Noda M, Kinoshita M (2003). Association of the cytoskeletal GTP-binding protein Sept4/H5 with cytoplasmic inclusions found in Parkinson's disease and other synucleinopathies. *J Biol Chem.* 278, 24095–24102.
- Isobe T, Ichimura T, Sunaya T, Okuyama T, Takahashi N et al. (1991). Distinct forms of the protein kinase-dependent activator of tyrosine and tryptophan hydroxylases. *J. Mol. Biol.* 217, 125–132.
- Iwai A, Masliah E, Yoshimoto M, Ge N, Flanagan L, Silva HA de et al. (1995). The precursor protein of non-A beta component of Alzheimer's disease amyloid is a presynaptic protein of the central nervous system. *Neuron.* 14, 467–475
- Iwai A, Yoshimoto M, Masliah E, Saitoh T (1995a). Non-A beta component of Alzheimer's disease amyloid (NAC) is amyloidogenic. *Biochemistry.* 34, 10139–10145.
- Jakes R, Spillantini MG, Goedert M (1994). Identification of two distinct synucleins from human brain. *FEBS Lett.* 345, 27–32.
- Jao CC, Der-Sarkissian A, Chen J, Langen R (2004). Structure of membrane-bound alpha-synuclein studied by site-directed spin labeling. *Proc. Natl Acad. Sci. USA*, 101, 8331–8336.
- Jarrett JT, Lansbury PT Jr (1993). Seeding “one-dimensional crystallization” of amyloid: A pathogenic mechanism in Alzheimer's disease and scrapie? *Cell*, 73, 1055–1058.
- Jenco JM, Rawlingson A, Daniels B, Morris AJ (1998). Regulation of phospholipase D2: selective inhibition of mammalian phospholipase isoenzymes by α - and β -synuclein. *Biochemistry*, 37, 4901–4909.
- Jensen PH, Hager H, Nielsen MS, Hojrup P, Gliemann J, Jakes R (1999). Alpha-synuclein binds to tau and stimulates the protein kinase A-catalyzed tau phosphorylation of serine residues 262 and 356. *J. Biol. Chem.* 274, 25481–25489.
- Jensen PH, Hojrup P, Hager H, Nielsen MS, Jacobsen L, Olesen OF et al. (1997). Binding of A-beta to alpha- and beta-synucleins: identification of segments in alpha-synuclein/ NAC precursor that bind A-beta and NAC. *Biochem. J.* 323, 539–546.
- Jensen PH, Nielsen MS, Jakes R, Dotti CG, Goedert M (1998). Binding of alpha-synuclein to brain vesicles is abolished by familial Parkinson's disease mutation. *J. Biol. Chem.* 273, 26292–26294.

- Jensen PH, Sorensen ES, Petersen TE, Gliemann J, Rasmussen LK (1995). Residues in the synuclein consensus motif of the alpha-synuclein fragment, NAC, participate in transglutaminase-catalysed cross-linking to Alzheimer-disease amyloid beta peptide. *Biochem. J.* 310, 91–94.
- Jo E, McLaurin JA, Yip CM, St George-Hyslop PH, Fraser PE (2000). α -Synuclein membrane interactions and lipid specificity. *J. Biol. Chem.* 275, 34328–34334.
- Jones DH, Ley S, Aitken A (1995). Isoforms of 14-3-3 protein can form homo and hetero dimers in vivo and in vitro: implications for function as adapter proteins. *FEBS Lett.* 368, 55–58.
- Kaiser U, Schardt C, Brandscheidt D, Wollmer E, Havemann K (1993). Expression of insulin-like growth factor receptors I and II in normal human lung and in lung cancer. *J. Cancer Res. Clin. Oncol.* 119, 665–668.
- Kawamata H, McLean PJ, Sharma N, Hyman BT (2001). Interaction of alpha-synuclein and synphilin-1: effect of Parkinson's disease-associated mutations. *J Neurochem.* 77, 929–934.
- Kawamoto Y, Akiguchi I, Nakamura S, Budka H (2002a). Accumulation of 14-3-3 proteins in glial cytoplasmic inclusions in multiple system atrophy. *Ann Neurol.* 52, 722–731.
- Kawamoto Y, Akiguchi I, Nakamura S, Budka H (2004). 14-3-3 proteins in Lewy body-like hyaline inclusions in patients with sporadic amyotrophic lateral sclerosis. *Acta Neuropathol (Berl).* 108, 531–537.
- Kawamoto Y, Akiguchi I, Nakamura S, Honjyo Y, Shibasaki H, Budka H (2002b). 14-3-3 proteins in Lewy bodies in Parkinson disease and diffuse Lewy body disease brains. *J Neuropathol Exp Neurol.* 61, 245–253.
- Kayed R, Head E, Thompson JL, McIntire TM, Milton SC et al. (2003). Common structure of soluble amyloid oligomers implies common mechanism of pathogenesis. *Science.* 300, 486–489.
- Kelly JW (1996). Alternative conformations of amyloidogenic proteins govern their behavior. *Curr Opin Struct Biol.* 6, 11–17.
- Kim et al. (2007). Seed-dependent Accelerated Fibrillation of α -Synuclein Induced by Periodic Ultrasonication Treatment. *J. Microbiol. Biotechnol.* 17, 2027–2032
- Kowalewski T, Holtzman DM (1999). In situ atomic force microscopy study of Alzheimer's β -amyloid peptide on different substrates: new insights into mechanism of β -sheet formation. *Proc. Natl. Acad. Sci. USA,* 96, 3688–3693.
- Kruger R, Kuhn W, Muller T, Woitalla D, Graeber M, Kosel S, Przuntek H, Epplen JT, Schols L, Riess O (1998). Ala30Pro mutation in the gene encoding α -synuclein in Parkinson's disease. *Nat Genet.* 18, 106–108.
- Lambert MP, Barlow AK, Chromy BA, Edwards C, Freed R, Liosatos M, Morgan TE, Rozovsky I, Trommer B, Viola KL, Wals P, Zhang C, Finch CE, Krafft GA, Klein WL (1998). Diffusible nonfibrillar ligands derived from A β 1-42 are potent central nervous system neurotoxins. *Proc. Natl. Acad. Sci. USA,* 95, 6448–6453.
- Lansbury PT Jr (1999). Evolution of amyloid: What normal protein folding may tell us about fibrillogenesis and disease. *Proc. Natl. Acad. Sci. USA,* 96, 3342–3344.
- Lashuel HA, Hartley D, Petre BM, Walz T, Lansbury Jr PT (2002). Neurodegenerative disease: amyloid pores from pathogenic mutations. *Nature,* 418 (6895), 291.
- Lavedan C, Leroy E, Dehejia A, Buchholtz S, Dutra A, Nussbaum RL et al. (1998). Identification, localization and characterization of the human gamma-synuclein gene. *Hum. Genet.* 103, 106–112.

- Layfield R, Fergusson J, Aitken A, Lowe J, Landon M et al. (1996). Neurofibrillary tangles of Alzheimer's disease brains contain 14-3-3 proteins. *Neurosci. Lett.* 209, 57–60.
- Lee C, Kim HJ, Lee J, Cho H, Kim J, Chung KC, Jung S, Paik SR (2006). Dequalinium-induced protofibrils formation of α -synuclein. *J. Biol. Chem.* 281, 3463–3472.
- Leffers H, Madsen P, Rasmussen HH, Honore B, Andersen AH et al. (1993). Molecular cloning and expression of the transformation sensitive epithelial marker stratifin. A member of a protein family that has been involved in the protein kinase C signalling pathway. *J. Mol. Biol.* 231, 982–998.
- Lemere CA, Lopera F, Kosik KS, Lendon CL, Ossa J et al. (1996). The E280A presenilin 1 Alzheimer mutation produces increased A-beta 42 deposition and severe cerebellar pathology. *Nat. Med.* 2, 1146–1150.
- Lewis J, Dickson DW, Lin WL, Chisholm L, Corral A et al. (2001). Enhanced neurofibrillary degeneration in transgenic mice expressing mutant tau and APP. *Science.* 293, 1487–1491.
- Li S, Resnicoff M, Baserga R (1996). Effect of mutations at serines 1280–1283 on the mitogenic and transforming activities of the insulin-like growth factor I receptor. *J. Biol. Chem.* 271, 12254–12260.
- Li X, Romero P, Rani M, Dunker AK, Obradovic Z (1999). Predicting protein disorder for N-, C-, and internal regions. *Genome Inform. Ser Workshop Genome Inform.* 10, 30–40.
- Liu D, Bienkowska J, Petosa C, Collier RJ, Fu H et al. (1995). Crystal structure of the zeta isoform of the 14-3-3 protein. *Nature*, 376, 191–194.
- Lowe J, Blanchard A, Morrell K, Lennox G, Reynolds L, Billett M, Landon M, Mayer RJ (1988). Ubiquitin is a common factor in intermediate filament inclusion bodies of diverse type in man, including those of Parkinson's disease, Pick's disease, and Alzheimer's disease, as well as Rosenthal fibres in cerebellar astrocytomas, cytoplasmic bodies in muscle, and mallory bodies in alcoholic liver disease. *J Pathol*, 155, 9–15.
- Lowe R, Pountney DL, Jensen PH, Gai WP, Voelcker NH (2004). Calcium(II) selectively induces α -synuclein annular oligomers via interaction with the C-terminal domain. *Protein Sci.* 13, 3245–3252.
- Lucking et al., (2000). Alpha-synuclein and Parkinson's disease. *CMLS, Cell. Mol. Life Sci.* 57, 1894-1908.
- Luhrs T, Ritter C, Adrian M, Riek-Loher D, Bohrmann B, Dobeli H, Schubert D, Riek R (2005). 3D structure of Alzheimer's A β (1-42) fibrils, Proc. *Natl. Acad. Sci. USA*, 102, 17342–17347.
- Luo ZJ, Zhang XF, Rapp U, Avruch J (1995). Identification of the 14.3.3 zeta domains important for self-association and Raf binding. *J. Biol. Chem.* 270, 23681–23687.
- Mann DM, Brown A, Prinja D, Davies CA, Landon M et al. (1989). An analysis of the morphology of senile plaques in Down's syndrome patients of different ages using immunocytochemical and lectin histochemical techniques. *Neuropathol. Appl. Neurobiol.* 15, 317–329.
- Manning-Bog AB, McCormack AL, Li J, Uversky VN, Fink AL, Di Monte DA (2002). The herbicide paraquat causes upregulation and aggregation of alpha-synuclein in mice: paraquat and alpha-synuclein. *J. Biol. Chem.* 277, 1641–1644.
- Maroteaux L, Scheller RH (1991). The rat brain synucleins: family of proteins transiently associated with neuronal membrane. *Brain Res. Mol. Brain Res.* 11, 335–343.

- Maroteaux L, Campanelli JT and Scheller RH (1988). Synuclein: a neuron-specific protein localized to the nucleus and presynaptic nerve terminal. *J. Neurosci.* 8, 2804–2815.
- Martin H, Patel Y, Jones D, Howell S, Robinson K et al. (1993). Antibodies against the major brain isoforms of 14-3-3 protein: an antibody specific for the N-acetylated amino-terminus of a protein. *FEBS Lett.* 331, 296–303.
- Mathur AB, Collinsworth AM, Reichert WM, Kraus WE, Truskey GA. (2001). Endothelial, cardiac muscle and skeletal muscle exhibit different viscous and elastic properties as determined by atomic force microscopy. *J Biomech.* 34(12), 1545–1553.
- Mattson MP, Goodman Y (1995). Different amyloidogenic peptides share a similar mechanism of neurotoxicity involving reactive oxygen species and calcium, *Brain Res.* 676, 219–224.
- McDonald JD, Daneshvar L, Willert JR, Matsumura K, Waldman F et al. (1994). Physical mapping of chromosome 17p13.3 in the region of a putative tumor suppressor gene important in medulloblastoma. *Genomics.* 23, 229–232.
- McLean JA, Savory J, Sparks NHC (2002). Welfare of male and female broiler chickens in relation to stocking density, as indicated by performance, health and behaviour. *Anim. Welf.* 11:55–73.
- McNulty BC, Young GB, Pielak GJ (2006). Macromolecular crowding in the Escherichia coli periplasm maintains alphasynuclein disorder. *J. Mol. Biol.* 355, 893–897.
- Meredith GE, Sonsalla PK, Chesselet MF (2008). Animal models of Parkinson’s disease progression. *Acta Neuropathol.* 115, 385–398.
- Mesquida P, Riener C, MacPhee C, McKendry R (2007). Morphology and mechanical stability of amyloid-like peptide fibrils. *J. Mater. Sci. Mater. Med.* 18, 1325–1331.
- Mezey E, Dehejia A, Harta G, Papp MI, Polymeropoulos MH, Brownstein MJ (1998). Alpha synuclein in neurodegenerative disorders: murderer or accomplice? *Nat. Med.* 4, 755–757.
- Morris JC, Storandt M, McKeel DW Jr, Rubin EH, Price JL et al. (1996). Cerebral amyloid deposition and diffuse plaques in “normal” aging: Evidence for presymptomatic and very mild Alzheimer’s disease. *Neurology.* 46, 707–719.
- Morrison D (1994). 14-3-3: modulators of signaling proteins? *Science.* 266, 56–57.
- Moussavian M, Potolicchio S, Jones R (1997). The 14-3-3 brain protein and transmissible spongiform encephalopathy. *N. Engl. J. Med.* 336, 873–874.
- Munishkina L A, Phelan C, Uversky VN, Fink AL (2003). Conformational behavior and aggregation of alpha-synuclein in organic solvents: modeling the effects of membranes. *Biochemistry.* 42, 2720–2730.
- Munishkina LA, Cooper EM, Uversky VN, Fink AL (2004). The effect of macromolecular crowding on protein aggregation and amyloid fibril formation. *J. Mol. Recognit.* 17, 456–464.
- Nakanishi K, Hashizume S, Kato M, Honjoh T, Setoguchi Y et al. (1997). Elevated expression levels of the 14-3-3 family of proteins in lung cancer tissues. *Hum. Antib.* 8, 189–194.
- Narhi L, Wood SJ, Steavenson S, Jiang Y, Wu GM, Anafi D et al. (1999). Both familial Parkinson’s disease mutations accelerate alpha-synuclein aggregation. *J. Biol. Chem.* 274, 9843–9846.

- Naslund J, Haroutunian V, Mohs R, Davis KL, Davies P et al. (2000). Correlation between elevated levels of A β -peptide in the brain and cognitive decline. *JAMA*. 283, 1571–1577.
- Necula M, Kaye R, Milton S, Glabe CG (2007). Small molecule inhibitors of aggregation indicate that amyloid beta oligomerization and fibrillization pathways are independent and distinct. *J. Biol. Chem.* 282, 10311–10324.
- Nelson R, Sawaya MR, Balbirnie M, Madsen A, Riekel C et al. (2005). Structure of the cross-beta spine of amyloid-like fibrils. *Nature*. 435, 773–778.
- Obradovic Z, Peng K, Vucetic S, Radivojac P, Dunker AK (2005). Exploiting heterogeneous sequence properties improves prediction of protein disorder. *Proteins* 61(Suppl. 7), 176–182.
- Ostrerova N, Petrucelli L, Farrer M, Mehta N, Choi P, Hardy J, Wolozin B (1999). α -Synuclein shares physical and functional homology with 14-3-3 proteins. *J Neurosci*. 19, 5782–5791.
- Pawson T, Scott JD (1997). Signaling through scaffold, anchoring, and adaptor proteins. *Science*. 278, 2075–2080.
- Perrin RJ, Woods WS, Clayton DF, George JM (2000). Interaction of human α -synuclein and Parkinson's disease variants with phospholipids. *J. Biol. Chem.* 275, 34393–34398.
- Petosa C, Masters SC, Bankston LA, Pohl J, Wang B et al. (1998). 14-3-3zeta binds a phosphorylated Raf peptide and an unphosphorylated peptide via its conserved amphipathic groove. *J. Biol. Chem.* 273, 16305–16310.
- Podlisny MB, Walsh DM, Amarante P, Ostaszewski BL, Stimson ER et al. (1998). Oligomerization of endogenous and synthetic amyloid beta-protein at nanomolar levels in cell culture and stabilization of monomer by Congo red. *Biochemistry*. 37, 3602–3611.
- Polymeropoulos MH et al. (1996). Mapping of a gene for Parkinson's disease to chromosome 4q21-q23. *Science*. 274, 1197–1199.
- Polymeropoulos MH et al. (1997). Mutation in the α -synuclein gene identified in families with Parkinson's disease. *Science*. 276, 2045–2047.
- Putman CAJ, van der Werf KO, de Grooth BG, van Hulst NF, Greve J (1994b). Tapping mode atomic-force microscopy in liquid. *Appl. Phys. Lett.* 64, 2454–2456.
- Putman CAJ, van der Werf KO, de Grooth BG, van Hulst NF, Greve J (1994). Viscoelasticity of living cells allows high-resolution imaging by tapping mode atomic-force microscopy. *Biophys. J.* 67, 1749–1753.
- Qin et al. (2007). Role of Different Regions of α -Synuclein in the Assembly of Fibrils. *Biochemistry*. 46, 13322–13330.
- Rapoport M, Dawson HN, Binder LI, Vitek MP, Ferreira A (2002). Tau is essential to beta amyloid-induced neurotoxicity. *Proc. Natl. Acad. Sci. USA*, 99, 6364–6369.
- Rekas A et al. (2004). Interaction of the molecular chaperone alphaB-crystallin with alpha-synuclein: effects on amyloid fibril formation and chaperone activity. *J Mol Biol.* 340, 1167–1183.
- Ribeiro CS, Carneiro K, Ross CA, Menezes JR, Engelender S (2002). Synphilin-1 is developmentally localized to synaptic terminals, and its association with synaptic vesicles is modulated by alpha-synuclein. *J Biol Chem.* 277, 23927–23933.

- Richard M, Biacabe AG, Streichenberger N, Ironside JW, Mohr M, Kopp N, Perret-Liaudet A (2003). Immunohistochemical localization of 14.3.3 zeta protein in amyloid plaques in human spongiform encephalopathies. *Acta Neuropathol (Berl)*. 105, 296–302.
- Rittinger K, Budman J, Xu J, Volinia S, Cantley LC et al. (1999). Structural analysis of 14-3-3 phosphopeptide complexes identifies a dual role for the nuclear export signal of 14-3-3 in ligand binding. *Mol. Cell*. 4, 153–166.
- Romero P, Obradovic Z, Li X, Garner EC, Brown CJ and Dunker AK (2001). Sequence complexity of disordered protein. *Proteins*. 42, 38–48.
- Samii A, Nutt JG, Ransom BR (2004). Parkinson's disease. *Lancet*. 363, 1783–1793.
- Sandal M, Valle F, Tessari I, Mammi S, Bergantino E, Musiani F, Brucale M, Bubacco L, Samori B (2008). Conformational equilibria in monomeric α -synuclein at the single-molecule level. *PLoS Biol*. 6 e6.
- Sato S, Chiba T, Sakata E, Kato K, Mizuno Y, Hattori N, Tanaka K (2006). 14-3-3eta is a novel regulator of parkin ubiquitin ligase. *Embo J*. 25, 211–221.
- Scheuner D, Eckman C, Jensen M, Song X, Citron M, et al. (1996). Secreted amyloid betaprotein similar to that in the senile plaques of Alzheimer's disease is increased in vivo by the presenilin 1 and 2 and APP mutations linked to familial Alzheimer's disease. *Nat. Med*. 2, 864–870.
- Schmidt ML, Murray J, Lee VM, Hill WD, Wertkin A, Trojanowski JQ (1991). Epitope map of neuro filament protein domains in cortical and peripheral nervous system Lewy bodies. *Am. J. Pathol*. 139, 53–65.
- Schubert D, Behl C, Lesley R, Brack A, Dargusch R, Sagara Y, Kimura H (1995). Amyloid peptides are toxic via common oxidative mechanism. *Proc. Natl. Acad. Sci. USA*, 92, 1989–1993.
- Selkoe DJ (2001). Alzheimer's disease results from the cerebral accumulation and cytotoxicity of amyloid β -protein. *J. Alzheimer's Dis*. 3, 75–80.
- Selkoe DJ (1999). Translating cell biology into therapeutic advances in Alzheimer's disease. *Nature*. 399, 23–31.
- Selkoe DJ (1996). Amyloid β -protein and the genetics of Alzheimer's disease. *J Biol Chem*. 271, 18295–18298.
- Serpell LC (2000). Alzheimer's amyloid fibrils: Structure and assembly. *Biochim. Biophys. Acta*. 1502-1516.
- Serpell LC, Berriman J, Jakes R, Goedert M, Crowther R A (2000). Fiber diffraction of synthetic α -synuclein filaments shows amyloid-like cross- β conformation. *Proc. Natl Acad. Sci. USA*, 97, 4897–4902.
- Shibasaki Y, Baillie DA, St. Clair D, Brookes AJ (1995). High-resolution mapping of SNCA encoding alphasynuclein, the non-A beta component of Alzheimer's disease amyloid precursor, to human chromosome 4q21.3-->q22 by fluorescence in situ hybridization. *Cytogenet. Cell Genet*. 71, 54–55.
- Shimura H, Schlossmacher MG, Hattori N, Frosch MP, Trockenbacher A, Schneider R, Mizuno Y, Kosik KS, Selkoe DJ (2001). Ubiquitination of a new form of alpha-synuclein by parkin from human brain: implications for Parkinson's disease. *Science*. 293, 263–269.
- Skovronsky DM et al. (2006). Neurodegenerative disease: New Concepts of Pathogenesis and Their Therapeutic Implications. *Annurev.pathol*. Vol. 1, 151-170.
- Smith MJ, Kwok JB, McLean CA, Kril JJ, Broe GA et al. (2001). Variable phenotype of Alzheimer's disease with spastic paraparesis. *Ann. Neurol*. 49, 125–129.

- Soto C, Estrada LD (2008). Protein misfolding and neurodegeneration. *Arch Neurol*. 65, 184–189.
- Soto C. (2001). Protein misfolding and disease: protein refolding and therapy. *FEBS Lett*. 498, 204–207.
- Soto C. (2003). Unfolding the role of protein misfolding in neurodegenerative diseases. *Nature Rev Neurosci*. 4, 49–60.
- Souza JM, Giasson BI, Chen Q, Lee VM, Ischiropoulos H (2000). Dityrosine cross-linking promotes formation of stable alpha-synuclein polymers. Implication of nitrate and oxidative stress in the pathogenesis of neurodegenerative synucleinopathies. *J. Biol. Chem*. 275, 18344–18349.
- Spillantini MG, Crowther RA, Jakes R, Cairns NJ, Lantos PL, Goedert M (1998a). Filamentous alpha-synuclein inclusions link multiple system atrophy with Parkinson's disease and dementia with Lewy bodies. *Neurosci. Lett*. 251, 205–208.
- Spillantini MG, Divane A, Goedert M (1995). Assignment of human alpha-synuclein (SNCA) and beta-synuclein (SNCB) genes to chromosomes 4q21 and 5q35. *Genomics*. 27, 379–388.
- Spillantini MG, Schmidt ML, Lee VM, Trojanowski JQ, Jakes R, Goedert M (1997). Alpha-synuclein in Lewy bodies. *Nature*. 388, 839–840.
- Spillantini MG, Crowther RA, Jakes R, Hasegawa M, Goedert M (1998). α -Synuclein in filamentous inclusions of Lewy bodies from Parkinson's disease and dementia with Lewy bodies. *Proc. Natl Acad. Sci. USA*, 95, 6469–6473.
- Srinivasan R, Marchant RE, Zagorski MG (2004). A β 1 peptide associated with familial British dementia forms annular and ring-like protofibrillar structures. *Amyloid*. 11, 10–13.
- Syme CD, Blanch EW, Holt C, Jakes R, Goedert M, Hecht L, Barron LD (2002). A Raman optical activity study of rheomorphism in caseins, synucleins and tau. New insight into the structure and behaviour of natively unfolded proteins. *Eur. J. Biochem*. 269, 148–156.
- Takahashi RH, Almeida CG, Kearney PF, Yu F, Lin MT et al. (2004). Oligomerization of Alzheimer's beta-amyloid within processes and synapses of cultured neurons and brain. *J. Neurosci*. 24, 3592–3599.
- Tang SJ, Suen TC, McInnes RR, Buchwald M (1998). Association of the TLX- 2 homeodomain and 14-3-3eta signaling proteins. *J. Biol. Chem*. 273, 25356–25363.
- Thorson JA, Yu LW, Hsu AL, Shih NY, Graves PR et al. (1998). 14-3-3 proteins are required for maintenance of Raf-1 phosphorylation and kinase activity. *Mol. Cell Biol*. 18, 5229–5238.
- Toyooka K, Muratake T, Tanaka T, Igarashi S, Watanabe H et al. (1999). 14-3-3 protein eta chain gene (YWHAH) polymorphism and its genetic association with schizophrenia. *Am. J. Med. Genet*. 88, 164–167.
- Ueda K, Fukushima H, Masliah E, Xia Y, Iwai A, Yoshimoto M et al. (1993). Molecular cloning of cDNA encoding an unrecognized component of amyloid in Alzheimer disease. *Proc. Natl. Acad. Sci. USA*. 90, 11282–11286
- Ulmer TS, Bax A, Cole NB, Nussbaum RL (2005). Structure and dynamics of micelle-bound human alpha-synuclein. *J. Biol. Chem*. 280, 9595–9603.

- Umahara T, Uchihara T, Tsuchiya K, Nakamura A, Ikeda K, Iwamoto T, Takasaki M (2004). Immunolocalization of 14-3-3 isoforms in brains with Pick body disease. *Neurosci Lett.* 371, 215–219.
- Uversky VN (2002a). Natively unfolded proteins: a point where biology waits for physics. *Protein Sci.* 11, 739–756.
- Uversky VN (2002b). What does it mean to be natively unfolded? *Eur. J. Biochem.* 269, 2–12.
- Uversky VN (2003). A protein-chameleon: conformational plasticity of alpha-synuclein, a disordered protein involved in neurodegenerative disorders. *J. Biomol. Struct. Dyn.* 21, 211–234.
- Uversky VN (2004). Neurotoxicant-induced animal models of Parkinson's disease: understanding the role of rotenone, maneb and paraquat in neurodegeneration. *Cell Tissue Res.* 318, 225–241.
- Uversky VN et al. (2002b). Accelerated alpha-synuclein fibrillation in crowded milieu. *FEBS Lett.* 515, 99–103.
- Uversky VN, Gillespie JR, Fink AL (2000). Why are 'natively unfolded' proteins unstructured under physiologic conditions? *Proteins.* 41, 415–427.
- Uversky VN, Lee HJ, Li J, Fink AL, Lee SJ (2001e). Stabilization of partially folded conformation during alpha-synuclein oligomerization in both purified and cytosolic preparations. *J. Biol. Chem.* 276, 43495–43498.
- Uversky VN, Li J, Fink AL (2001a). Evidence for a partially folded intermediate in alpha-synuclein fibril formation. *J. Biol. Chem.* 276, 10737–10744.
- Uversky VN, Li J, Fink AL (2001b). Metal-triggered structural transformations, aggregation, and fibrillation of human alpha-synuclein. A possible molecular link between Parkinson's disease and heavy metal exposure. *J. Biol. Chem.* 276, 44284–44296.
- Uversky VN, Li J, Fink AL (2001c). Pesticides directly accelerate the rate of alpha-synuclein fibril formation: a possible factor in Parkinson's disease. *FEBS Lett.* 500, 105–108.
- Uversky VN, Li J, Fink AL (2001d). Trimethylamine-N-oxide-induced folding of alpha-synuclein. *FEBS Lett.* 509, 31–35.
- Uversky VN, Li J, Bower K, Fink AL (2002a). Synergistic effects of pesticides and metals on the fibrillation of alpha-synuclein: implications for Parkinson's disease. *Neurotoxicology.* 23, 527–536.
- Uversky VN, Li J, Souillac P, Millett IS, Doniach S, Jakes R, Goedert M, Fink AL (2002d). Biophysical properties of the synucleins and their propensities to fibrillate: inhibition of alpha-synuclein assembly by beta- and gamma-synucleins. *J. Biol. Chem.* 277, 11970–11978.
- Uversky VN, Oldfield CJ, Dunker AK (2005a). Showing your ID: intrinsic disorder as an ID for recognition, regulation and cell signaling. *J. Mol. Recognit.* 18, 343–384.
- Uversky VN, Yamin G, Munishkina LA, Karymov MA, Millett IS, Doniach S, Lyubchenko YL, Fink AL (2005b). Effects of nitration on the structure and aggregation of alpha-synuclein. *Brain Res. Mol. Brain Res.* 134, 84–102.
- Uversky VN, Yamin G, Souillac PO, Goers J, Glaser CB, Fink AL (2002c). Methionine oxidation inhibits fibrillation of human alpha-synuclein in vitro. *FEBS Lett.* 517, 239–244.

- Uversky VN, Li J, Fink AL (2001a). Evidence for a partially folded intermediate in α -synuclein fibril formation. *J. Biol. Chem.* 276, 10737-10744.
- Van der Werf KO, Putman CAJ, de Grooth BG, Greve J (1994). Adhesion force imaging in air and liquid by adhesion mode atomic-force microscopy. *Appl. Phys. Lett.* 65, 1195-1197.
- Van Raaij ME, van Gestel J., Segers Nolten IMJ, de Leeuw S, Subramaniam V (2008). Concentration dependence of α -synuclein fibril length assessed by qualitative atomic force microscopy and statistical-mechanical modeling. *Biophys. J.* 95, 4871-4878.
- Varadarajan S, Yatin S, Aksenova M, Butterfield DA (2000). Alzheimer's amyloid β peptide-associated free radical oxidative stress and neurotoxicity. *J. Struct. Biol.* 130, 184-208.
- Vincenz C, Dixit VM (1996). 14-3-3 proteins associate with A20 in an isoform specific manner and function both as chaperone and adapter molecules. *J. Biol. Chem.* 271, 20029-20034.
- Wakabayashi K, Engelender S, Yoshimoto M, Tsuji S, Ross CA, Takahashi H (2001). Synphilin-1 is present in Lewy bodies in Parkinson's disease. *Ann Neurol.* 47, 521-523.
- Wakabayashi K, Fukushima T, Koide R, Horikawa Y, Hasegawa M, Watanabe Y et al. (2000). Juvenile-onset generalized neuroaxonal dystrophy (Hallervorden-Spatz disease) with diffuse neurofibrillary and Lewy body pathology. *Acta Neuropathol. (Berl.)* 99, 331-336.
- Walker JR, Corpina RA, Goldberg J (2001). Structure of the Ku heterodimer bound to DNA and its implications for double-strand break repair. *Nature* 412: 607-614.
- Walsh DM, Klyubin I, Fadeeva JV, Cullen WK, Anwyl R, Wolfe MS, Rowan MJ, Selkoe DJ (2002). Naturally secreted oligomers of amyloid beta protein potently inhibit hippocampal long-term potentiation in vivo. *Nature.* 416, 535-539.
- Walsh DM, Selkoe DJ (2004). Oligomers on the brain: The emerging role of soluble protein aggregates in neurodegeneration. *Protein Pept. Lett.* 11, 213-228.
- Walsh DM, Hartley DM, Kusumoto Y, Fezoui Y, Condron MM, Lomakin A et al. (1999). Amyloid beta-protein fibrillogenesis. Structure and biological activity of protofibrillar intermediates. *J Biol Chem.* 274, 25945-25952.
- Walsh DM, Selkoe DJ. (2007). A β oligomers a decade of discovery. *J. Neurochem.* 101, 1172-1184.
- Walsh DM, Tseng BP, Rydel RE, Podlisny MB, Selkoe DJ (2000). The oligomerization of amyloid beta-protein begins intracellularly in cells derived from human brain. *Biochemistry.* 39, 10831-10839.
- Wang B, Yang H, Liu Y, Jelinek T, Zhang L et al. (1999). Isolation of high-affinity peptide antagonists of 14-3-3 proteins by phage display. *Biochemistry.* 38, 12499-12504.
- Wang H, Zhang L, Liddington R, Fu H (1998). Mutations in the hydrophobic surface of an amphipathic groove of 14-3-3 ζ disrupt its interaction with Raf-1 kinase. *J. Biol. Chem.* 273, 16297-16304.
- Wang W, Shakes DC (1996). Molecular evolution of the 14-3-3 protein family. *J. Mol. Evol.* 43, 384-398.
- Weinreb PH, Zhen W, Poon AW, Conway KA, Lansbury PT Jr (1996). NACP, a protein implicated in Alzheimer's disease and learning, is natively unfolded. *Biochemistry.* 35, 13709-13715.
- Wolfe MS, Esler WP, Das C (2002). Continuing strategies for inhibiting Alzheimer's gamma-secretase. *J. Mol. Neurosci.* 19, 83-87.

- Wood SJ, Wypych J, Steavenson S, Louis JC, Citron M, Biere AL (1999). Alpha-synuclein fibrillogenesis is nucleation-dependent: implications for the pathogenesis of Parkinson's disease. *J. Biol. Chem.* 274, 19509–19512
- Xiao B, Smerdon SJ, Jones DH, Dodson GG, Soneji Y et al. (1995). Structure of a 14-3-3 protein and implications for coordination of multiple signalling pathways. *Nature.* 376, 188–191.
- Yaffe MB, Rittinger K, Volinia S, Caron PR, Aitken A, et al. (1997). The structural basis for 14-3-3:phosphopeptide binding specificity. *Cell.* 91, 961–971.
- Yamin G, Uversky VN, Fink AL (2003). Nitration inhibits fibrillation of human alpha-synuclein in vitro by formation of soluble oligomers. *FEBS Lett.* 542, 147–152.
- Yang ZR, Thomson R, McNeil P, Esnouf RM (2005). RONN: the bio-basis function neural network technique applied to the detection of natively disordered regions in proteins. *Bioinformatics.* 21, 3369–3376.
- Yang G, Woodhouse KA, Yip CM (2002). Substrate-facilitated assembly of elastin like peptides: studies by variable-temperature in situ atomic force microscopy. *J. Am. Chem. Soc.* 124, 10648–10649.
- Yang S, Dammer SM, Bremond N, Zandvliet HJW, Kooij ES, Lohse D (2007). Characterization of nanobubbles on hydrophobic surfaces in water. *Langmuir.* 23, 7072–7077.
- Yankner BA (1996). Mechanisms of neuronal degeneration in Alzheimer's disease. *Neuron.* 16, 921–932.
- Yoshimoto M, Iwai A, Kang D, Otero DA, Xia Y, Saitoh T (1995). NACP, the precursor protein of the nonamyloid beta/A4 protein (A beta) component of Alzheimer disease amyloid, binds A-beta and stimulates A-beta aggregation. *Proc. Natl. Acad. Sci. USA,* 92, 9141–9145.
- Zarranz JJ, Alegre J, Gomez-Esteban JC, Lezcano E, Ros R, Ampuero I, Vidal L, Hoenicka J, Rodriguez O, Atares B, Llorens V, Gomez Tortosa E, del Ser T, Munoz DG, de Yebenes JG (2004). The new mutation, E46K, of alpha-synuclein causes Parkinson and Lewy body dementia. *Ann Neurol.* 55, 164–173.
- Zhang L, Chen J, Fu H (1999). Suppression of apoptosis signal-regulating kinase 1-induced cell death by 14-3-3 proteins. *Proc. Natl. Acad. Sci. USA,* 96, 8511–8515.
- Zhang L, Wang H, Liu D, Liddington R, Fu H (1997). Raf-1 kinase and exoenzyme S interact with 14-3-3zeta through a common site involving lysine 49. *J. Biol. Chem.* 272, 13717–13724.
- Zhang L, Wang H, Masters SC, Wang B, Barbieri JT et al. (1999a). Residues of 14-3-3zeta required for activation of exoenzyme of *Pseudomonas aeruginosa*. *Biochemistry.* 38, 12159–12164.
- Zhang S, Xing H, Muslin AJ (1999b). Nuclear localization of protein kinase alpha is regulated by 14-3-3. *J. Biol. Chem.* 274, 24865–24872.
- Zhu M, Han S, Zhou F, Carter S.A, Fink AL (2004). Annular oligomeric amyloid intermediates observed by in situ atomic force microscopy. *J. Biol. Chem.* 279, 24452–24459.
- Zhu M, Souillac PO, Ionescu-Zanetti C, Carter SA, Fink AL (2002). Surface catalyzed amyloid fibril formation. *J. Biol. Chem.* 277, 50914–50922.

Curriculum Vitae

DHRUV KUMAR

E-mail: dhruv.kumar2@unibo.it
: dhruvbhu@gmail.com
Mob: +39-333-752-3338

OBJECTIVE

- ✓ To achieve a challenging position in the field of Research and Development of Molecular/Cellular Biology, Protein-complex structure, Drug Designing, Atomic force microscopy, Image analysis, Biophysics, Biochemistry, Nano-Biotechnology, Microscopy and Bioinformatics in Project with a high growth oriented organization, University and Laboratories.

EDUCATION

- ✓ **2009-present:** Ph.D. in Cellular, Molecular and Industrial Biology, Ph.D. School in Biological, Biomedical and Biotechnological Sciences. NanoBioScience Lab, Department of Biochemistry, University of Bologna, Italy.
- ✓ **Thesis topic:** Atomic force microscopy studies of the amyloidogenic processes of intrinsically unstructured proteins related to neurodegenerative disease.
- ✓ **Thesis advisor:** Prof. Bruno Samori, Ph.D., Coordinator of NanoBioScience lab, Department of Biochemistry, University of Bologna, Italy.
- ✓ **2006-2008:** Master of Science (M.Sc.) in Bioinformatics, first Division with Distinction from University of Allahabad, India. 68 credits out of 68.
- ✓ **Thesis topic:** Insilico Analysis of Interaction between HIV-1 Proteases and derivatives of Cyclic Urea Inhibitor and its ADME Toxicity Properties.
- ✓ **Thesis advisor:** Prof. D.K. Gupta, Ph.D., Coordinator of Bioinformatics, Center of Bioinformatics, IIDS, University of Allahabad (AU), India.
- ✓ **2003-2006:** Bachelor of Science (B.Sc.) in Chemistry (Hons.) with First Division from Department of Chemistry (Center for advance studies), Faculty of Science, Banaras Hindu University (BHU), India.

AWARDS

- ✓ **Young Scientist Award**, International Academy of Physical Science, Allahabad, India, Jun 2011.
- ✓ **8th EBSA European Biophysics Congress Bursaries Award** to attained conference in Budapest, Hungary, August 23rd-27th 2011.
- ✓ **Italian Government Scholarship Award**, for Higher studies in Italy. From Jan 2009 – Jun 2012.

- ✓ **Brains in Competition Award** for free residence at Residenza studio di superiori (Institute of Advance studies, University of Bologna, Italy). From Jan 2009 - Dec 2011.

BIOINFORMATICS SKILLS

- ✓ Software: Python, Autodock, NCBI software suits, Rasmol, Clustal-X and W, VMD, Phylip, Tree view, Pymol, Arguslab and Genscan etc.
- ✓ Biological Databases: Genbank, EMBL, DDBJ, Pfam, PDB, Swiss prot, TrEMBL etc. User friendly with Proteomics server Expasy.

INFORMATION TECHNOLOGY SKILLS

- ✓ Well versed with Windows+LINUX, MS-Project, MS-Access, MS-Office and Internet applications.
- ✓ Languages: MATLAB, HTML, DOS, C++, VISUAL BASIC, ORACLE9i (SQL-PLUS).

CONFERENCE and WORKSHOP ATTENDED

- ✓ *“International symposium cum training workshop on recent trends in bioinformatics, system biology and biomolecular interactions”* University of Allahabad, India, January 8th-10th, 2012.
- ✓ *“8th EBSA European Biophysics Congress, Budapest”* Hungary, August 23rd-27th, 2011.
- ✓ *“Nanobiotechnology (Satellite Conference), Budapest”* Hungary, August 22nd-23rd, 2011.
- ✓ *“36th FEBS Congress (“Biochemistry for tomorrow's medicine”)”* Torino, Italy, June 25th-30th, 2011.
- ✓ *“NMR in Biology (Bio-NMR Satellite Meeting)”* Torino, June 25th, 2011.
- ✓ *“CONIAPS-XIII: 13th Conference of International Academy of Physical Sciences”* Dehradun, Uttarakhand, India, June 14th-16th, 2011.
- ✓ *“International Biophysics school on the Molecular Mechanisms of neurodegeneration”* Venice, Italy, January 25th-29th, 2010.
- ✓ *“Course in Genetics and Molecular Pathology of Age Related Neurodegenerative Diseases”* European Genetics Foundation, Bologna, Italy, 2010.
- ✓ *“7th EBSA European Biophysics Congress”* Genoa, Italy, July 11th-15th 2009.
- ✓ *“Two days workshop on Drug Designing and Sequence analysis”* Vittal Mallaya Research Foundation, Bangalore, India, 2007.
- ✓ *“National Symposium on Recent Advances in Microbial Biofertilizers, production and Utilization technology”* University of Allahabad, India, 2007.

TALK and POSTER PRESENTATION

- ✓ α -Synuclein: A target for Parkinson's Disease, **International symposium cum training workshop on recent trends in bioinformatics, system biology and biomolecular interactions**, University of Allahabad, India, January 8th-10th 2012. (**Invited Talk**)
- ✓ A Simple and Facile Method for Preparation and Characterization of CdS Nanoparticles by SEM, TEM and AFM. **International Symposium on Advanced Complex Inorganic Nanomaterials**, Namur, Belgium, September 11th-14th 2011. (**Poster**)
- ✓ Effect of 14-3-3 η on α -synuclein aggregation intermediates. **8th EBSA European Biophysics Congress**, Budapest, Hungary, August 23rd-27th 2011. (**Poster**)

- ✓ α -synuclein aggregation intermediates influenced by chaperone like protein molecule (14-3-3 η). **CONIAPS-XIII: 13th Conference of International Academy of Physical Sciences**, June 14th-16th 2011, Dehradun, Uttarakhand, India. (**Contributed talk**)
- ✓ 14-3-3 η acts as a molecular chaperon on α -synuclein aggregation intermediates. **36th FEBS Congress "Biochemistry for tomorrow's medicine"**, June 25th-30th 2011, Torino, Italy. (**Poster**)
- ✓ Multi-scale insights into the α -Synuclein aggregation process: from single- molecule manipulation to mature amyloid fibril characterization. **FUNMARCH workshop**, CNR Bologna, Italy, May 5th-7th 2010. (**Contributed Talk**)
- ✓ Chaperones prevent Protein Aggregation: Mechanism of action investigated by Atomic Force Microscope (AFM). **University of Bologna**, Italy, May 28th-29th 2010. (**Poster**)
- ✓ Insight into the aggregation process of α -Synuclein: Structural characterization of Synuclein dimers. **55th National Meeting of the Italian Society of Biochemistry and Molecular Biology (SIB)**, University of Milan, Italy, September 14th-17th 2010. (**Poster**)

PROFESSIONAL MEMBERSHIP

- ✓ **Life Member:** International Academy of Physical Sciences, Allahabad, India.
- ✓ **Life Member:** The international NanoScience community, Budapest, Hungary.
- ✓ **Life Member:** Blue Planet Society, Allahabad, India.
- ✓ **Member:** Parkinson's disease online research (Michael J. Fox Foundation)

EXTRA CURRICULAR ACTIVITIES

- ✓ **Certificate course in Information Technology** with Good Grade from National Institute of Information Technology (NIIT), Varanasi, India, 2006.
- ✓ **Yoga training for better Living** from B.H.U Varanasi, (Award for best Yoga Practice) India, 2006.
- ✓ **Painting Classes** from Allahabad museum (Painting selected for National Painting Exhibition) India, 2007.

PUBLICATIONS

- ✓ "Chaperone like protein 14-3-3 η interacts with human α -synuclein aggregation intermediates rerouting the intracellular amyloidogenic pathway" - Manuscript Under preparation.
- ✓ "Structure and aggregation of Alpha-Synuclein covalent tandem dimers" - Manuscript Under preparation.
- ✓ "Insilico Analysis of Interaction between HIV-1 Proteases and derivatives of Cyclic Urea Inhibitor and its ADME Toxicity Properties". Dhruv kumar, D.K.Gupta, Biofrontiers, 1, 2, (2010).

BOOKS and CHAPTER CONTRIBUTION

- ✓ **Mechanochemistry: Coupling mechanical forces and chemical reactions** (Book chapter) by Dhruv kumar and Bruno Samori for Molecular Manipulation with Atomic Force Microscopy (Book), **CRC Press-publication date: Dec 01 2011**, ISBN No -9781439809662

- ✓ **Nanophosphors-Nanogold immunoconjugates in Isolation of Biomembranes and in Drug Delivery** (Book chapter) for Recent Advances in Nanomedicine (Book), **VBRI Press, 2011**, ISBN No-9788192006803
- ✓ **Insilico analysis of Docking between HIV-1 PR and derivatives of CUI** (Docking between HIV-1 proteases and cyclic urea inhibitors: A step towards drug designing against AIDS) by Dhruv kumar, **Lambert Academic Publishing, 2011**, ISBN No -9783844384765

AREA OF INTEREST

- ✓ Any area which adds experience and needs attentive mind thinking and an area where I could come and under their shadow.

PERSONAL DETAIL

- ✓ **Present Address:** Dhruv Kumar, C/o- Prof. Bruno Samori, Via S. Giacomo-11, Nanobioscience lab, Department of Biochemistry, University of Bologna, Bologna, Italy. Pin-40126.
- ✓ **Permanent Address:** S/o Sri Jagdhari Pandey, Vill-Manpura, P.O-Goroul, Dist-Vaishali (Bihar), India. Pin-844118.
- ✓ **Date of Birth:** March 01, 1982.

REFERENCES

1. Prof. Bruno Samori

Coordinator of Nanobiotechnology and Nanobioscience lab,
Department of Biochemistry,
University of Bologna,
Via S. Giacomo-11, Bologna, Italy
E-mail: bruno.samori@unibo.it
Tel: +39 051 209 4387

2. Prof. Dwijendra K. Gupta

Coordinator of Bioinformatics
Center of Bioinformatics
Nehru Science Center, IIDS
University of Allahabad, India
E-mail: dwijenkumar@gmail.com
Tel: +91 9335150718

3. Prof. Vincenzo Scarlato

Professor of Molecular Biology
Department of Biology
University of Bologna,
Via Selmi 3, Bologna, Italy
E-mail: vincenzo.scarlato@unibo.it
Tel: +39 051 209 4204

4. Dr. Marco Brucale

Senior Scientist
Consiglio Nazionale delle Ricerche (CNR)
Istituto per lo Studio dei Materiali Nanostrutturati (ISMN)
Via Salaria km 29.3 - 00015 Monterotondo, Roma, Italy
Email: marco.brucale@ismn.cnr.it
Tel: +39 069 067 2410